PORE-GAS DYNAMICS
IN OVERBURDEN AND
RECLAMATION SOIL COVERS

A Thesis submitted to the College of
Graduate and Postdoctoral Studies
in partial fulfilment of the requirements
for the degree of
Doctorate of Philosophy
in the Department of
Civil, Geological and Environmental Engineering
University of Saskatchewan
Saskatoon, Saskatchewan, Canada

By
KYLE O. SCALE
2017

PERMISSION TO USE

In presenting this thesis in partial fulfillment of the requirements for a Postgraduate degree from the University of Saskatchewan, I agree that the Libraries of the University may make it freely available for inspection. I further agree that permission for copying this thesis in any manner, in whole or in part, for scholarly purposes may be granted by the professor or professors who supervised my thesis work or, in their absence, by the Head of the Department or the Dean of the College in which my thesis work was done. It is understood that any copying or publication or use of this thesis or parts thereof for financial gain shall not be allowed without my written permission. It is also understood that due recognition shall be given to me and to the University of Saskatchewan in any scholarly use which may be made of any material in my thesis.

Requests for permission to copy or to make other use of material in this thesis in whole or in part should be addressed to:

Head of the Department of Civil, Geological and Environmental Engineering
57 Campus Drive
Saskatoon, SK
S7N 5A9

ABSTRACT

Large above-grade overburden landforms comprised of low-grade lean oil sands (LOS) are amassed during the surface mining of oil sands in northern Alberta, Canada. Reclamation soil covers consisting of locally-salvaged soils are subsequently placed above the LOS landforms in single and multi-layered configurations. The soil covers are intended to 1) provide sufficient pore-gas O2 to facilitate the growth of native boreal forest vegetation and to 2) oxidize methane (CH4) produced in the anaerobic zones of the LOS before being exhausted to the atmosphere as a greenhouse gas.

Prior to covering the LOS with soil covers, rates of CO2 efflux from the surface of the LOS to the atmosphere ranged from 0.1-7.1 kg/m2/a. Pore-gas concentrations within the uncovered LOS ranged from 0-18% for oxygen (O2), 3-21% for carbon dioxide (CO2), and 0-12% for CH4. Following placement of soil covers, peak rates of CO2 efflux were 2.3 kg/m2/a from the surface of the soil covers to the atmosphere and 1.8 kg/m2/a from the LOS into the soil covers. Peak rates of O2 influx from the atmosphere through the soil covers was 18 kg/m2/a. Pore-gasses within the overlying soil covers and uppermost LOS were typically below the threshold that poses a risk to the survivability of reclamation vegetation, >10% O2 and <15% CO2. Pore-gasses deeper than 2 m within the LOS surpassed this threshold with O2 falling to 0% and CO2 rising to >16%.

Rates of CH4 oxidation were quantified in batch soil column experiments for the soil cover materials and LOS in single and multi-layered configurations. Oxidation rates were sensitive to variations in temperature, moisture content, and bulk density. The results of the column experiments indicate that CH4 generated deeper than 2 m within the LOS landform will be partially oxidized in both the soil covers and uppermost LOS horizon.

Statistical analyses and finite difference numerical modelling were conducted to guide mine operators regarding practical issues involving the construction of LOS landforms, design of soil cover systems, and management of reclamation sites. Based on these exercises, it appears that the characteristics of the LOS landform are more important to pore-gas dynamics than the design of the soil cover systems.

ACKNOWLEDGEMENTS

I am sincerely grateful to Dr. Ian Fleming for providing the opportunity and supporting me throughout graduate studies and for the time and effort invested by the members of my committee, Matt Lindsay, Terry Fonstad, and Grant Ferguson.

The staff at Syncrude's Environmental department at Mildred Lake were a pleasure work with, specifically Wendy Kline, Lori Cyprien, Jess Piercy, Janna Lutz, and Chris Beierling. I can't over-emphasise my appreciation for Marty Yarmuch at Syncrude for thoroughly reviewing my work and providing thoughtful and constructive feedback. The staff at O'Kane Consultants were helpful in the field and in the office, specifically Larissa Doucette, Sophie Kessler, Lindsay Tallon and Dave Christensen. Also, many thanks as well to all the members of C.O.S.I.A. that believed in this project and provided the funding to complete the research – I literally couldn't have done this without your support.

I'd like to give a shout-out to the many helpful people at the University of Saskatchewan, Cynthia Hanke, Adam Hammerlindl, Doyin Adesokan, Helen Yin, Doug Fisher, David Parker, Kevin Matheson, Tomasz Korbas, Andrew Ireson, and Matthew Fleming.

Lastly, I dedicate this effort to the special people in my life that I've lost since starting graduate studies, my grandma Bertha Lloyd, my best friend Mohammad Taherian, my father-in-law Les Cantin, and my beloved dog Fergus.

Table of Contents

Table of Figures

List of Tables

List of acronyms

Abbreviation	
A	Area
ASCS	Aurora Soil Capping Study
ANOVA	Analysis of variance
ASTM	American Society for Testing of Materials
BC	Boundary condition
BGS	Below ground surface
BTEX	Benzene/ Toluene/ Ethylene/ Xylene
C	Concentration
CCME	Canadian Council of Ministers of Environment
CH4	Methane gas
CO2	Carbon dioxide gas
D	Diffusion coefficient
GC	Gas chromatography
GHG	Greenhouse gas
F	Mass flux
F_A/F_D	Ratio of advection to diffusion
FC	Flux chamber
FID	Flame ionization detection
FTIR	Fourier transform infrared
H	Henry's Law coefficient
Ha	Hectare
L	Length
LFH	Leaf-litter, fibric, humic
Loc.	Location
LOI	Loss on ignition
LOS	Lean oil sands
M	Mass
M-Q	Millington & Quirk
MET	Meteorological station
MLSC	Multi-layered soil column

NAFC	Napthenic acid fraction component
O_2	Oxygen gas
PHC	Petroleum hydrocarbon
PSD	Particle-size distribution
PVC	Polyvinyl chloride
R^2	Coefficient of determination
RMSE	Root mean squared error
SCL	Syncrude Canada Limited
SFC	Static flux chamber
SVP	Soil vapour probe
SWCC	Soil water characteristic curve
t	Time
T	Temperature
TC	Total carbon
TIC	Total inorganic carbon
TOC	Total organic carbon
Tr	Treatment #
US EPA	United States Environmental Protection Agency
V	Volume
VWC	Volumetric water content

1.0 INTRODUCTION

1.1 Study Motivation

Above-grade overburden landforms are amassed during the surface mining of oil sands in northern Alberta, Canada. To facilitate the reclamation of these landforms, engineered soil covers ranging in thickness from 0.3 m to 1.5 m are placed onto the landforms and subsequently planted with native boreal forest plant and tree species (reclamation vegetation). Restrictions in soil-atmosphere gas exchange within the plant rooting zone of the soil covers develop into conditions of O_2 deficiency and CO_2 toxicity by inhibiting the ingress of atmospheric oxygen (O_2) and efflux of carbon dioxide (CO_2). It is therefore essential that sufficient soil-atmosphere gas exchange be maintained in order to preclude concentrations of pore-gasses within the soil covers from surpassing the threshold that poses a risk to the growth and survivability of reclamation vegetation.

This thesis is intended to provide C.O.S.I.A. operators (listed below) with a scientific basis for the site-specific estimation of the risk of gas-related toxicity to plant growth during the re-vegetation phase of the reclamation of lean oil sands landforms. The findings in this thesis may inform mine operators regarding issues involving the construction of lean oil sands landforms, design of soil covers, and future management of the reclamation site.

Funding for this thesis is provided by C.O.S.I.A. – the Canadian Oil Sands Innovation Alliance. Contributing C.O.S.I.A. members include Syncrude Canada Ltd., Suncor Energy Inc., Shell Canada Energy, Imperial Oil, Total E&P Canada Ltd., and Canadian Natural Resources Limited. This thesis is a continuation of the “Hydrocarbon Mobility and Degradation Study” started by Dr. I.R. Fleming.

1.2 Overview

With production rates surpassing 1 million barrels of oil per day (CAPP 2015), the surface mining of oil sands in Alberta, Canadsa operates on a massive scale in terms of project size, mineable area, and land disturbance. The Athabasca, Peace River, and Cold Lake bitumen deposits underlie a 140,000 km^2 area in Alberta and are estimated to contain 170 billion barrels

of recoverable oil (Alberta Energy 2016). Of the three bitumen deposits, the Athabasca oil sands region (AOSR) is the largest in mineable area and recoverable reserves.

Syncrude Canada Limited (SCL) is one of the leading mine operators in the AOSR with two active mines situated 50 km and 80 km north of Fort McMurray, Alberta. The Aurora soil capping Study (ASCS) is a field-scale mine cover testing site located at SCL's northernmost Aurora North mine. The ASCS is a multi-disciplinary collaboration between industry, universities, and consultants that aims to systematically investigate the effectiveness of single and multi-layered coarse-textured locally-salvaged soil covers placed over "lean" oil sands (LOS) consisting of ≤7% petroleum hydrocarbons (Barber et al 2015).

Regulations in Alberta mandate that oil sands operators must prepare long-term site closure plans and implement the associated land reclamation programs. For LOS, operators are required to design and grade closure landforms prior to covering the landforms with 1.2-1.5 m of locally-salvaged soil (Government of Alberta 2007). Subsequently, native boreal forest vegetation are planted with >90% of the rooting zone concentrated in the uppermost 0.6 m (Van Rees 1997). A major risk to the growth and survivability of the reclamation vegetation is whether rates of gas exchange between the soil covers and the atmosphere (atmospheric O_2 moving downwards into the soil covers and LOS; CO_2 and CH_4 moving upwards from the LOS to the soil covers and atmosphere) are sufficient to preclude the development of conditions of O_2 deficiency and CO_2 toxicity within the plant rooting zone. The research presented in this dissertation supplements the multi-disciplinary ASCS research by developing a comprehensive understanding of the storage, transportation, and reactions of pore-gasses in single and multi-layered soil covers and in the underlying lean oil sands landform.

1.3 Research Objectives

Understanding pore-gas dynamics in reclamation soil covers and lean oil sands (LOS) is fundamental to understanding the risks of gas-related toxicity to plant growth during the re-vegetation stage of the reclamation of boreal forest ecosystems. The objective of this dissertation is to develop a scientific basis to estimate the site-specific risk of gas-related

toxicity to reclamation vegetation in order to inform mine operators regarding practical issues related to construction of LOS landforms, design of soil covers, and future management of the reclamation site. The following specific objectives are addressed within the four manuscripts comprising this dissertation:

1. characterise LOS degradation rates and pore-gasses within the uncovered LOS landform;
2. characterise pore-gasses at various depths in the single and multi-layered soil covers and LOS landform following placement of soil covers;
3. quantify rates of O_2 ingress through the soil covers and CO_2 efflux from the soil covers;
4. estimate O_2 and CO_2 flux rates resulting from pressure-gradient driven advection and concentration-gradient driven diffusion;
5. quantify the relative importance of advection and diffusion to total gas transport;
6. quantify methane oxidation rates in the laboratory while controlling for temperature, moisture content, and bulk density; and
7. evaluate the factors controlling the storage and transport of pore-gasses in the soil covers and LOS, including air temperature, soil temperature, soil moisture, soil-atmosphere pressure gradients, petroleum hydrocarbon content of the LOS, in-situ bulk density of the LOS, soil cover thickness, and soil cover material.

This dissertation contains four research manuscripts. Manuscript 1 is presented in Chapter 2 and addresses objective 1. This manuscript was prepared by K. Scale based on the raw data collected in the field and laboratory by Tomasz Korbas for his M.Sc. (2014). It should be noted that much of the fieldwork was performed collaboratively with both Korbas and Scale working together at the field site. While most of the basic data collection had been completed by T. Korbas, considerable additional calculations, modelling, and analyses were carried out by K. Scale as part of the preparation of this manuscript. While not wholly the work of K. Scale, this chapter represents a starting point for the work that was completed independently by K. Scale and is presented in the later chapters. The manuscript is separated into field and laboratory

sections. In the field section, concentrations of O_2, CO_2, and CH_4 pore-gasses within the LOS landform are characterised in-situ using a combination of single-point soil vapour probes (SVP) and a re-purposed landfill gas analyser. Rates of CO_2 efflux from the uncovered LOS are directly measured using static flux chambers. In the laboratory section, rates of CO_2 efflux, PHC degradation, and PHC volatilization are measured in soil column experiments. Furthermore, the fractions of F1-F4 petroleum hydrocarbons comprising the LOS are measured with analytical laboratory techniques.

Manuscript 2 is presented in Chapter 3 and addresses objectives 2-5. Following placement of soil covers, concentrations of O_2, CO_2, and CH_4 pore-gasses within the soil covers and LOS are characterised using a combination of SVP and a re-purposed landfill gas analyser. Static flux chambers were used to directly measure CO_2 effluxes from the surface of the soil covers. A novel subsurface flux chamber is custom designed and fabricated to measure CO_2 effluxes from the LOS into the soil covers and O_2 ingress from the atmosphere through the soil covers. Fluxes of O_2 and CO_2 through the soil covers driven by concentration-gradient driven diffusion are indirectly measured based on pore-gas profiles and estimations of diffusivity based on vertical profiles of soil temperature and soil moisture. Fluxes of O_2 and CO_2 through the soil covers driven by pressure-gradient driven advection are indirectly measured based on pore-gas profiles and in-situ measurements of air conductivity and vertical profiles of gas pressures. The relative importance of advection and diffusion is quantified at each gas sampling location.

Manuscript 3 is presented in Chapter 5 and addresses objective 6. Methane oxidation rates in soil cover materials and lean oil sands are quantified in the laboratory using transient “batch” soil column experiments. Oxidation rates in single and multi-layered configurations of locally salvaged soils (peat, subsoil, LFH) and LOS are characterised over the range of CH_4 fluxes characterised in the field. Temperature, moisture content, and bulk density are controlled in the experiments.

Manuscript 4 is presented in Chapter 4 and addresses objective 7. The aim of this manuscript is to guide mine operators in practical issues involving the construction of LOS landforms,

design of soil cover systems, and future management of reclamation sites. Statistical analyses are conducted to evaluate the storage of pore-gasses in the context of on-site conditions, measurable soil parameters, soil cover design, petroleum hydrocarbon content of the LOS, and in-situ bulk density of the LOS. Finite difference numerical modelling is conducted to evaluate the transport of pore-gasses by simulating the diffusive and advective-diffusive flux of CO_2 through multi-layered soil covers.

Findings from this research are applicable to mine operators using engineered soil covers to reclaim LOS deposits consisting of low petroleum hydrocarbon content oil sands.

1.4 Literature Review

1.4.1 Pore-gasses and plant growth

Reclamation vegetation planted in soil covers require sufficient pore-gas O_2 in the rooting zone to facilitate essential biological processes like metabolism and respiration (Geigenberger 2003). Reductions in pore-gas O_2 may arise from biological activity or restrictions in air porosity from over-compaction or elevated soil moisture conditions. Symptoms of O_2 deficiency generally manifest at pore-gas concentrations less than 10% (Flower 1981; Kozlowski 1985), while CO_2 may be phytotoxic at pore-gas concentrations greater than 15% (Flower 1981; Whitton 1991).

Physiological impairments from deficient O_2 or excess CO_2 include drying of leaves (desiccation), loss of pigmentation (chlorosis), shedding of leaves (abscission), impeded nutrient absorption, reduced photosynthesis (and thus reduced growth rates), and the production of organic compounds such as ethylene (Chang and Loomis 1955; Leone 1977; Flower 1981; Kozlowski 1985; Wong 1988; Whitton 1991; Pezeshki et al 1993; Bartholomeus et al 2008).

1.4.2 Flux chambers

Soil gas effluxes are commonly measured using the static flux chamber (SFC) method. The upper section of the static flux chamber is sealed to atmospheric gasses and the lower section is permeable to soil gasses. The lower section of the flux chamber is embedded into the soil

to minimize intrusion of atmospheric O_2. The efflux of gasses is calculated from the rate of increase of gasses within the enclosed headspace over an incremental time.

Equation 1.1 is the general equation used to calculate gas fluxes using the SFC method:

$$F_i = \frac{V_C}{A_C}\frac{\Delta C_i}{\Delta t} \quad [1.1]$$

Where F_i is the mass flux of a gaseous species into the closed chamber [$ML^{-2}T^{-1}$], V_c is the volume of the chamber headspace [L^3], A_c is the area enclosed by chamber [L^2], and $\Delta C_i/\Delta t$ = concentration change of the gaseous species in the headspace over a time interval [$ML^{-3}T^{-1}$].

The main systematic error involved with SFC measurements is the underestimation of flux rates due to accumulation of gasses in the headspace to concentrations surpassing levels representative of the natural environment, thus reducing the concentration gradient that drives diffusive gas transport (Fick 1855; Nay 1994; Hutchinson et al 2000; Davidson et al 2002; Pumpanen 2004; Heinemeyer and McNamara 2011; Pihlatie 2012).

1.4.3 Diffusion

Gaseous diffusion is the movement of gasses from regions of higher concentration to regions of lower concentration. For soil covers, the dominant O_2 and CO_2 concentration gradient exists between the atmosphere and soil. With O_2 the gradient is positive since O_2 decreases with depth below ground surface (BGS); for CO_2 the gradient is negative since CO_2 typically increases with depth BGS.

Diffusion of soil gasses driven by concentration gradients is explained by Fick's Law that molecules move from regions of higher to lower concentration at a rate proportional to the diffusion coefficient, D (Fick 1855). Fick's Law is expressed in Equation 1.2.

$$F = -D * \frac{\Delta C}{\Delta z} \quad [1.2]$$

Where D is the bulk diffusion coefficient [L^2T^{-1}] and $\Delta C/\Delta z$ is the concentration gradient [ML^{-4}].

A “harmonic” diffusion coefficient as described by Aubertin et al (2000) in Equation 1.3 takes into account variations in the diffusion coefficient in layered soils by considering the layers above (for O_2 diffusing downward) and layers below (for CO_2 diffusing upward):

$$\bar{D_1} = \frac{\Sigma t_i}{\Sigma t_i / D_i} \quad [1.3]$$

Where D_i is the diffusion coefficient of a given soil layer [L^2T^{-1}] and t_i is the corresponding thickness of the soil layer [L].

The “bulk” diffusion coefficient D assumes unrestricted diffusion through free air. To practically reflect the physical constraints of gaseous diffusion in soil pores, the diffusion coefficient accounts for irregularities along the flow path by incorporating tortuosity (τ) and constrains the pore volume to the air-filled fraction by incorporating air porosity (θ_a). The modified diffusion coefficient presented in Equation 1.4 is expressed as D_p for single-phase flow and is expressed as tortuosity (τ) multiplied by the diffusion coefficient in air, Da_0. Tortuosity describes irregularities along the flow path that reduce the flow rate of gasses travelling through porous media.

$$D_p = Da_0 * \tau \quad [1.4]$$

Where Da_0 is the diffusion coefficient in air [L^2T^{-1}] and τ is the coefficient for tortuosity [LL^{-1}].

Dual-phase diffusion takes into account diffusion through the water-filled fraction of the pore-volume in addition to the air-filled fraction by incorporating the coefficient for diffusion in water Dw_0, with units of [L^2T^{-1}], which is orders of magnitude smaller than the coefficient for diffusion in air (Cussler 2009, Haynes 2013). Dual-phase models, as presented in Equation 1.5, are expressed as the “effective” diffusion coefficient (Collin and Rasmuson 1988):

$$D_e = Dp_0 + HDw_0 \quad [1.5]$$

Where D_e is the effective diffusion coefficient [L^2T^{-1}] and H is Henry’s law equilibrium coefficient for a solution of gas in water.

1.4.4 Soil concentration gradient method

The soil concentration gradient method (CGM) enables soil-atmosphere diffusive fluxes to be calculated using position-dependent gas concentrations and a known diffusion coefficient (de Jong and Schappert 1972; Maier and Schack-Kirchner 2014; Kanako et al 2008; Billings et al 1998; Risk et al 2002; Sihota et al 2011). The equation to estimate gas fluxes using CGM is based on Fick's law and is presented in Equation 1.6:

$$F_{CGM} = D_e \frac{C_s - C_a}{\Delta z} \quad [1.6]$$

Where C_s is the concentration of a gaseous species in the subsurface [ML^{-3}], C_a is the atmospheric gas species concentration [ML^{-3}], and Δz is the vertical distance between gas sampling location and ground surface [L].

The CGM has several advantages to estimating gas fluxes using static flux chambers. Since the process involves measuring vertical gas profiles, it is possible to account for gaseous storage in pore-spaces (Risk et al 2002). The depth of gas sources (e.g. CO_2 production) and gas sinks (e.g. O_2 consumption) can be estimated (Martin and Schack-Kirchner 2015). Lastly, CGM negates errors inherent to static flux chambers such as the systematic under-estimation of gas fluxes due to accumulation of gasses in the chamber headspace (Maier and Schack-Kirchner 2014).

Although CGM has advantages to static flux chambers, there are also limitations to the approach. One such limitation is that diffusion is restricted to the vertical direction and thus neglects lateral diffusion (Maier and Schack-Kirchner 2014). Moreover, diffusion is assumed to be at steady-state and doesn't consider temporal variations in gas production or consumption (Martin and Schack-Kirchner 2015). There are also limitations to the applicability of Fick's Law to for multi-component gas mixtures (Jaynes and Rogowski 1983; Leffelaar 1987; Thorstenson and Pollock 1989; Voudrias and Chiayang 1992). Fick's laws don't consider Knudsen diffusion, which occurs in finer-grained soils when molecules collide more

with pore walls than with other molecules (Klinkenberg 1941). Moreover, Fick's Laws aren't applicable for stagnant gasses with no fluxes, sources or sinks (Scanlon 2002).

In order to assign position-dependent diffusion coefficients to multi-layered soils, the diffusion coefficient must be assumed to abruptly change between soil layers (Liu and Si 2008). This may be a poor assumption in some cases because it is rare for natural soils to be stratified with sharp or level transitions (Liu and Si 2008). At the ASCS, however, this is likely a valid and defensible assumption since the soil covers were precisely graded with GPS-assisted graders and dozers.

1.4.5 Barometric pressures and gas transport

Barometric pressure is the weight exerted on Earth's surface by atmospheric gasses. Temporal variations in barometric pressures occur due to i) transient low and high pressure weather systems; ii) changes in density of atmospheric gasses resulting from diurnal temperature and gravity variations; iii) precipitation and subsequent moisture infiltration; and iv) fluctuations in the groundwater table (Auer 1996; Hillel 2003; Dong-mei Sun 2015).

Barometric pressure influences rates and direction of soil-atmosphere gas exchange (Buckingham 1905; Fukuda 1955; Jaynes and Rogowski 1983, Thorstenson and Pollock 1989, Nilson et al 1991; Auer et al 1996; Boeckx 1996; Cepiel 1996; Christophersen 2001; Poulsen 2003; Massman 2006; Gebert 2011; Redecker 2015). This phenomenon is denoted in the literature as "barometric pumping"; falling pressures induce gas flow from soils to atmosphere, whereas rising pressures suppress gas flow from atmosphere to soils (Young 1990; Czepiel 1996; Christophersen 2001; Massman 2006; Gebert 2011).

1.4.6 Advection

Equation 1.7 presents the relationship for one-dimensional fluxes of pore-gasses due to advection for a single phase is derived from Darcy's Law (Darcy 1856; Falta et al 1989; Seely et al 1994; Hillel 2003; Kim and Benson 2004; Kjeldsen et al 2005):

$$F_a = \nu C_i = -\left(\frac{k_a \rho_g g}{\theta_a \mu_g} \nabla P\right) * C_i \qquad [1.7]$$

Where F_a is advective flux of species i [$ML^{-2}T^{-1}$], k_a is intrinsic air permeability of the porous media [L^2], ρ_g is gas density [ML^{-3}], g is gravitational constant [LT^{-2}], μ is dynamic viscosity of the gas [$ML^{-1}T^{-1}$], C_i is concentration of species i, and ∇P is soil-atmosphere pressure gradient [ML^{-4}].

The coefficient of gas permeability, k_a, can be estimated with Equation 1.8 by modifying Freeze and Cherry's (1979) relationship:

$$k_a = \frac{K_a \mu_g}{\rho_g g} \quad [1.8]$$

Where K_a is the air conductivity [LT^{-1}]. Air conductivity through a porous soil is reduced at higher soil moisture contents.

1.4.7 Biochemistry of CH_4 oxidation

Methanogenic biodegradation of petroleum hydrocarbon substrates occurs under anaerobic conditions when O_2 is unavailable to be terminal electron acceptor (Grishchenkov et al 2000, Salminen et al 2004). The product, gaseous CH_4, may be subsequently exposed to O_2 in the aerobic zone of an overlying cover soil. Methanotrophic microorganisms (methanotrophs) in the aerobic zone of the cover soil can facilitate reduction-oxidation reactions (methane oxidation) by transferring electrons from electron-donating CH_4 to electron-accepting O_2.

All methanotrophs are characterised by the methane monooxygenase enzyme (Anthony 1982; Hanson and Hanson 1996). The only energy source for methanotrophs is the carbon in methane (Anthony 1982); the energy gained in the electron transfer is used to carry out cell functioning while the carbon is incorporated into biomass. The net reaction for methane oxidation is presented in Equation 1.9 and results in the consumption of O_2 and CH_4 and production of CO_2 and water:

$$CH_4 + 2O_2 \rightarrow CO_2 + 2H_2O \quad [1.9]$$

Based on this stoichiometric relationship, 2 moles of O_2 are consumed for every 1 mole of CH_4 consumed; this means pore-gas CH_4 concentrations greater than 10% could potentially fuel the consumption of all O_2 in the pore space and lead to anoxic conditions in the cover soil.

There are 2 types of methanotrophs that are of interest in this study: 1) high capacity/low affinity (typically present at CH_4 concentrations >40 ppm) and 2) low capacity/ high affinity (typically present at CH_4 levels <1.7 ppm). Low affinity methanotrophs survive by utilizing the abundant carbon supplied by relatively high fluxes of CH_4. On the other hand, it is still a mystery how high affinity methanotrophs avoid starvation with the relatively low CH_4 fluxes (Knief and Dunfield 2005): they may survive by consuming low levels of atmospheric CH_4 (Bender and Conrad 1994), using alternate substrates like methanol (Jensen et al 1998), or relying on intermittent bursts of methanogenic activity (Dunfield et al 1995). The first to observe methane oxidation at low, atmospheric-level CH_4 concentrations (<1.7 ppm_v) were Bender and Conrad (1992, 1994) before a novel species of methanotroph was later isolated by Bull et al (2000).

1.4.8 Statistical procedures

Multiple statistical procedures are used in the following dissertation to i) evaluate the goodness of fit of various models with R^2 and adjusted R^2; ii) determine if data sets were correlated with ANOVA, T-test, and F-test; and iii) estimate the relationships between a dependent variable and one or more independent variables with single-variable and and multi-variate regression.

i) Goodness of fit

The coefficient of determination, R^2, is an indicator of how well a regression model approximates measured values when one independent variable (regressor) is being evaluated (Montgomery and Runger 2014). The formula for calculating R^2 is presented in Equation 1.10:

$$R^2 = \frac{SS_R}{SS_T} = \frac{\Sigma(Y_{est} - \overline{Y_{est}})^2}{\Sigma(Y - \overline{Y})^2} \quad [1.10]$$

Where, SS_R is residual sum of squares, SS_T is total sum of squares, Y_{est} is the estimated Y value from the model, $\overline{Y_{est}}$ is the mean estimated Y value, Y is the measured Y value, $\overline{Y}$ is the mean measured Y value.

When more than one regressor is being evaluated in multi-variate linear regression, the R^2 needs to be adjusted to account for the additional variables (Zar 1999). The adjusted R^2,

presented in Equation 1.11, reduces the R^2 with each added regressor. It is useful quantity to examine when comparing multi-variate regression models with various combinations of regressors.

$$R^2_{adj} = 1 - \left[\frac{(1-R^2)(n-1)}{n-k-1}\right] \quad [1.11]$$

Where n is the number of data points and k is the number of regressors (variables) in the model.

ii) Data correlation

Analysis of variance (ANOVA) is a test to evaluate if multiple groups of data (3 or more) are statistically correlated. The results of ANOVA tests that are analysed herein are the p-value, the F-value, and the F-critical value.

P-values are the estimated probability that a null hypothesis should be rejected, where the null hypothesis is that data sets are not significantly different (Montgomery and Runger 2014). P-values are compared to alpha values in order to determine whether to accept or reject the null hypothesis, where: alpha = 1 – confidence level (CI). For example, the alpha values for 95% CI and 99% CI are 0.05 and 0.01, respectively. Therefore, if p-values are larger than alpha, the values aren't statistically different and the null hypothesis is accepted; conversely, if p-values are less than alpha, the values are considered statistically different and the null hypothesis is rejected.

F-values are also compared when examining results of ANOVA. The F-test mesures the significance of the difference between sample variances (McBean and Rovers 1998). Re-phrased, the F-test is the ratio of variance between groups to variance within groups. Therefore, large values of F indicate more variance between different groups than within groups; thus, the groups are statistically different and the null hypothesis should likely be rejected (McBean and Rovers 1998). The F-value is compared to the F-critical value; if F is larger than F-critical than the null hypothesis should likely be rejected.

ANOVA is an omnibus test, meaning the results don't predict which of the groups compared is different, only that there is a difference between groups. Therefore, if results of ANOVA produce p-values less than alpha, signifying that the groups are statistically different, further *post-hoc* statistical analyses need to be done to determine precisely which groups are different.

The post-hoc statistical procedures used herein were t-tests with Bonferroni correction applied. The T-test is used to evaluate whether means of two groups are different from each other. The issue with conducting multiple T-tests in post-hoc testing, however, is that it compounds the likelihood of Type 1 errors. Note, a type 1 error is equal to alpha; it is the error that the null hypothesis was true, but was wrongly rejected.

When multiple comparisons are made using T-tests, a "Bonferroni correction" is applied to reduce compounding of Type I errors (Dunn 1961). The Bonferroni correction divides alpha by the number of post-hoc comparisons made. For example, for a 95% CI, the alpha value is 0.05; if 3 comparisons are made with T-tests at 95% CI, then the Bonferonni adjusts alpha to: alpha = 0.05/3 = 0.0167.

iii) Regeression

Regression analysis is a statistical procedure to quantify the relationship between a dependent variable and one or more independent variables. The results of regression tests analysed herein are the p-value, the F-value, and the F-significance value.

As mentioned previously, the p-value is the probability that the null hypothesis should be rejected. The F-value, when applied to regression analysis, can be stated as the ratio of the variance that can be explained to the variance that is unexplained; therefore, the higher the F-value, the more variance in the dependent variable that is explained by the independent variable.

The results of regression analysis are analyzed with a similar procedure as ANOVA results. P-values are compared to alpha values to assess whether to accept or reject the null

hypothesis. F-values are compared to F-significance values; if F is larger than F-significance than the independent variable is likely a good predictor of the dependent variable.

References

Alberta Energy. 2016. **About Oil Sands: Facts and Statistics**. [Accessed October 2016] Available at: http://www.energy.alberta.ca/oilsands/791.asp

Anthony C. 1982. **The Biochemistry of Methylotrophs**. Academic Press, New York.

Aubertin M, Aachib M, and Authier K. 2000. **Evaluation of Diffusive Gas Flux through Covers with a GCL**. Geotextiles and Geomembranes. (18): 215-233. DOI: 10.1016/S0266-1144(99)00028-X

Auer LH, Rosenberg ND, Birdsell KH, and Whitney EM. 1996. **The Effects of Barometric Pumping on Contaminant Transport**. Journal of Contaminant Hydrology. (24) 145-166. DOI: 10.1016/S0169-7722(96)00010-1

Barber LA, Bocksette J, Christensen DO, Tallon, LK, and Landhausser SM. 2015. **Effect of Soil Cover System Design on Cover System Performance and Early Tree Establishment**. Mine Closure 2015, Vancouver, Canada.

Bartholomeus RP, Witte JP, Bodegom PM, Van Dam JC, and Aerts R. 2008. **Critical Soil Conditions for Oxygen Stress to Plant Roots: Substituting the Feddes-function by a Process-based Model**. Journal of Hydrology (360): 147-165. DOI: 10.1016/j.jhydrol.2008.07.029

Bender M and Conrad R. 1992. **Kinetics of CH4 Oxidation in Oxic Soils Exposed to Ambient Air or High CH4 Mixing Ratios**. FEMS Microbiology Letters. (101): 261-270. DOI: 10.1111/j.1574-6968.1992.tb05783.x

Bender M and Conrad R. 1994. **Methane Oxidation Activity in Various Soils and Freshwater Sediments: Occurrence, Characteristics, Vertical Profiles, and Distribution on Grain Size Fractions**. Journal of Geophysical Research. (99): 16531-16540. DOI: 10.1029/94JD00266

Billings SA, Richter DD, Yarie J 1998: **Soil carbon dioxide fluxes and profile concentrations in two boreal forests**. Canadian Journal of Forest Research. (28): 1773–1783. DOI: 10.1139/x98-145

Boeckx P, Van Cleemput O, and Villaralvo I. 1996. **Methane emission from a landfill and the methane oxidising capacity of its covering soil**. Soil Biology and Biochemistry. (28): 1397-1405. DOI: 10.1016/S0038-0717(96)00147-2

Buckingham E. 1904. **Contributions to our Knowledge of Aeration of Soils**. Bulletin 25. Bureau of Soils, U.S. Department of Agriculture, Washington, D.C.

Bull ID, Parekh NR, Hall GH, Ineson P, and Evershed RP. 2000. D**etection and Classification of Atmospheric Methane Oxidizing Bacteria in Soil**. Nature. (405): 175-178. DOI: 10.1038/35012061

CAPP (Canadian Association of Petroleum Producers). 2016. **Basic Statistics**. [Accessed October 2016] Available at: http://www.capp.ca/publications-and-statistics/statistics/basic-statistics

Chang HT and Loomis WE 1955. **Effect of carbon dioxide on absorption of water and nutrients by roots**. Plant Physiology. (30): 155-161.

Christophersen M, Kjeldsen P, Holst H, and Chanton J. 2001. **Lateral gas transport in soil adjacent to an old landfill: Factors governing emissions and methane oxidation**. Waste Management Research. (19): 595-612. DOI: 10.1177/0734242X0101900616

Collin M and Rasmuson A. 1988. **A Comparison of Gas Diffusivity Models for Unsaturated Porous Media**. Soil Science Society of America Journal. (52): 1559-1565. DOI: 10.2136/sssaj1988.03615995005200060007x

Cussler EL**.** 2009**. Diffusion: Mass Transfer in Fluid Systems 3rd Edition.** Cambridge University Press.

Czepiel PM, Mosher B, Crill PM, and Harriss RC. 1996. **Quantifying the effect of oxidation on landfill methane emissions**. Journal of Geophysical Research. (101): 721-759. DOI: 10.1029/96JD00222

De Jong E and Schappert HJV. 1972. **Calculation of Soil Respiration and Activity from CO2 Profiles in the Soil**. Soil Science. (113): 328-333.

Dong-mei S, Yong-ge Z, and Semprich S. 2015. **Effects of Airflow Induced by Rainfall Infiltration on Unsaturated Soil Slope Stability**. Transport in Porous Media. (107): 821-841. DOI: 10.1007/s11242-015-0469-x

Dunfield PF, Topp E, Archambault C, and Knowles R. 1995. **Effect of Nirtogen Fertilizers and Moisture Content on CH4 and NH4 Fluxes in a Humisol: Measurements in the Field and Intact Soil Cores.** Biogeochemistry. (29): 199-222. DOI: 10.1007/BF02186048

Dunn OJ. 1961. **Multiple Comparisons among Means.** Journal of the American Statistical Association. (56): 52-64. DOI: 10.1080/01621459.1961.10482090

Fick A. 1855. **On liquid diffusion**. Ann. Phys. (170): 59–86. doi:10.1002/andp.18551700105. 94: 59

Flower, FB. 1981. **Landfill gas, what it does to trees and how its injurious effects may be prevented**. Journal of Arboriculture. (7): 43-52

Fukuda H. 1955. **Air and Vapor Movement in Soil Due to Wind Gustiness**. Soil Science (79): 249-256.

Gebert J, Rower IU, Scharff H, Roncato CDL, and Cabral AR. 2011. **Can soil gas profiles be used to assess microbial CH4 oxidation in landfill covers?** Waste

Management. (31): 987-994. DOI: 10.1016/j.wasman.2010.10.008

Geigenberger P. 2003. **Response of plant metabolism to too little oxygen**. Current Opinion in Plant Biology. (6): 247–256. *DOI*: 10.1016/S1369-5266(03)00038-4

Government of Alberta. 2007. **Alberta Environmental Protection and Enhancement Act.**

Grischenkov, V. et. Al. 1999. **Degradation of Petroleum Hydrocarbons by Facultative Anaerobic Bacteria under Aerobic and Anaerobic Conditions**. Process Biochemistry. (35): 889-896. DOI: 10.1016/S0032-9592(99)00145-4

Hanson RS and Hanson TE. 1996. **Methanotrophic Bacteria**. Microbiology Reviews. (60): 439-471

Haynes WM. 2013. **CRC Handbook of Chemistry and Physics: 94th Edition**.

Hillel D. 2003. **Introduction to Environmental Soil Physics**. Academic Press.

Jaynes DB and Rogowski AS. 1983. **Applicability of Fick's Law to Gas Diffusion**. Soil Science Society of America Journal. (47): 425-430.

Jensen S, Prieme A, and Bakken L. 1998. **Methanol Improves Methane Uptake in Starved Methanotrophic Microorganisms**. Applied Environmental Microbiology. (64): 1143-1146.

Kanako K, Sawamoto T, Hu R, and Hatano R. 2008. **Comparison of the closed-chamber and gas concentration methods for measurements of CO2 and N2O fluxes in two upland field soils**. Soil Science and Plant Nutrition. (54): 777-785. DOI:10.1111/j.1747-0765.2008.00292.x

Klinkenberg LJ. 1941. **The permeability of porous media to liquids and gasses**. Drilling and Production Practice, American Petroleum Institutte: 200–213.

Knief C and Dunfield PF. 2005. **Response and Adaptation of Different Methanotrophic Bacteria to Low Methane Mixing Ratios**. Environmental Microbiology. (7): 1307-1317. DOI: 10.1111/j.1462-2920.2005.00814.

Kozlowski T. 1985. **Soil aeration, flooding, and tree growth. Journal of Arboriculture**. (11:3)

Leffelaar PA. 1987. **Dynamic Simulation of Multinary Diffusion Problems Related to Soil**. Soil Science. (143). DOI: 10.1097/00010694-198702000-00001

Leone IA. 1977. **Damage to woody species by anaerobic landfill gasses**. Journal of Arboriculture.(3): 221-225

Liu G and Si BC. 2008. **Analytical Modeling of One-dimensional Diffusion Layered Systems with Position-dependent Diffusion Coefficients. Advances in Water Resources**. (31): 251-268. DOI: 10.1016/j.advwatres.2007.08.008

Maier M and Schack-Kirchner H. 2014. **Using the gradient method to determine soil gas flux: A review**. Agricultural and Forest Meteorology. (192-193): 78-95. DOI: 10.1016/j.agrformet.2014.03.006

Martin M and Schack-Kirchner H. 2015. **Using the Gradient Method to Measure Soil Gas Flux: Limitations and Pitfalls**. Geophysical Research Abstracts. (17)

Massman WJ. 2006. **Advective transport of CO2 in permeable media induced by atmospheric pressure fluctuations: 1 An analytical model**. Journal of Geophysical Research. (111). DOI: 10.1029/2006JG000163

McBean EA and Rovers FA. 1998. **Statistical Procedures for Analysis of Environmental Monitoring and Risk Assessment Vol. 3**. Prentice Hall PTR Environmental Management & Engineering Series.

Montgomery DC and Runger GC. 2014. **Applied Statistics and Probability for Engineers 6th Edition**. Wiley.

Nilson RH, Peterson EW, Lie KH, Burkhard NR, and Hearst JR. 1991. **Atmospheric Pumping: A mechanism Causing Vertical Transport of Contaminated Gasses through Fractured Permeable Media**. Journal of Geophysical Research. (96): 933-948.

Pezeshki SR, Pardue JH, and Delaune RD. 1993. **The Influence of Soil Oxygen Deficiency on Alcohol Dehydrogenase Activity, Root Porosity, Ethylene Production and Photosynthesis in Spartina Patens.** Environmental and Experimental Botany. (33): 565-573.

Poulsen T, Christophersen M, Moldrup P, and Kjeldsen P. 2003. **Relating Landfill Gas Emissions to Atmospheric Pressure using Numerical Modelling and State-space Analysis**. Waste Management and Research. (21): 356-366. DOI: 10.1177/0734242X0302100408.

Redecker KR, Baird AJ, and The YA. 2015. **Quantifying Wind and Pressure Effects on Trace Gas Fluxes across the Soil-Atmosphere Interface**. Biogeosciences. (12): 7423-7434. DOI: 10.5194/bg-12-7423-2015

Risk D, Kellman L, and Beltrami H. 2002. **Carbon Dioxide in Soil Profiles: Production and Temperature Dependence**. Geophysical Research Letters. (29) DOI: 10.1029/2001GL014002

Salminen JM, Tuomi PM, Suortti A-M, and Jorgensen KS. 2004. **Potential for Aerobic and Anaerobic Biodegradation of Petroleum Hydrocarbons in Boreal Subsurface**. Biodegradation. (15): 29-39. DOI: 10.1023/B:BIOD.0000009954.21526.e8

Scanlon, B.R. et al. 2002. **Soil Physics Companion: Soil Gas Movement in Unsaturated Systems**. CRC Press, pp 297-341.

Sihota NJ, Singurindy O, Mayer KU. 2011. **CO2-efflux measurements for evaluating source zone natural attenuation rates in a petroleum hydrocarbon contaminated aquifer**. Environmental Science and Technology. (45): 482–488. DOI: 10.1021/es1032585.

Thorstenson DC and Pollock DW. 1989. **Gas Transport in Unsaturated Zones: Multicomponent Systems and the Adequacy of Fick's Laws**. Water Resources Research. (25): 477-507. DOI: 10.1029/WR025i003p00477

Van Rees KCJ. 1997. **Rooting patterns of boreal tree species**. Prince Albert Model Forest vaAssociation, Inc. Prince Albert, SK.

Voudrias EA and Chiayang L. 1992. **Importance of Knudsen Diffusion on Benzene Vapor Transport in Unsaturated Soil**. Chemosphere. (25): 651-663. DOI: 10.1016/0045-6535(92)90428-T

Whitton BA, Chan GYS, and Wong MH. 1991. **Effects of Landfill Gas on Subtropical Woody Plants**. Environmental Management. 15(3): 411-431.

Wong MH. 1988. **Soil and plant characteristics of landfill sites near Merseyside, England**. Environmental Management. (12): 491-499

Young A. 1990. **Volumetric Changes in Landfill Gas Flux in Response to Variations in Atmospheric Pressure. Waste Management and Research**. (8) 379-385.

Zar JH. 1999. **Biostatistical Analysis**. Prentice-Hall, Upper Saddle River, NJ, USA.

2.0 DEGRADATION AND MOBILITY OF PETROLEUM HYDROCARBONS IN OILSANDS WASTE

Preface

This manuscript was prepared by K. Scale based on the raw data collected in the field and laboratory by T. Korbas for his M.Sc. (2014). It should be noted that while much of the basic data collection had been completed by T. Korbas, additional calculations, modelling, and analyses were carried out by K. Scale as part of the preparation of this manuscript. This chapter, while not wholly the work of K. Scale, represents a starting point for much of the work independently completed by K. Scale as presented in the subsequent chapters.

Massive above-grade lean oil sands (LOS) overburden landforms will be a permanent feature of reclaimed landscapes in the Alberta oilsands. This manuscript focuses on characterizing the degradation and mobility of petroleum hydrocarbons within the LOS. In the field, pore-gas O_2, CO_2, and CH_4 concentrations within the uncovered LOS landform were measured in single-point probes using a repurposed landfill gas analyser; CO_2 effluxes from the LOS were measured using static flux chambers. In the laboratory, PHC fractions, degradation rates, and CO_2 flux rates were characterized for the LOS. This research helps to develop a baseline for the concentrations of pore-gasses and rates of CO_2 efflux from the uncovered LOS landform.

Reference: Scale KO, Korbas TK and Fleming IR. 2016. **Degradation and Mobility of Petroleum Hydrocarbons in Oil Sand Waste.** Environmental Geotechnics, DOI: 10.1680/jenge.15.00035

Abstract

In Northern Alberta, Canada, large volumes of low-grade “lean” oil sands (LOS) overburden are translocated during the surface mining of oil sands and remain in future reclaimed landscapes. The objectives addressed in this paper are to (1) characterise in-situ petroleum hydrocarbon (PHC) content of LOS; (2) evaluate the effect of LOS temperature on rates of CO_2 flux and PHC biodegradation; and (3) evaluate the potential for PHC to leach from LOS into groundwater. Results show that LOS is predominantly composed of heavier F3 and F4 PHC fractions,

temperature appears to affect CO_2 fluxes and PHC degradation rates, and it is unlikely that the presence of LOS in reclamation soils will release significant quantities of PHC into groundwater.

2.1 Introduction

Massive quantities of “lean” oil sands (LOS) overburden consisting of ≤7% petroleum hydrocarbons (PHC) are trans-located during the surface mining of oil sands in Alberta, Canada to access underlying deposits of bitumen-rich ore (CEMA 2011). Surface mining is the primary extraction method for shallower (<75 m) oil sand deposits and involves the complete removal of inter-connected (upland) boreal forest ecosystems and (lowland) wetland ecosystems. Land reclamation programs are enforced by the Alberta Environmental Protection and Enhancement Act (Alberta Government 2007) to return areas disturbed by mining to a land capability similar to what existed prior to disturbance.

In practice, oil sands are excavated in active mining zones and hauled to extraction facilities where they are processed to extract bitumen for upgrading to useable petroleum products. The remaining material, LOS, is uneconomical to process and is placed in large capacity LOS landforms. There are concerns regarding the risks to ecological receptors arising from the fate and transport of the bituminous substrate that remains in the reclaimed landscape.

The Fort Hills LOS disposal area at Syncrude Canada Limited’s (SCL) Aurora North mine spans more than 1000 hectare with a maximum height of 100 m and final capacity of ~615 Mm^3. Within the Fort Hills LOS disposal area, 36 hectare was designated for the purpose of conducting reclamation research, including surface landform grading of the LOS, placement of various configurations of soil cover, and planting of native tree species of differing stocking densities. This study, termed the “Aurora soil capping study” (ASCS), is a multi-disciplinary and collaborative effort to evaluate the efficacy of various soil cover designs placed over LOS in order to re-establish a self-sustaining native boreal forest ecosystem with tree species of the local region. The location of the ASCS within SCL’s Aurora North mine is depicted in Figure 2.1.

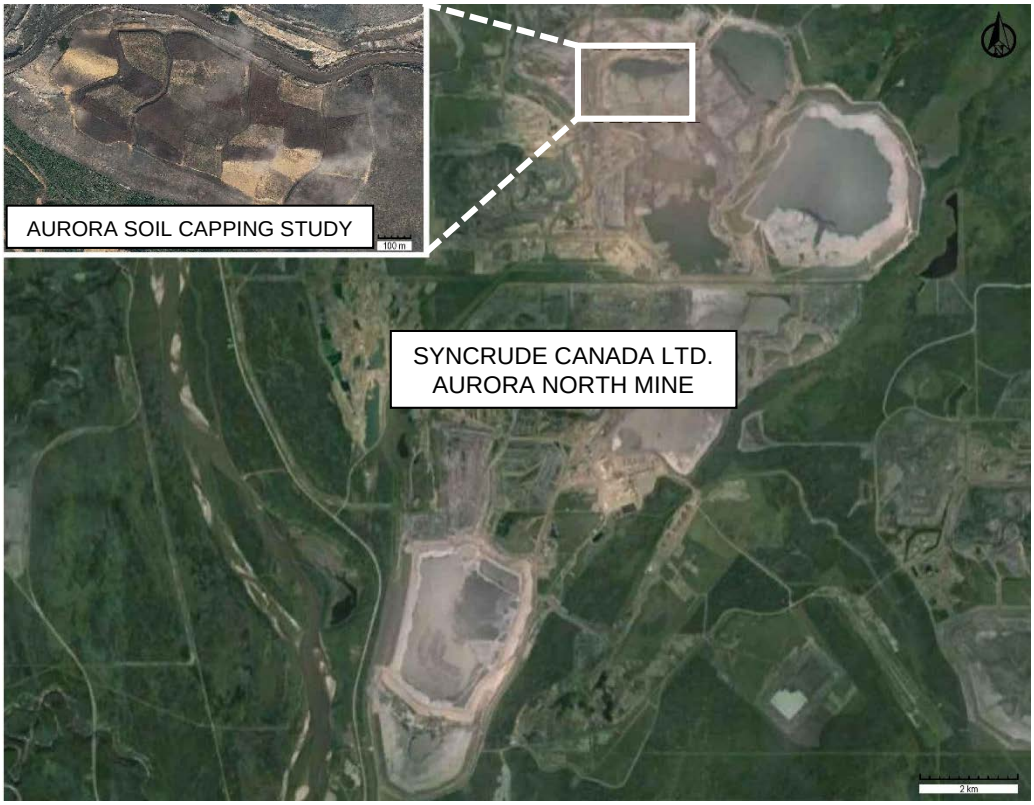

Figure 2.1 Syncrude Canada Limited's Aurora North Mine (right) Location of the Aurora Soil Capping Study within the Aurora North Mine (inlet left)

As part of this larger research effort, the main objectives described in this study are to i) characterise pore-gasses within the LOS overburden landform; ii) quantify rates of CO_2 efflux and PHC biodegradation over a range of temperatures; iii) characterise in-situ petroleum hydrocarbon (PHC) content of LOS material and leachate; and iv) evaluate potential for PHC mobilized from LOS leachate to enter groundwater.

Part I – Field study

The field portion of this study involves i) estimating CO_2 effluxes from LOS using the static flux chamber (SFC) method and ii) measuring gas concentrations at various depths below the surface of a LOS deposit.

2.2 Materials and methodology

2.2.1 Flux chambers

Gas efflux from the LOS into the soil covers may pose a risk to the growth and survivability of reclamation vegetation as a result of the accumulation of pore-gas CO_2 and consequent depletion/ displacement of pore-gas O_2 (Chan 1997; Trotter and Cooke 2005).

To measure CO_2 efflux from the LOS to the atmosphere, custom-fabricated circular gas flux chambers were temporarily installed on 16 discrete locations at the ASCS prior to placement of soil covers. The test locations were selected to be representative of the 36 ha surface area of the Fort Hills LOS disposal area. SFC measurements were taken during successive field trips before placement of reclamation soil material and re-vegetation planting in order to evaluate the repeatability of collected data and sensitivity of gas flux to temperature and moisture content.

Each gas flux chamber consisted of two parts: a lower part (the ring) and upper part (cap). The diameter of the upper and lower parts was 0.70 m. The heights of the rings and caps were 0.20 m and 0.15 m, respectively. Prior to conducting measurements, the lower ring was installed in the surface to a depth of 0.04-0.08 m (depending on the soil's hardness) and sealed around the edges with bentonite clay. The circular gas flux chamber is illustrated in Figure 2.2.

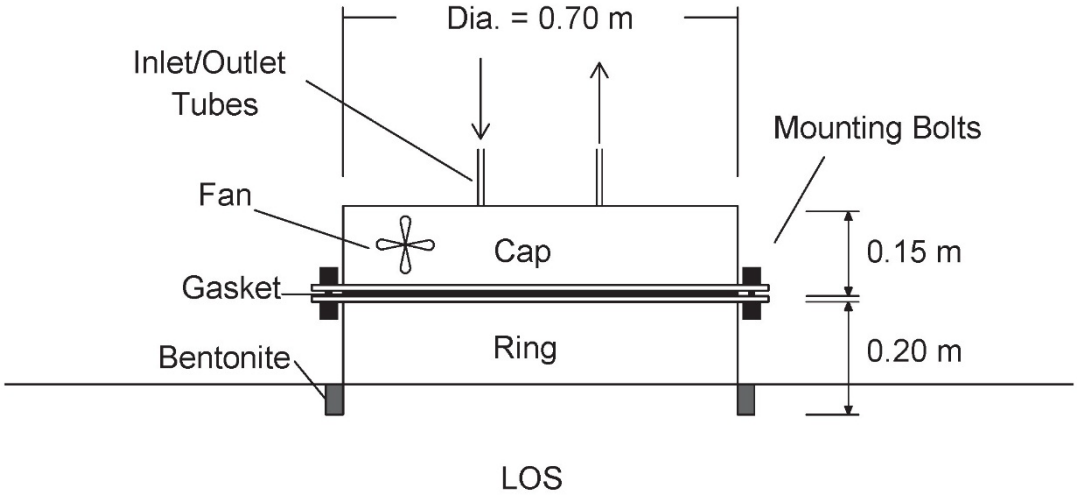

Figure 2.2 Illustration of custom-fabricated static flux chamber field setup

A minimum of 1 day after installation, the upper cap was placed on the ring and the flanges and gasket were tightened to ensure a tight seal. Two tubes, one for inlet and one for outlet, were attached to the top of the chamber. The outlet tube was connected to the Fourier-transform infrared (FTIR) and oxygen sensor, whereupon data was collected on a portable laptop computer.

Before each sampling event, the chamber headspace was purged with 99.998% purity compressed nitrogen (N_2) gas. Gas concentrations in the SFC headspace were measured using a GasTec DX4015® field portable FTIR system in line with a Varsalla paramagnetic O_2 sensor. The equipment was connected to a computer that enabled data to be measured and recorded at pre-determined 1 and 2 minute time intervals. Changes in CO_2 concentrations within the chamber headspace over time at each location were collected on three separate occasions in order to investigate spatial/ temporal variability and the repeatability of collected data. No physical calibration was required in the field; however, the FTIR was purged with N_2 gas prior to each sampling event.

The rate of gas flux at each location was estimated based on the measured CO_2 concentrations and the known dimensions of the SFC using Equation 2.1:

$$F_{CO2} = \frac{V_C}{A_C}\frac{\Delta C_i}{\Delta t} \quad [2.1]$$

Where F_i is the mass flux of a gaseous species into the closed chamber [$ML^{-2}T^{-1}$], V_c is the volume of the chamber headspace [L^3], A_c is the area enclosed by the chamber [L^2], and $\Delta C_i/\Delta t$ is the concentration change of the gaseous species in the headspace over a time interval [$ML^{-3}T^{-1}$].

2.2.2 Soil vapour probes

Soil vapour probes were installed at various depths in the uncovered LOS overburden landform. The soil vapour probe system consists of a drive-point gas vapour tip connected to plastic tubing driven into the ground using specially constructed rods (AMS sampling system and Gas Vapour Probe Kit®). The metal rods are then removed, thus leaving the gas vapour probe tip embedded in the LOS at the desired depth below ground surface. The holes were backfilled with bentonite clay to seal out atmospheric gasses. Approximately 1 m of tubing was left above the ground surface to allow for future sampling. Thirty-one soil vapour probes were successfully installed at 13 locations across the site at depths ranging from 0.5-7.5 m below ground surface during 3 site visits in 2010 and 2011.

Partial pressures of and O_2, CO_2 and CH_4 were monitored using LandTEC Gem 2000® (NDIR/ paramagnetic) field portable gas analyser. Measurements were conducted the following day after installation and at several times afterwards to ensure repeatability of the data. The GEM 2000® was physically calibrated with high-purity O_2, CO_2 and CH_4 calibration gasses daily during field sampling events. Gas bottles used for calibration include 1% CH_4, 4% O_2, and a mixture of 50% CH_4/ 35% CO_2, all with a balance of undetectable nitrogen (N_2) gas.

2.3 Results

2.3.1 Flux chambers

In October 2010, the average air temperatures fluctuated between 6-10˚C, with temperatures as low as 0˚C measured by the end of the sampling event. In July 2011, the site conditions appeared wetter due to recent multi-day precipitation events, while the daytime air temperatures ranged from 20-30°C. In September 2011, the site conditions appeared dry due to lack of precipitation during the previous 3 to 4 weeks, while daily air temperatures ranged from 15-25°C. Note that field samples of the LOS were not obtained, so it was not possible to quantify soil water contents on site. However, it is expected that restrictions in air porosity at higher water contents will lead to reductions in gas flux.

CO_2 flux rates calculated using Equation 2.1 averaged between 0.1-0.4 kg/m^2/a in October 2010 with peaks of 0.8-1.1 kg/m^2/a. In July 2011, CO_2 flux rates averaged between 0.1-1.2 kg/m^2/a with a peak of 7.1 kg/m^2/a. In September 2011, estimated CO_2 flux rates averaged between 0.4-1.5 kg/m^2/a with a peak of 2.3 kg/m^2/a.

The high CO_2 flux rate of 7.1 kg/m^2/a measured in July 2011 was associated with an area of relatively loose sand (compared to more compact, finer-textured LOS material with increased bitumen at the surface across most of the site). This area may have represented a zone of high air permeability and preferential flow.

Low CO_2 flux rates were estimated in July 2011 at two locations that appeared to correspond to higher levels of soil saturation caused by heavy rainfall events. An example of this is that in September 2011 the CO_2 flux rate was 1.5 kg/m^2/a during relatively dryer conditions; however,

the CO_2 flux rate was only 0.1 mg/m^2/h in July 2011 at the same location during relatively wetter conditions.

The summary of CO_2 flux results from the three site visits is presented in Table 2.1. Tabulated values represent the averaged CO_2 flux rates from repeated testing using the SFC method. Note that it was not possible to sample each location during each visit.

Table 2.1 Summary of gas flux measurements recorded during three site visits

Sampling Period	CO_2 fluxes [kg/m^2/a]
October, 2010	0.1 – 1.1
July, 2011	0.1 – 7.1
September, 2011	0.4 – 2.3

Concentrations of trace gasses other than carbon dioxide (CO_2) were monitored in the SFC headspace. Methane (CH_4) was present at low and steady concentrations that fluctuated between 2.5-4 ppm. Other trace gasses such as nitrous oxide (N_2O), ammonia (NH_3), sulphur dioxide (SO_2), nitrogen dioxide (NO_2), ethylene (C_2H_4) and carbon disulfide (CS_2) were found at very low concentrations (≤1 ppm) or could not be detected at all at some locations.

2.3.2 Soil vapour probes

Installation of soil vapour probes was difficult in dense clays and several installations were found clogged on subsequent visits. Clogging is presumed to result from bitumen and/or clay moving in and sealing the gas vapour vents. Furthermore, several probes have drawn water in measureable quantities, indicating zones of perched shallow groundwater conditions below the surface.

Soil vapour concentrations measured during the three sites visits in 2010 and 2011 typically ranged from 0-18% for O_2, CO_2 ranged from 3-21%, and CH_4 ranged from 0-12%.

2.3.3 Purge tests

Due to the unique design of the surface and buried flux chambers, it was not possible to conduct standard closed chamber tests, which involve enclosing a volume of air and measuring the accumulation of gasses within that volume over an incremental time period.

Instead, the chamber headspaces were purged with N_2, while a vent was left open to the atmosphere to prevent pressure build up inside the headspace. Headspace gasses were periodically sampled during purging, which was deemed complete after repeated non-detect measurements of O_2, CO_2, and CH_4.

During testing, headspace gasses were pumped in a continuous loop through the analysers and returned to the chamber headspace. This cycle was repeated for up to 10 channels, resulting in a sampling interval of roughly 10 minutes to 1 hour. By sampling in a continuous loop, sampling-induced pressure changes were largely avoided.

Part II – Laboratory study

The laboratory portion of this study involved i) characterizing the PHC content of LOS; ii) characterizing the composition of LOS leachate; iii) estimating rates of PHC biodegradation; and iv) measuring rates of CO_2 gas flux.

2.4 Materials and methodology

2.4.1 Soil columns

The LOS material used in the column study was collected from the ASCS site and delivered to the University of Saskatchewan. The LOS material was stored in a climate chamber at 4°C before being used to study the effects of PHC degradation.

Six custom-designed Teflon lined steel columns (0.3 m diameter and 1 m height) were manufactured at the University of Saskatchewan machine shops for the soil column experiment. To minimize potential sorption or catalytic effects in the columns, all interior surfaces were lined with Teflon or glass. Each column was designed to enable a glass access tube to run vertically down the centre of the column as shown in Figure 2.4. The purpose of the glass access tube was to provide access for a SenTek EnviroScan® soil moisture probe, which operates on the principle of frequency-domain reflectometry (Sentek Sensor Technologies, Australia).

Six soil columns were prepared using the methodology outlined in the following paragraph. The bottom of each column was filled with approximately 0.1 m of coarse silica sand (0.5-1

mm particle size) to create a capillary break within the LOS/overburden material. On top of the sand layer, approximately 0.6 m of LOS material was carefully placed in equal increments of 0.01 m and compacted to dry densities ranging from 1.5-1.8 T/m^3. The remaining space (approximately 0.3 m) provided a headspace for monitoring volatilized gasses. On average, approximately 2.8 kg of hydrocarbons were placed in each column.

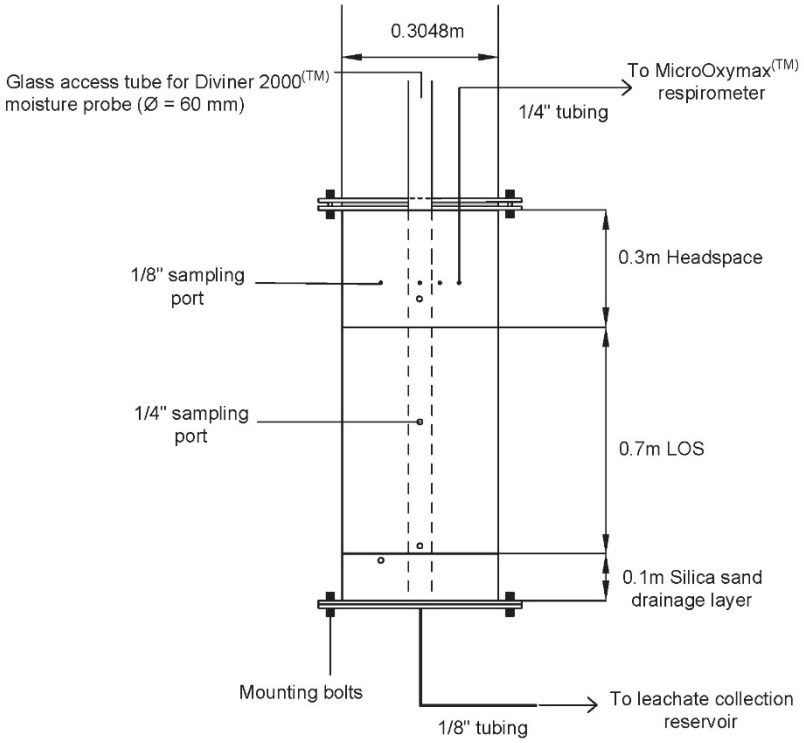

Figure 2.4 Illustration of cross-section of Teflon-lined steel soil column used in laboratory experiments

Special connections were made in the wall of each column in order to connect to the Micro-Oxymax® respirometer (Columbus Instruments, Columbus, OH, USA). The Micro-Oxymax® is an aerobic/anaerobic respiratory system that continuously measures changes in concentrations of CO_2, O_2 and CH_4 in the headspace as a surrogate of microbial activity.

In the column study, each individual test was carried out in triplicate to ensure the accuracy and repeatability of the collected data. Three columns were set up at room temperature (22° C), while another three columns were set up in the climate chamber at varying cooler temperatures (from 2°C-14°C) for a period of several weeks.

2.4.2 Particle-size distribution

Grain size distributions were performed on a total of 12 samples of LOS (two from each column) in order to determine the average particle size distribution for the material in the columns. The American Society for Testing of Materials (ASTM) D2422-63 “Standard Test Method for Particle-Size Analysis of Soils” method was used for each of the 12 samples (ASTM 2007).

2.4.3 Leachate composition

The columns were operated under unsaturated conditions using a low-flow peristaltic pump to supply demineralized water in order to replicate field conditions. The amount of water provided daily to each column was determined to be 30 mL added 3 times per day based on an average annual precipitation for Fort McMurray (460 mm/year).

The daily addition of water to the columns resulted in the production of leachate. Leachate was collected from a reservoir at the bottom of each column on a weekly basis and analysed for TC (total carbon) and TOC (total organic carbon). All carbon analyses in water samples were conducted on the Tekmar-Dohrman Phoenix 8000® UV/persulphate gas chromatograph.

Along with TC/TOC analyses, every three weeks a small sample of leachate was collected and sent to Exova analytical laboratories in Calgary, Alberta for analysis of BTEX, F1, F2 and F3 hydrocarbons with the CCME Tier-1 method (2008) for petroleum hydrocarbons (PHC) in soil using an Agilent 7890 gas chromatograph (GC) system that included a CompiPal system to conduct simultaneous flame ionization (FID) detection and mass spectrometry.

Furthermore, a sample of leachate was also sent to Exova labs to be tested for “oil and grease” in order to weigh all organic compounds, not just hydrocarbons. Oil and grease was tested using the United States Environmental Protection Agency (USEPA) partition-gravimetric method, which uses liquid-liquid extraction with normal hexane as the extraction solvent (USEPA 1999).

2.4.4 PHC characterization data

In Canada, PHC fractions are defined as follows (CCME 2008):

Table 2.2 Definition of hydrocarbon fractions

Fraction	Equivalent carbon number
F1	C6 to C10
F2	>C10 to C16
F3	>C16 to C34
F4	C34+

Lighter F1-F2 PHC fractions are of potentially more risk to the environment than heavier F3-F4 because they are generally more soluble, mobile, and bioavailable. When considered in terms of fate and transport, the less mobile, heavier hydrocarbon fractions tend to degrade slower and be more persistent in the environment. The more mobile and soluble lighter fractions, however, can potentially be transported in pore water and impact ecological receptors further from the source (CCME 2010).

In total, 60 soil samples were collected from all six experimental columns and analyzed for PHC content according to the CCME (2008) Tier-1 method for "Canada-wide standards for petroleum hydrocarbons (PHC) in soil." Visser (2008) and Fleming (2012) also used the CCME (2008) Tier-1 method to evaluate the PHC contents of LOS and conglomerated masses of bitumen known as "tarballs," respectively. Visser's (2008) results were that the PHC content of LOS is comprised mainly of F2-F4 fractions: 0.15% F1, 8.6% F2, 37.7% F3, and 53.8% F4. Fleming's (2012) results were that the PHC content of tarballs were primarily comprised heavier F3 and F4 fractions: 0.01% F1, 0.09% F2, 4.07% F3, and 95.8% F4.

2.4.5 PHC biodegradation

During aerobic biodegradation, oxygen is consumed by microorganisms in order to degrade hydrocarbons into simpler organic compounds and eventually reduce them to compounds such as carbon dioxide and water. The relationship presented in Equation 2.2 below was used by Zytner et al. (2001) to provide a simplified stoichiometric equation for the complete biodegradation of a diesel molecule by microbial activity:

$$C_{16}H_{34} + 24.5O_2 \rightarrow 17H_2O + 16CO_2 \qquad [2.2]$$

Estimated PHC degradation was determined by applying Zytner's relationship to CO_2 production; this includes the total cumulative CO_2 produced by respiration and the total concentration of dissolved CO_2 that was monitored in leachate over the course of this study. Calculations for CO_2 dissolved in water were based on i) regular monitoring of volume of leachate removed from system; measured values of TIC (Total Inorganic Carbon), which was converted to a mass of total dissolved CO_2 using the relationship $C + O_2 \rightarrow CO_2$; and $CO_{2(g)} + H_2O \rightarrow CO_{2(l)}$, which forms carbonic acid H_2CO_3. At measured pH values of 6.8, H_2CO_3 dissociates to bicarbonate HCO_3^- ion only; therefore, CO_2 dissolved in the leachate will be present mostly as bicarbonates and free CO_2 as equivalent of H_2CO_3 (Snoeyink and Jenkins 1980).

2.4.6 Volatile hydrocarbons

The LOS material used in the experiment contained a significant amount of PHCs and their volatiles. Accordingly, an activated charcoal trap (Orbo 302® charcoal sorbent tube) was used to collect volatiles and prevent the Micro-Oxymax® gas sensors from being damaged (Micro-Oxymax® user's manual). At the end of the study, one such charcoal tube that had collected volatilized gasses for 5 months was eluted for analysis of volatile PHCs.

2.4.7 CO_2 flux rates

Based on the cumulative slopes of CO_2 production, the long-term gas fluxes for each column were estimated for various temperatures. The individual CO_2 gas fluxes were estimated based on calculations using best fit linear regression applied to the cumulative slopes of the CO_2 production at various temperatures.

2.5 Results

2.5.1 Particle-size distribution

The average particle size distribution curve is shown in Figure 2.5 and represents the sandy loam type of soil according to the USCS soil classification. In general, LOS contained approximately 10% clay, 35% silt and 55% sand. These values were relatively consistent

between all 6 columns. However, in a field scenario the ratio between sand and fines may be different due to the variability of the material.

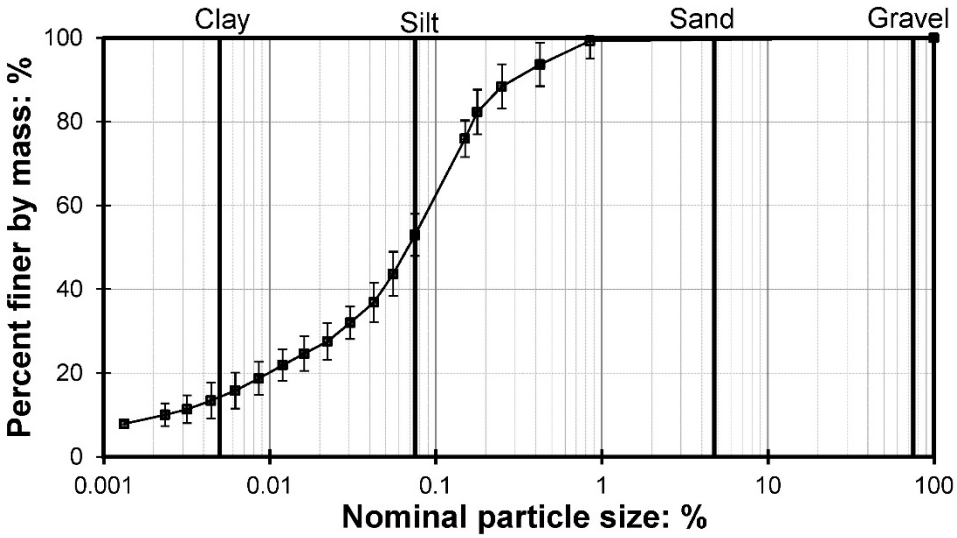

Figure 2.3 Particle-size distribution curve for LOS tested in the laboratory based on the average of 12 samples

2.5.2 Leachate composition

The water analyses for chromatographable PHCs measured a small amount of F2 and F3 fractions in the leachate, but did not detect F1 or BTEX fractions. The hydrocarbon content in the leachate is shown separately in Figure 2.6 for the two sets of column experiments (columns 1-3 and 4-6).

For the columns 1-3 at room temperature (23°C), concentrations of F2 hydrocarbons decreased over time from an average across all columns of 0.97 mg/L to 0.27 mg/L and concentrations of F3 hydrocarbons remained stable with an average across all columns of 0.6 mg/L to 0.5 mg/L from July 6, 2012 when the experiment began to October 16, 2012 when the experiment ended. For the columns in the 4°C climate chamber (columns 4-6), concentrations of F2 hydrocarbons increased from an average across all columns of 0.1 mg/L to 0.2 mg/L and concentrations of F3 hydrocarbons increased from an average across all columns of 0.2 mg/L to 0.4 mg/L from September 6, 2012 when the experiment began to October 16, 2012 when the experiment ended. Moreover, at the end of the experiment F2 and F3 concentrations spiked in a relatively short time due to the temperature in climate chamber increasing from 4°C to 9˚C. F2 concentrations averaged across all columns increased from 0.4 mg/L to 0.6

mg/L and F3 concentrations averaged across all columns increased from 0.4 mg/L to 0.7 mg/L from October 16, 2012 to November 13, 2012. Peak F2 and F3 concentrations for columns at 23°C were 2.2 mg/L and 1.2 mg/L, respectively, both measured at the beginning of the experiment on July 6, 2012. Peak F2 and F3 concentrations for columns at 4°C were lower at 0.6 mg/L and 0.7 mg/L, respectively, both measured at the end of the experiment on November 13, 2012.

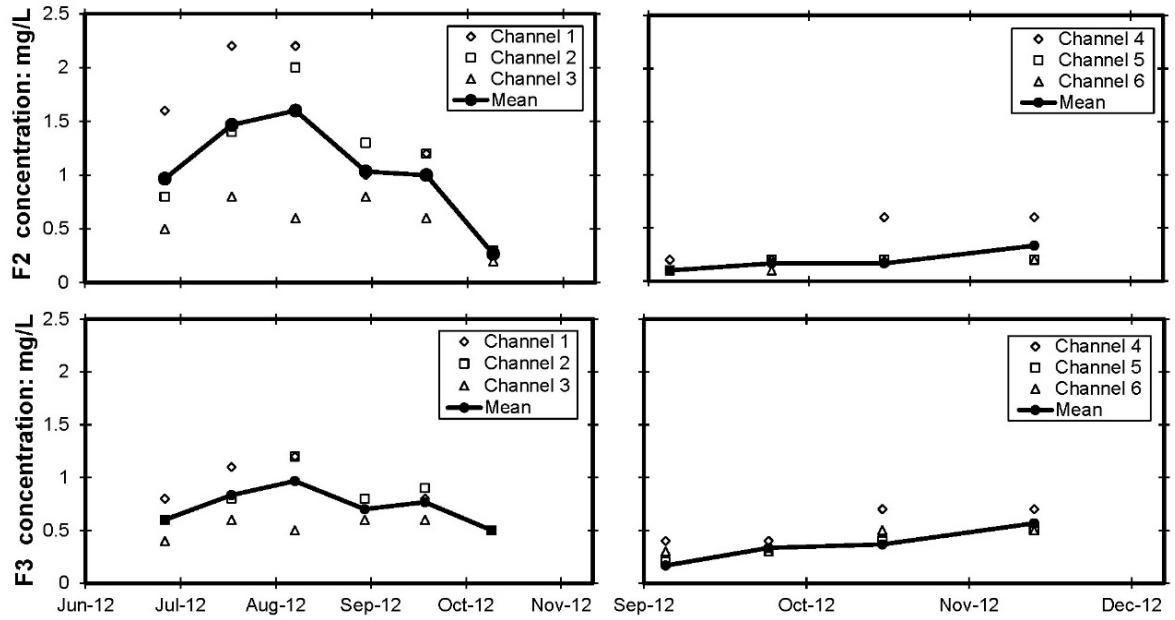

Figure 2.4 F2 and F3 concentrations in leachate for soil columns at room-temperature from June 5 to Sept 16, 2012. F2 and F3 concentrations in leachate for soil columns in the climate chamber from Sept 6 to Nov 13, 2012

The results from oil and grease tests revealed the presence of some BTEX and light diesel (most abundant at ~C20). There were also some indications of heavier materials not detected by the chromatogramph. The total average concentration of oil and grease in the leachate was 49 mg/L.

The results suggested that other organic compounds may be present in the leachate at increased concentrations. Accordingly, additional leachate analyses test were conducted at Environment Canada for the presence of organic acids known as the Naphthenic acid fraction

component (NAFC) and other acid-extractables. These tests revealed the presence of a NAFC's at concentrations averaging approximately 150 mg/L.

Monitoring of TC and TOC was conducted in order to estimate the mobility and quantity of organic/inorganic material in the leachate. As seen in Figure 2.7, the concentrations of TC and TOC decreased over time. The organic carbon concentrations measured in the leachate analysis were several orders of magnitude higher than the reported concentration of chromatographable PHCs presented earlier in Figure 2.6.

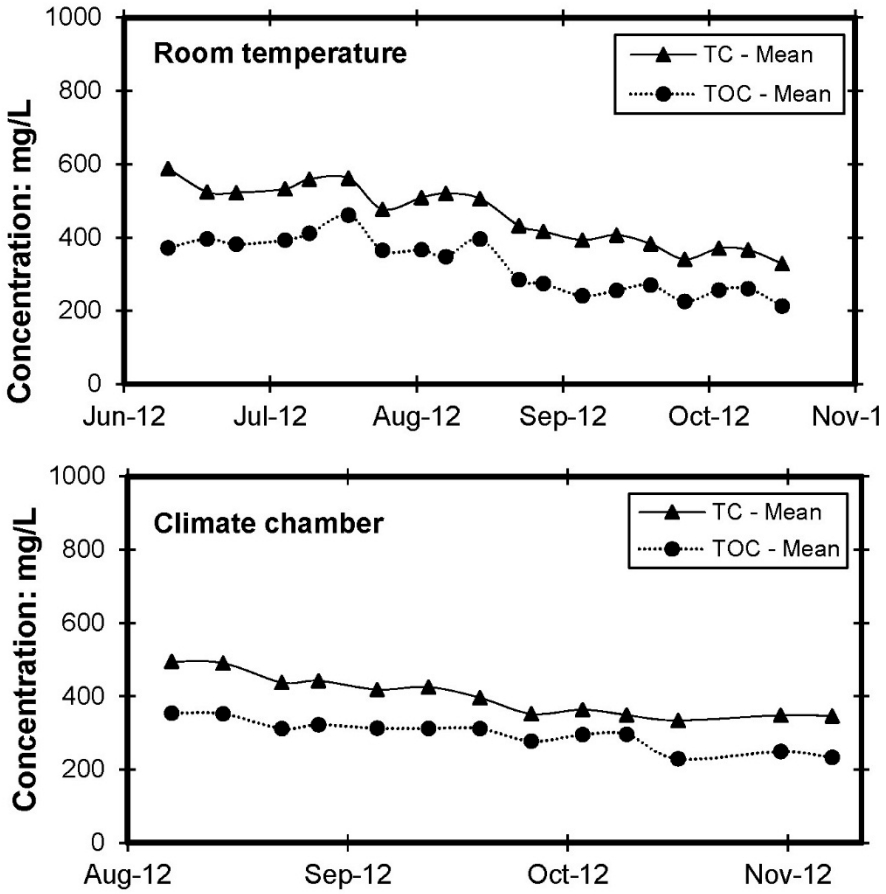

Figure 2.7 Total Carbon and Total Organic Carbon in leachate for columns at room-temperature and in climate chamber

2.5.3 PHC characterization

The characterization of the PHC content of the LOS was similar to the PHC content determined in Visser (2008). Results showed that LOS is comprised mostly of high molecular weight and not readily degradable F3 (47%) and F4 (45%) hydrocarbons. The remaining PHC fractions present in the LOS contained small amounts of volatile and easily degraded F1

(0.1%; excluding undetectable BTEX) and F2 (8.3%) hydrocarbons. The detailed summary of collected data is presented in Table 2.3. Note that samples from columns 1-3 and columns 4-6 were evaluated at different times and are presented in separate columns accordingly.

Table 2.3 Summary of PHC data for all columns

PHC Fraction	Units	Columns 1-3		Columns 4-6	
		Mean	STDEV[#]	Mean	STDEV
BTEX	mg/kg	non-detect	N/A	non-detect	N/A
F1 C6-C10	mg/kg	40	20	30	10
F2 C10-C16	mg/kg	2,900	800	1,700	400
F3 C16-C34	mg/kg	16,300	5,700	9,400	1,800
F4HTGC C34-50+	mg/kg	15,500	6,700	9,300	2,200
F4G	mg/kg	53,300	15,000	23,400	3,700

The analytical results for PHC content of the LOS are presented relative to the results from Visser's (2008) study on LOS and Fleming's (2012) study on LOS inclusions in soil reclamation material (Figure 2.8).

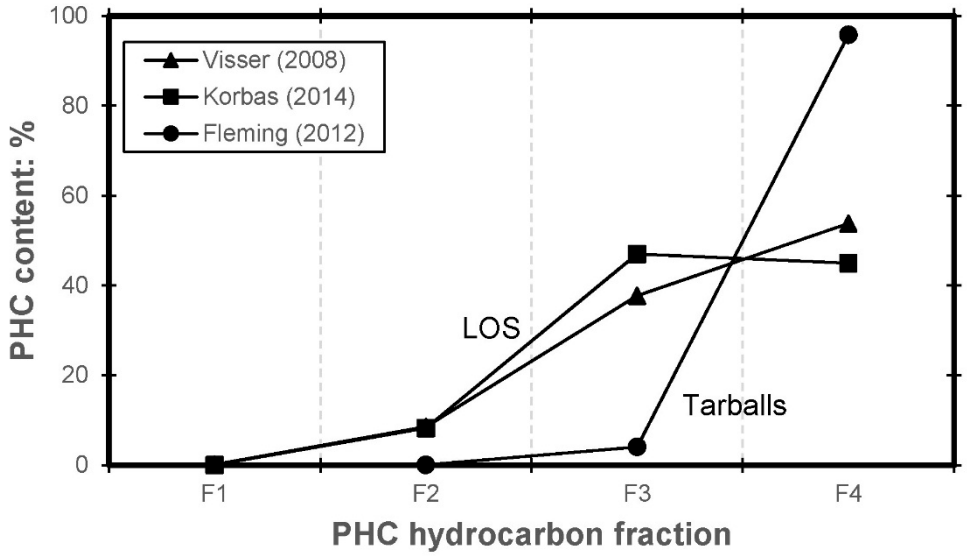

Figure 2.8 PHC content for LOS and tarball materials present in soil covers during the reclamation of boreal forest ecosystems

2.5.4 PHC biodegradation

The Micro-Oxymax® respiratory system continuously monitored changes in O_2, CO_2 and CH_4 gas concentrations in the headspace of the steel columns. Oxygen consumption and carbon dioxide production were monitored as a surrogate for microbial activity.

Cumulative data collected by the Micro-Oxymax® represents the total amount of gas expressed in (L) or (mg) that has been produced or consumed (expressed as negative values) since the beginning of the experiment. The average cumulative CO_2 production and O_2 consumption for the columns at room temperature (22˚C) over period of 196 days were approximately 47 L and 93 L, respectively. The total cumulative average CO_2 production and O_2 consumption for the columns in the climate chambers (at temperatures between 2 and 14˚C) over period of 168 days were approximately 8.8 L and 21.6 L, respectively. The cumulative consumption of O_2 and production of CO_2 for all columns are presented in Figures 2.9.

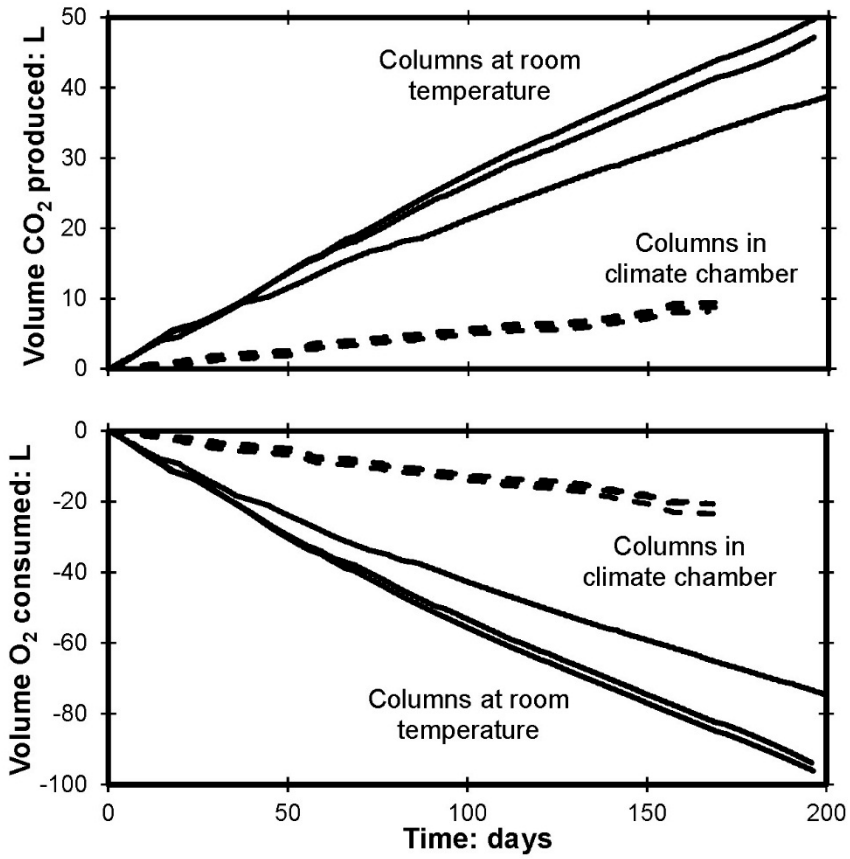

Figure 2.9 Total cumulative O_2 consumption and CO_2 production measured during laboratory study using MicroOxymax® respirometer

For columns at room temperature (22ºC) for 196 days, the total average amount of CO_2 produced by microbial activity was estimated to be approximately 100 g as a result of the degradation of 22 g of PHC. For columns running at cooler temperatures (2-14°C) for 196 days, the total average amount of CO_2 produced by microbial activity was estimated to be

approximately 32 g as a result of the degradation of 7 g of PHC. The total estimated PHC degradation from respiration was 60 g/year and 15 g/year at room temperature and cooler temperatures, respectively. Methane production was found to be very low and was representing a very small fraction (0.1%) of total CO_2 production. It was therefore concluded the experiments were running primarily in an aerobic environment as planned.

2.5.5 Volatile hydrocarbons

Results from the elution of the activated charcoal trap are shown in Table 2.4. Results indicated the presence of hydrocarbons on the downstream module of the two-module trap, suggesting that the tube may have been overloaded. Accordingly, the mass of hydrocarbons reported in Table 4 underestimate, by an unknown margin, the true mass volatilized. The relative mass of volatilized PHC of the various fractions may provide some insight into the sort of PHC's that may partition to the gas phase under field conditions. The entire mass of PHC collected in the tube was 131 mg, of which 123 mg was within the lighter part of the F2 fraction (up to C20), reflecting the limitation of the GC instrument used which could only quantify up to C20; therefore, the F3 fraction content only represents PHCs between C16 to C20.

Table 2.4 BTEX and total hydrocarbons in the charcoal tube for CH2

Analyte	Mass volatiles [mg]
BTEX	0.093
F0 (C4-C6)	0.025
F1 (C6-C10)	5.8
F2 (C10-C16)	122.8
F3 (C16-C20)	2.4
Sum	**131.2**

2.5.6 CO_2 flux rates

The average cumulative CO_2 production at various climate chamber temperatures was estimated by calculating the CO_2 production rate for each incremental change in LOS temperature. The results of these estimates are presented in Figure 2.10 and show a linear relationship between CO_2 gas fluxes and LOS temperature.

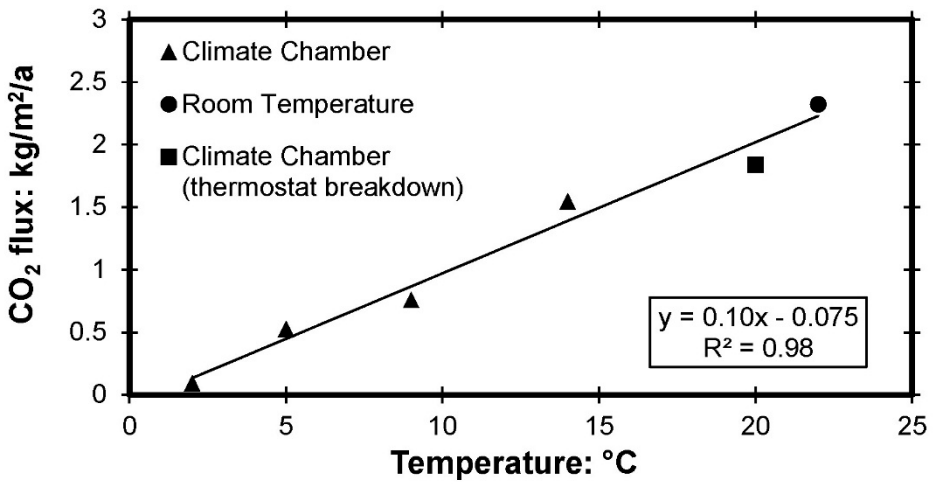

Figure 2.10 Relationship between LOS temperature and CO_2 gas flux rates for all columns

2.6 Discussion and conclusions

Surficial CO_2 flux measurements were taken at 16 locations across ASCS on three separate occasions. Temperature was observed to have an effect on the rate of PHC degradation as indicated by variations in gas fluxes at different times of the year. It was also observed that higher levels of soil moisture caused by rainfall events may have temporarily reduced CO_2 flux rates.

The results show that gas flux rates in the field varied spatially and temporally. Occasionally, elevated concentrations in the soil of up to 21% CO_2 and up to 12% CH_4 were detected. It is hypothesized that high CO_2 and CH_4 pore-gas concentrations may have been caused by the presence of low-permeability layers of bitumen in the subsurface inhibiting free flow of gas to the surface. This would explain why elevated gas concentrations were measured below these layers.

High concentrations of CO_2 and CH_4 at these depths in the soil may have some negative impact on plant growth. For example, CH_4 entering a well-aerated cover soil at concentrations greater than 10% can potentially consume all oxygen in the soil atmosphere due to the stoichiometry of methane oxidation ($CH_4 + 2O_2 \rightarrow CO_2 + 2H_2O$). Furthermore, O_2 concentrations less than 10% may be detrimental to tree and root growth as a result of insufficient energy being available to perform essential root function and mineral uptake (Kozlowski 1985). CO_2 concentrations greater than 15-20%, meanwhile, can potentially

impact nutrient and water absorption and be lethal to plants (Chang and Loomis 1955; Whitton 1991).

The LOS/overburden material collected from ASCS and used in the column study contained PHC's predominantly composed of F3 (47%) and F4 (45%) hydrocarbon fractions (i.e. heavy molecular hydrocarbons that are not readily degradable). The remaining PHC fractions present in the LOS contained small amounts of volatile and more easily degraded F1 (0.1% excluding undetectable BTEX) and F2 (8.3%).

The results from the PHC mobility study suggest that the LOS material will likely have a low environmental impact to surface or groundwater quality. The F1 fraction (including BTEX) was not detected in the column leachate. The F2 fraction slightly exceeded clean water guidelines on a few occasions at temperatures ≥ 22°C. At low temperatures, ≤ 4°C, the concentration of F2 hydrocarbons was near the 0.1 mg/L detection limit. The F3 hydrocarbons were present at low concentrations, but are not regulated for groundwater. It should be noted that based on measurements made at the site, the LOS temperature beneath 0.3-1.5 m of reclamation cover ranged from 17°C to -7°C, with an average annual temperature of 4.2°C.

The results from the leachate analysis showed that organic carbon concentrations were several orders of magnitude higher than the reported concentrations of chromatographable hydrocarbons, which indicates the presence of other organic compounds. Additional tests conducted on leachate water revealed the presence of 49 mg/L concentrations of oil and grease and 150 mg/L of NAFC's and other acid extractables. Organic acids found in the leachate were complex and detailed quantification was not carried out for individual compounds in this study.

Based on soil respiration, the rate of biodegradation is apparently dependent on temperature as it is widely described in the literature (Atlas 1981; Leahy and Colwell 1990). The total estimated PHC degradation from respiration was 60 g/year at 22°C and 15 g/year at temperatures from 2 to 14°C. However, these amounts constitute only a small portion of the approximately 2.8 kg of hydrocarbons present in each column. Thus, the results indicate that

the degradation of hydrocarbons from LOS material is occurring at relatively slow rates. For comparison, Fleming at al. (2012) showed that degradation of PHC from naturally-occurring oil sand inclusions in native surface soils in the region, (as determined in soil column studies at 20°C) was on average 8.5 g/year, which is nearly half of the rate measured for LOS in this study. PHC volatilization at rates of 0.3 g/year was observed to be two orders of magnitude less than that of PHC degradation of LOS.

Controlling temperature during the experiments allowed the effects of temperature on PHC degradation and CO_2 production to be investigated. Temperature dependence became further evident during climate chamber failure when the temperature in the climate chamber abruptly increased from 4-23°C within 24 hr and resulted in a spike in gas flux rates. The estimated CO_2 flux rates showed a linear relationship between CO_2 gas fluxes and temperatures. The gas flux rates ranged from 0.1 kg/m^2/a at 2°C to 2.3 kg/m^2/a at 22°C. Interestingly, the gas flux results obtained under controlled steady lab conditions were comparable with the gas flux rates obtained in the field prior to placement of reclamation cover soil (while the LOS was exposed to atmospheric air temperatures). The CO_2 fluxes ranged from 0.1-1.5 kg/m^2/a with peaks of 2.3 and 7.1 kg/m^2/a. The results from the field and laboratory respiration studies were also relatively similar, indicating that the column study could be used to produce meaningful and low cost estimates of in situ PHC degradation.

Acknowledgements

Funding for this research was supported by CONRAD (Canadian Oilsands Network for Research and Development). We would like to thank staff at Syncrude Canada Ltd. in Edmonton, AB and Fort McMurray, AB for their assistance and accommodating this research.

References

Alberta Government. 2014. **Alberta Environmental Protection and Enhancement Act of 2007**. Alberta Queen's Printer, Edmonton, Alberta.

American Society for Testing and Materials (ASTM).2007. **D-422-63**: **Standard Test Method for Particle-Size Analysis of Soils**. ASTM. Philadelphia, Pa. DOI: 10.1520/D0422-63R07E02

Atlas RM. 1981. **Microbial Degradation of Petroleum Hydrocarbons: an Environmental Perspective**. Microbiological Reviews. 45(1): 180-209.

CCME (Canadian Council of Ministers of the Environment). 2008. **Canada-Wide Standards for Petroleum Hydrocarbons (PHCs) in Soil.** Available online at: http://www.ccme.ca/en/resources/canadian_environmental_quality_guidelines/ [Accessed January 16, 2016]

CCME (Canadian Council of Ministers of the Environment). 2010. **Canadian Soil Quality Guidelines for Protection of Environmental and Human Health.** http://www.ccme.ca/en/resources/canadian_environmental_quality_guidelines/ [Accessed January 16, 2016]

CEMA (Cumulative Environmental Management Association). 2011. **Best Management Practices for Conservation of Reclamation Materials in the Mineable Oil Sands Region of Alberta.**

Chang HT and Loomis WE. 1955. **Effect of carbon dioxide on absorption of water and nutrients by roots**. Plant Physiology 20(2): 155–161 DOI: http://dx.doi.org/10.1104/pp.20.2.221

Fleming M, Fleming I, Headley J, Du J, and Peru K. 2012. **Surficial bitumens in the Athabasca oil sands region, Alberta, Canada.** International Journal of Mining Reclamation & Environment. 26(2): 134-147. DOI: 10.1080/17480930.2011.570098

Fleming M. 2012. **Petroleum Hydrocarbon Content, Leaching and Degradation from Surficial Bitumens in the Athabasca Oil Sands Region***.* MSc Thesis. University of Saskatchewan, Saskatoon, Saskatchewan, Canada.

Kozlowski T. 1985. **Soil aeration, flooding, and tree growth**. Journal of Arboriculture 11(3): 85-95

Snoeyink, V and Jenkins D. 1980. **Water Chemistry**. Wiley.

USEPA (United States Environmental Protection Agency). 1999. **Method 1664, Revision A: N-Hexane Extractable Material (HEM; Oil and Grease) and Silica Gel Treated N-Hexane Extractable Material (SGT-HEM; Non-polar Material) By Extraction and Gravimetry***.* Washington, DC.

Visser S. 2008. **Petroleum Hydrocarbons (PHCs) in Lean Oil Sand (LOS): Degradation potential and toxicity to ecological receptors**. Technical report.

Whitton BA, Chan GYS and Wong MH. 1991. **Effects of Landfill Gas on Subtropical Woody Plants**. Environmental Management. **15(3)**: 411-431. DOI: 10.1007/BF02393888

Zytner RG, Salb A, Brook TR, Leunissen M, and Striver, WH. 2001. **Bioremediation of diesel fuel contaminated soil**. Canadian Journal of Civil Engineering. **28(1)**: 131-140.

3.0 PORE-GAS DYNAMICS IN OVERBURDEN AND RECLAMATION SOIL COVERS

Preface

Reclamation efforts using engineered soil covers depend on aeration of the rooting zone to freely allow O_2 ingress and CO_2/CH_4 effluxes. This manuscript focuses on characterizing pore-gas concentrations and quantifying gas flux rates in 8 composite single and multi-layer soil covers. Pore-gas O_2, CO_2, and CH_4 concentrations were measured in single-point probes using a repurposed landfill gas analyser. CO_2 effluxes from the cover soils were measured using surface static flux chambers. O_2 ingress into the cover soils and CO_2 efflux from the lean oil sands were measured using custom designed and fabricated subsurface static flux chambers. Relative contributions of advection & diffusion were calculated from soil gas profiles based on soil temperatures & soil moisture measured by O'Kane Consultants, air conductivity measured by Zettl et al (2013), and differential pressures measured herein. This research is fundamental to predicting the long-term success of reclamation efforts using engineered soil cover systems by providing insight into the pore-gas dynamics of the soil cover systems and lean oil sands.

Reference: Scale KO and Fleming

IR. 2017. **Pore-gasses Dynamics in Overburden and Reclamation Soil Covers.** Accepted June, 2017.

Pore-gas dynamics in single and multi-layered soil covers were characterised in a mine cover testing program for reclamation of lean oil sand overburden. Pore-gas concentrations of O_2 and CO_2 in the upper 1.5 m of soil covers and lean oilo sands did not reach a threshold that poses a risk for plant growth. Below 1.5 m in the LOS, O_2 dropped to 0% and CO_2 rose to >16%. Frozen moisture in peat coversoil at one sampling location was a barrier to gas exchange and resulted in accumulation of CH_4 (>35%). Novel subsurface flux chambers were designed and fabricated to directly measure O_2 ingress through soil covers and CO_2 effluxes from lean oil sands into soil covers. Soil cover material and placement thickness affected gas flux rates; O_2 fluxes peaked at 18.0 kg/m^2/a and CO_2 fluxes peaked at 2.3 kg/m^2/a. Diffusive fluxes were calculated from soil gas profiles by estimating diffusion coefficients from position-dependent soil moisture

and temperature. Advective fluxes were calculated from pressure gradients and in-situ air conductivity. Advection dominated over diffusion in soil covers except for one location that was a localized zone of PHC degradation and methane oxidation and/or the lean oil sands was coarser-textured and quickly responded to barometric pressure fluctuations.

3.1 Introduction

Surface mining of oil sands in Alberta, Canada, produces >1 million barrels of crude oil per day and has disturbed >700 km^2 of Canada's boreal forests (Alberta Energy 2016; CAPP 2015). Oil sands operators are mandated to reclaim areas disturbed by mining to a capability equivalent to pre-disturbance (Government of Alberta 2007). Establishing an appropriate soil cover design considering soil material type, horizon configuration, and capping thickness, is one of the most effective measures available for oil sand mine operations to mitigate the constituents of risk of a landform substrate. Soil reclamation cover designs are also used in upland reclamation to facilitate the growth of native boreal plant and tree species by providing sufficient nutrients, moisture, and an adequate supply of oxygen (O_2) for plants and biologically active soil microbial populations to remove methane gas (CH_4) in aerobic microbial reactions.

Overburden are landforms that will make up a significant portion of the closure mine landscape for oil sand mine operations. During the mine operation, overburden material above the oil sand deposit is removed and transported to a dedicated disposal area. Large above-grade overburden landforms are created in the operation which must later be reclaimed. For some oil sand mine operations in the Athabasca oil sands region, the overburden may contain a petroleum hydrocarbon (PHC) concentration up to the economical ore grade concentration of approximately 7%. This overburden substrate is referred to as lean oil sand (LOS) and there is uncertainty in the magnitude of risk associated with the removal, displacement, and placement of LOS in a new environment in the closure landscape. One of the risks associated with LOS involves degradation of PHCs near or within the root and biologically active cover soil zone, which may reduce plant-available O_2 by displacement with carbon dioxide (CO_2) or by consumption in CH_4 oxidation reactions (Leone et al 1977).

Current operating approvals for oil sand mine operations mandate placement of a minimum soil reclamation cover thickness ranging from 1.2 to 1.5 m for LOS. However, there is insufficient data available to evaluate the real risk of LOS and assess whether the current mandated minimum soil cover thickness is sufficient, optimal, or overly conservative to achieve the goal of “equivalent land capability”. Accordingly, there is an opportunity for research to address these uncertainties and provide information to support the establishment of an optimal soil cover design and thickness for the reclamation of LOS landforms. One specific research question relates to the potential for vegetation to experience distress as a result of pore-gas composition or pore-gas dynamics.

The Aurora Soil Capping Study (ASCS) is a 36 hectare soil cover research study constructed at Syncrude Canada Limited’s Aurora North mine (57°20’ N, -111°32’; Figure 3.1). The primary goal of the ASCS is to assess the effectiveness of single and multi-layered soil cover systems, as well as the optimal reclamation capping thickness to alleviate the risk(s) of LOS and meet targeted vegetation growth targets to achieve equivalent land capability. The study area was subdivided into 36 one hectare cells, each capped with one of twelve different soil cover configurations, denoted hereafter as *treatments*. Each cell was instrumented with moisture, temperature, and suction sensors; an on-site meteorological (MET) station collects data on wind-speeds, air temperature, precipitation, and barometric pressure. For the purposes of soil gas sampling, static flux chambers (SFC) were installed on 2 treatments and soil vapour probes (SVP) were installed in 8 of the soil cover treatments to a depth down to 4 m below ground surface (BGS).

Figure 3.1 Map showing location of Alberta on the map of Canada (left). Map of Alberta showing the location of Syncrude's Aurora North mine (right)

The objective of this paper is to supplement the multi-disciplinary research conducted at the ASCS (see Barber et al 2015) by developing an understanding of pore-gas dynamics in the soil covers and LOS. The tasks that are addressed in this paper are intended to achieve the following:

- characterise pore-gasses at various depths in the soil covers and LOS over a range of field conditions;
- directly measure O_2 ingress through the soil covers and CO_2 efflux from the LOS into the soil covers using static flux chambers and a novel subsurface static flux chamber;
- indirectly quantify O_2 fluxes resulting from concentration-gradient driven diffusion and pressure-gradient driven advection by evaluating soil gas concentration and pressure profiles in conjunction with soil moisture and temperatures; and
- quantify the relative importance of diffusion and advection to soil-atmosphere O_2 and CO_2 fluxes across the interface of the LOS and soil covers.

3.2 Background

The soil cover materials investigated herein were salvaged during oil sands mining activities and either directly placed at the study or stockpiled awaiting construction of the ASCS.

The soil reclamation materials comprising the ASCS were the following:

- **Peat** – salvaged from bogs and fens in the mine footprint, it is a cover soil (topsoil) horizon that provides organic carbon, nutrients, and improves water holding capacity (Rowland 2009). It was placed at a depth of 0.1 or 0.3 m at the ASCS. It should be noted that the organic carbon content of the peat in this study is lower than typical organic soils (Kroetsch et al 2011);
- **LFH** – surface litter layer, A horizon and potentially a portion of the B horizon salvaged from upland soils within the mine footprint. It was placed at a depth of 0.1 or 0.2 m at the ASCS; and
- **Subsoil** – coarse-textured (median texture of loamy sand), glaciofluvial surficial geology deposits within the mine development footprint containing a variable proportion of naturally-occurring hydrocarbons embedded in the soil matrix. Subsoil types varied depending on their salvage depth, ranging from approximately 0.15-0.5 m, 0.5-1.0 m or 0.15-2.5 m. Subsoil placement depth and configuration varied for the ASCS treatments; thickness varied from 0-1.5 m and consisted of 1 or 2 subsoil horizons (when subsoil present).

The soil cover treatments investigated herein are illustrated in Figure 3.2. LOS is present below every soil cover treatment; however, it is only illustrated in Figure 3.2 if present within 1.5 m of the surface.

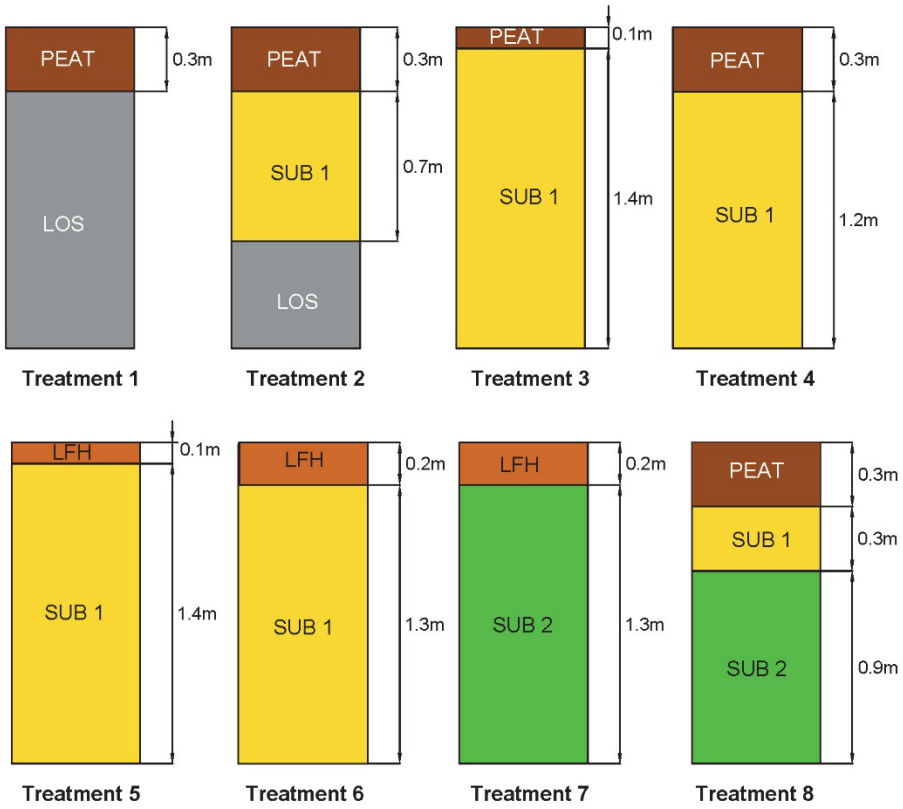

Figure 3.2 Single and multi-layer soil cover treatments at the Aurora soil capping study investigated in this research project. †

†Note: two types of subsoil are illustrated in the figure above: SUB 1 and SUB 2. The materials differ in their salvage depth but have similar particle-size distributions and soil-water characteristic curves. For simplicity, the two types of subsoil may be considered interchangeable for the purposes of this study and are both referred to as *subsoil* hereafter.

The treatments illustrated in Figure 3.2 were categorized based on capping thickness, soil texture, and gas sampling technique as listed in Table 3.1.

Table 3.1 Soil cover treatments grouped by capping thickness, soil cover design, and gas sampling technique.

Group	Soil Cover Design	Treatment[1]	Sampling Technique[2]
A (< 1.5 m thickness)	1 layer design of Peat coversoil (0.3 m)	1A	SVP
		1B	SVP
	2 layer design of Peat (0.3 and Subsoil (0.7 m)	2	SVP
B (1.5 m thickness)	2 layer design of Peat (0.1 or 0.3 m) and Subsoil (1.4 or 1.2 m)	3	SVP
		4	SVP
C (1.5 m thickness)	2 layer design of LFH (0.1 or 0.2 m) and Subsoil (1.4 or 1.3 m)	5A	SVP
		5B	SFC
		6	SVP
		7	SVP
D (1.5 m thickness)	3 layer design of Peat (0.3 m), SUB 1 (0.3 m) and SUB 2 (0.9 m) subsoils	8A	SVP
		8B	SVP
		8C	SVP
		8D	SFC

[1] Letters indicate replicate cells of treatments.
[2] SVP = soil vapour probe; SFC = static flux chamber.

Samples of soil reclamation materials and LOS at the ASCS were analyzed for particle-size distribution (PSD) in accordance with ASTM D422-63 (2007) and are presented in Figure 3.3.

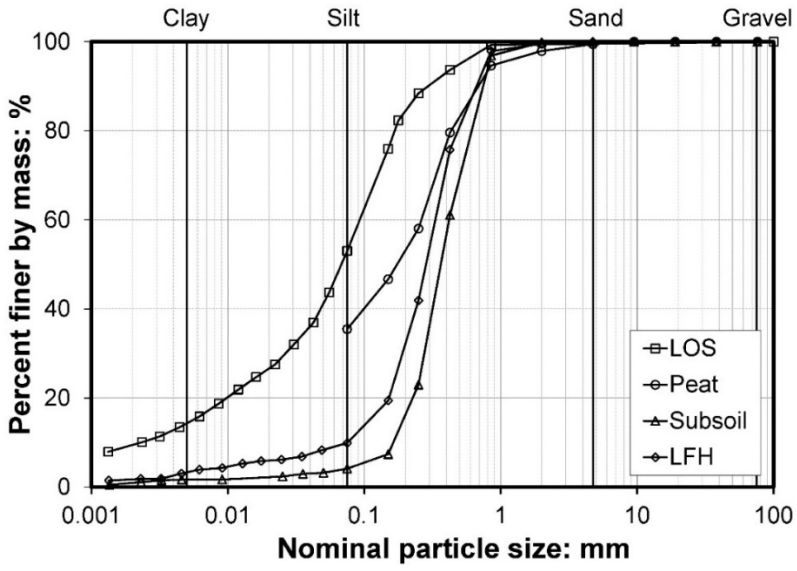

Figure 3.3 Particle-size distribution for soil reclamation materials and lean oil sand of the Aurora Soil Capping Study.

LOS, with the oil component removed, has more silt and clay relative to the cover soil materials. LFH and subsoil have similar particle sizes; however, LFH has slightly higher silt content. The peat was only classified for particle sizes ranging from 0.1-5 mm.

Laboratory measurements of the soil water characteristic curve (SWCC) for peat, subsoil, and LFH were conducted in accordance with ASTM D-6836-02 (2008). Measurements of the SWCC for LOS were conducted by Pernitsky et al (2016) using the suction table apparatus described by Dane and Topp (2002). Results of the SWCC tests are shown in Figure 4. Peat has the highest total porosity of approximately 78%, followed by LFH with a total porosity of 42%. LFH and subsoil have similar shaped SWCC's; however, the LFH curve is shifted slightly above the subsoil curve, likely due to the greater organic matter and silt content.

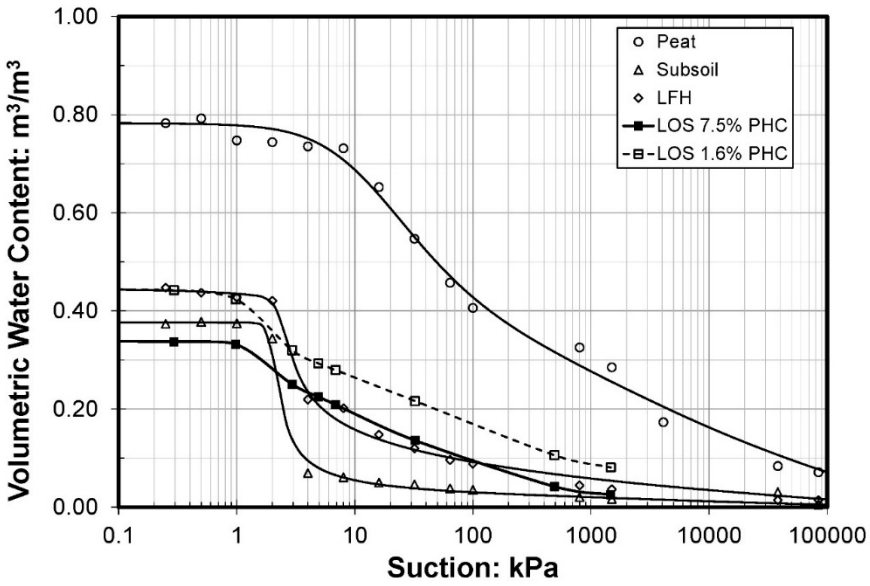

Figure 3.4 Laboratory-measured soil-water characteristic curves for soil reclamation materials and lean oil sand of the Aurora Soil Capping Study.

3.2.1 Significance of PHC degradation in reclamation soil covers

The methanogenic biodegradation of PHCs (such as the oil component of LOS) occurs under anaerobic conditions when O_2 is unavailable to be the terminal electron acceptor (Grishchenkov et al 2000; Salminen et al 2004). The products of this reaction are gaseous CH_4 and CO_2, which may subsequently enter the reactive aerobic zone of the overlying cover soils, whereupon methanotrophic microorganisms (methanotrophs) facilitate reduction-oxidation reactions (methane oxidation) by transferring electrons from electron-donating CH_4

to electron-accepting O_2. The net effect to the composition of pore gasses is the removal of O_2 and an increase in CO_2 and CH_4. Whether this effect is problematic is dependent upon the concentrations of CH_4 and O_2 to facilitate this reaction and the response of the reclamation vegetation to such changes in pore-gas composition.

Plants require sufficient O_2 in the rooting zone to facilitate essential biological processes (Geigenberger 2003). Reductions in pore O_2 may result from microbiological activity or restricted air porosity. Symptoms of O_2 deficiency generally manifest at concentrations less than 10% (Flower 1981; Kozlowski 1985). Moreover, CO_2 in the air-filled pore space can be phytotoxic at concentrations greater than 15% (Flower 1981; Whitton 1991).

Physiological impairments from deficient O_2 or excess CO_2 include drying of leaves (desiccation), loss of pigmentation (chlorosis), shedding of leaves (abscission), impeded nutrient absorption, reduced photosynthesis (and thus reduced growth rates), and the production of organic compounds such as ethylene (Chang and Loomis 1955; Leone et al 1977; Flower 1981; Kozlowski 1985; Wong 1988; Whitton 1991; Pezeshki et al 1993; Bartholomeus et al 2008). CH_4 and CO_2 produced during methanogenic biodegradation of the oil component of LOS can be transported by various gas transport processes into the aerobic pore space of the overlying unsaturated cover soil treatments.

3.2.2 Mass transport of pore gas in unsaturated reclamation cover soils

Gas transport processes that induce the movement of pore-gasses include concentration-gradient driven diffusive fluxes and pressure-gradient driven advective fluxes. Diffusive fluxes depend upon the assumed value of the diffusion coefficient, D_p, and there are a number of models published in the literature to estimate the diffusion coefficient. A sensitivity analysis was therefore conducted using six different models for the diffusion coefficient as listed in Table 3.2. Diffusive gas fluxes were calculated using the concentration gradient method (de Jong and Schappert 1972; Billings et al 1998; Risk et al 2002; Kanako et al 2008; Maier and Schack-Kirchner 2014). Values for the diffusion coefficients were determined from the various models and used with position-dependent gas concentrations.

Table 3.2. Diffusion coefficient models tested in sensitivity analysis.

Type	Model	Reference
Two-parameter	$\frac{D_p}{Da_0} = \frac{\theta_a^{10/3}}{\theta_T^2}$ [3.1]	Millington and Quirk (M-Q) (1961)
	$\frac{D_p}{Da_0} = \frac{\theta_a^2}{\theta_T^{2/3}}$ [3.2]	Millington and Quirk (1960)
Moisture-corrected	$\frac{D_p}{Da_0} = \left(2\theta_{a_{100}}^3 + 0.04\theta_{a_{100}}\right)\left(\frac{\theta_a}{\theta_{a_{100}}}\right)^{2+\frac{3}{b}}$ [3.3]	Moldrup (1996)
Dual-phase	$D_e = \frac{1}{\theta_T{}^2}[D_a^0\theta_a^P + HD_w^0\theta_w^P]$ [3.4]	Aachib et al (2004)
	$D_e = \tau D_a^0[1 - S_r]^\alpha + \frac{\tau S_r D_w^0}{H}$ [3.5]	Elberling (1993)
Density-corrected	$\frac{D_p}{Da_0} = 0.1\left[\left(\frac{\theta_a}{\theta_T}\right)^3 + 0.04\left(\frac{\theta_a}{\theta_T}\right)\right]$ [3.6]	Deepagoda (2011)

Advective fluxes, on the other hand, may be induced by soil-atmosphere barometric pressure gradients causing bulk movement of gasses into or out of soils (Christophersen 2001; Poulsen 2003; Massman 2006; Gebert 2011; Redecker 2015). Pressure gradients may also be induced by reactions; for example the simple stoichiometry of CH_4 oxidation results in a net decrease in pore-gas volume, while the production of CO_2 and CH_4 result in a net increase in pore-gas volume (Molins and Mayer 2007). The direction of flow depends on whether soil-atmosphere pressure gradients are positive (atmospheric pressure > pore-gas pressure) or negative (atmospheric pressure < pore-gas pressure) (Elberling et al 1998). Advection, especially in coarser-grained soils, can be orders of magnitude greater than diffusive gas transport (Nilson 1991; Redecker 2015).

One-dimensional flux of pore-gasses due to advection for a single phase is described by Darcy's Law (Seely et al 1994; Hillel 2003; Kim and Benson 2004; Kjeldsen et al 2005). At the field study site, the coefficient of gas permeability was determined based on in-situ air conductivity measured using an air permeameter and the soil-atmosphere pressure gradient

measured using a high-precision digital manometer attached to soil vapour probes as described in the following section.

3.3 Materials and Methodology

3.3.1 Flux chambers

Soil gas effluxes are commonly measured using the static flux chamber (SFC) method in which the upper section of the chamber is sealed to atmospheric gasses and the lower section is embedded into the soil and permeable to soil gasses. The ingress and efflux of gasses was calculated from the change in gas concentration within the enclosed headspace over an incremental time using the following general equation:

$$F_i = \frac{V_C}{A_C}\frac{\Delta C_i}{\Delta t} \quad [3.7]$$

Where F_i is the flux of a gaseous species into the closed chamber [$ML^{-2}T^{-1}$], V_c is the volume of the chamber headspace [L^3], A_c is the area enclosed by the chamber [L^2], and $\Delta C_i/\Delta t$ is the concentration change of the gaseous species in the headspace over a time interval [$ML^{-3}T^{-1}$].

Accumulation of gasses in the headspace may result in non-representative concentration gradients and reduce the concentration gradient driving diffusive gas flux (Fick 1855; Nay 1994; Hutchinson et al 2000; Davidson et al 2002; Pumpanen 2004; Heinemeyer and McNamara 2011; Pihlatie 2012). It should be noted that analysis of data from SFC tests was carried out to specifically address this potential systematic error.

Square 1.22 m by 1.22 m by 0.31 m surface and subsurface chambers were installed at the ASCS. The surface chambers were fabricated from PVC with holes drilled for inlet and outlet tubes. A solar-powered fan was inserted into the chamber to circulate headspace gasses. During installation, bentonite clay was placed in a groove around the perimeter of the chamber and hydrated to minimize gas exchange between the headspace and atmosphere. The surface chambers were moved periodically to locations within an approximate 20 m radius of the field laboratory.

For the steel subsurface flux chambers, the bottom was open and top covered by welded wire mesh (to support the weight of the overlying soil). A 0.053 mm aperture size gas-pervious stainless steel screen was fastened over the wire mesh. The upper surface of the chamber was comprised of two sealed compartments (to measure upward diffusion of gasses) and two open compartments (to account for downward diffusion of gasses from the surface). The compartments were staggered diagonally in an effort to account for non-uniform gas flow. The subsurface flux chamber is illustrated in Figure 3.5.

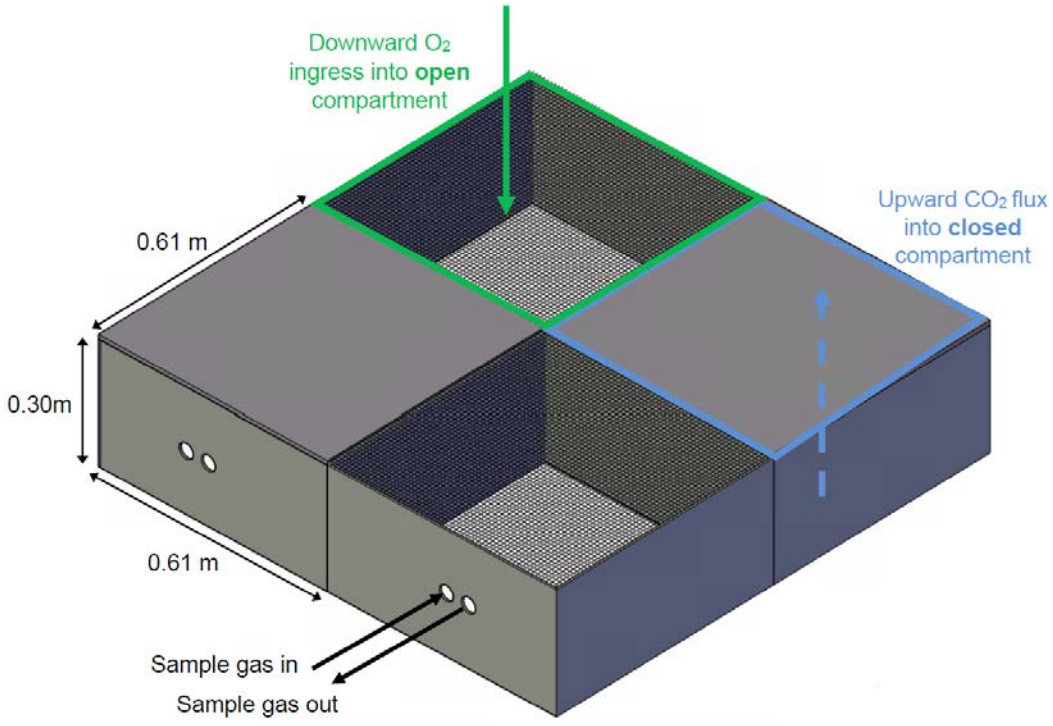

Figure 3.5 Illustration of the subsurface flux chamber. Not illustrated is welded wire mesh used to support weight of overlying soil.

The subsurface flux chambers were placed immediately on top of the LOS and in the soil reclamation material. Teflon tubing (6.4 mm diameter) was placed in a protective conduit and led to the surface and connected to an on-site instrumentation lab containing a 10 channel auto-sampling Columbus Instruments® Model 180-C™ gas analyser (Columbus Instruments, Columbus, Ohio, USA). The arrangement of the flux chambers and field laboratory is illustrated in Figure 3.6.

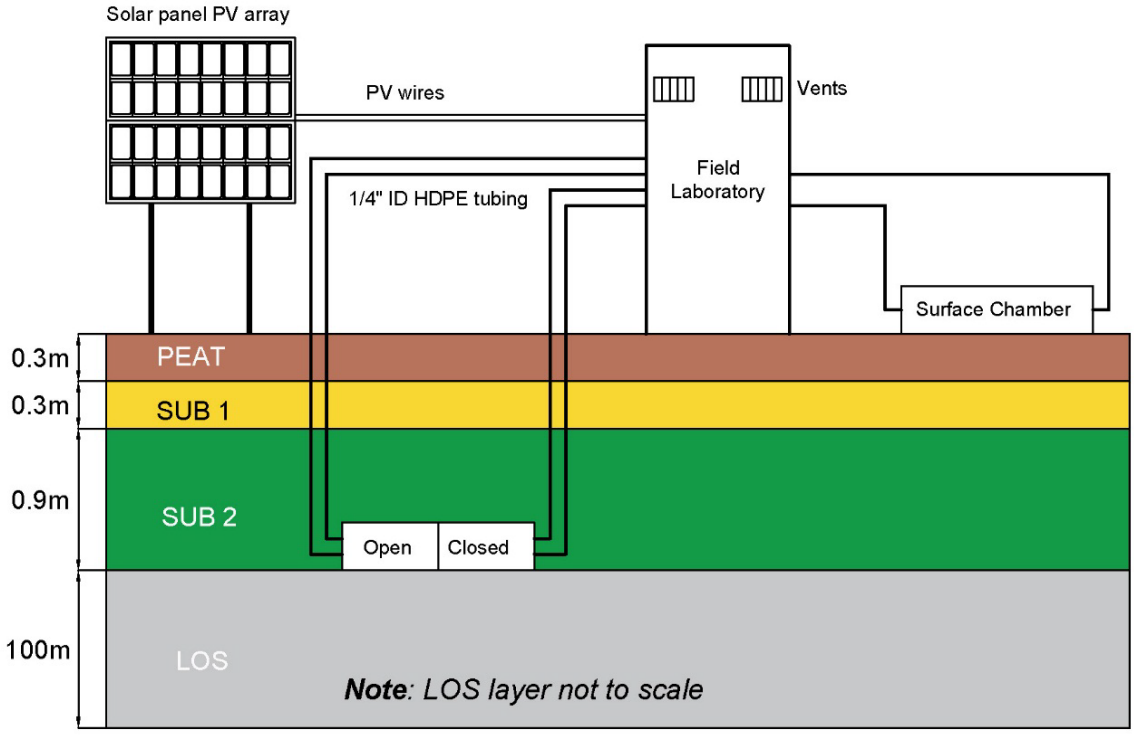

Figure 3.6 Cross-sectional illustration of field setup for sampling surface and subsurface flux chambers using Columbus Instruments® Model 180-C™ gas analyser.

3.3.2 Gas sampling

Gasses were pumped from the SFC headspace at a nominal flow rate of 0.5 L/min for 2 minutes per sampling interval. Excess moisture was removed from the gasses in the condensing air dryer unit. Gasses were further dried in the sample drier fitted with two desiccant columns containing Drierite ($CaSO_4$). Next, the gas passed through a 0-100% paramagnetic O_2 sensor and 0-1% and 0-30% single-beam non-dispersive infrared CO_2 and CH_4 sensors (4 sensors in total).

The gas analyser was calibrated before each site visit with O_2 at 20%, CO_2 at 0.8% and CH_4 at 25%. Calibration was conducted at temperatures from 0−40°C and measurements were within ±0.1% of the specified value, suggesting that temperature fluctuations from 0-40°C in the field laboratory should not have a significant effect on the measured gas concentrations.

3.3.3 Purge tests

Due to the unique design of the surface and buried flux chambers, it was not possible to conduct standard closed chamber tests, which involve enclosing a volume of air and

measuring the accumulation of gasses within that volume over an incremental time period. Instead, the chamber headspaces were purged with N_2, while a vent was left open to the atmosphere to prevent pressure build up inside the headspace. Headspace gasses were periodically sampled during purging, which was deemed complete after repeated non-detect measurements of O_2, CO_2, and CH_4.

During testing, headspace gasses were pumped in a continuous loop through the analysers and returned to the chamber headspace. This cycle was repeated for up to 10 channels, resulting in a sampling interval of roughly 10 minutes to 1 hour. By sampling in a continuous loop, sampling-induced pressure changes were largely avoided.

3.3.4 Soil vapour probes

Soil vapour probes (SVP) were installed in the LOS and the cover soils using the AMS® SVP Kit™. The tubing is attached to the "harpoon" tip (Figure 3.7), pulled through hollow steel rods and advanced into the subsurface with a slide hammer. In each SVP cluster, tubing was installed into the soil reclamation covers to depths ranging between 0.3 m and 1.5 m and into the LOS to a maximum total depth of 4 m as illustrated in Figure 3.7.

Pore-gas concentrations were measured in the SVP using a LandTEC® GEM 2000™ field portable gas analyser (LandTec 2010) which measures CH_4 and CO_2 using dual-beam infrared adsorption to ±0.3% at concentrations <5% and ±1% at concentrations up to 15%. Oxygen is measured to ±1% with a galvanic cell. This instrument is equipped with a digital manometer to measure differential pressures to ±0.25 Pa.

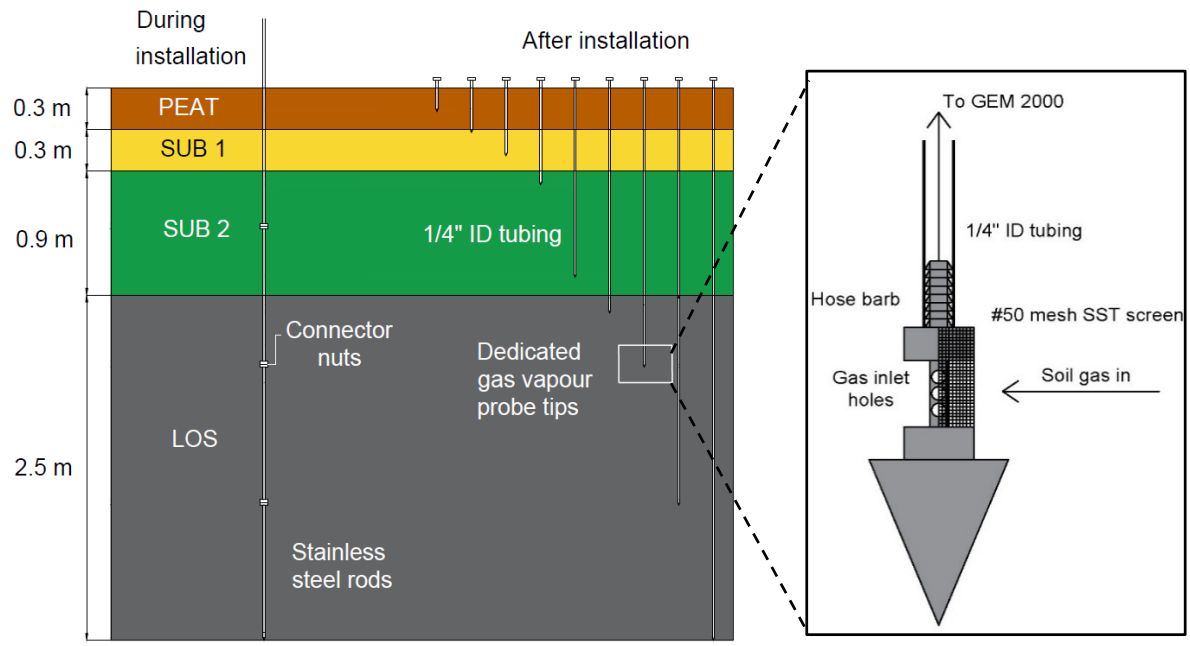

Figure 3.7 Cross-sectional illustration of field installations for a nest of soil vapour probes (Left). Illustration of AMS® dedicated soil vapour probe "harpoon" tip embedded in the soil for gas sampling (Right).

3.3.5 Air permeameter

As part of the multi-disciplinary ASCS research, air conductivity of the soil covers were measured in-situ to a depth of 0.4 m using a custom-fabricated portable air permeameter apparatus (Zettl 2013; Huang 2015). The apparatus involved inserting a 0.16 m diameter by 0.4 m length steel cylinder into the cover soil with a drop hammer and measuring pressure drops across the base and headspace of the cylinder while applying a constant flow rate of non-reactive gas. A detailed methodology is described in Huang et al (2015).

3.4 Results

3.4.1 Direct measurement of fluxes using flux chambers

The time vs. concentration results from the SFC purge tests indicated the accumulation of O_2 and CO_2 in the chamber headspaces. O_2 purge tests were conducted in the subsurface SFC placed at the soil cover/LOS interface below Treatment 5B (2 layer design of 0.1 m peat and 1.4 m subsoil) and below Treatment 8D (3 layer design of 0.3 m peat, 0.3 m subsoil 1, and 0.9 m subsoil 2). Using these results, O_2 flux rates through the soil covers were calculated using Equation 3.7. The geometric mean O_2 flux rates through the soil covers into the subsurface SFCs were plotted as shown for the subsurface SFC in Figure 3.8. Onset of O_2 ingress into

the chamber headspace was delayed by roughly 2 hr for both treatments. Flux rates increased for approximately 20 hours and peaked at 18 kg/m^2/a for Treatment 8D and approximately 8 kg/m^2/a for Treatment 5B.

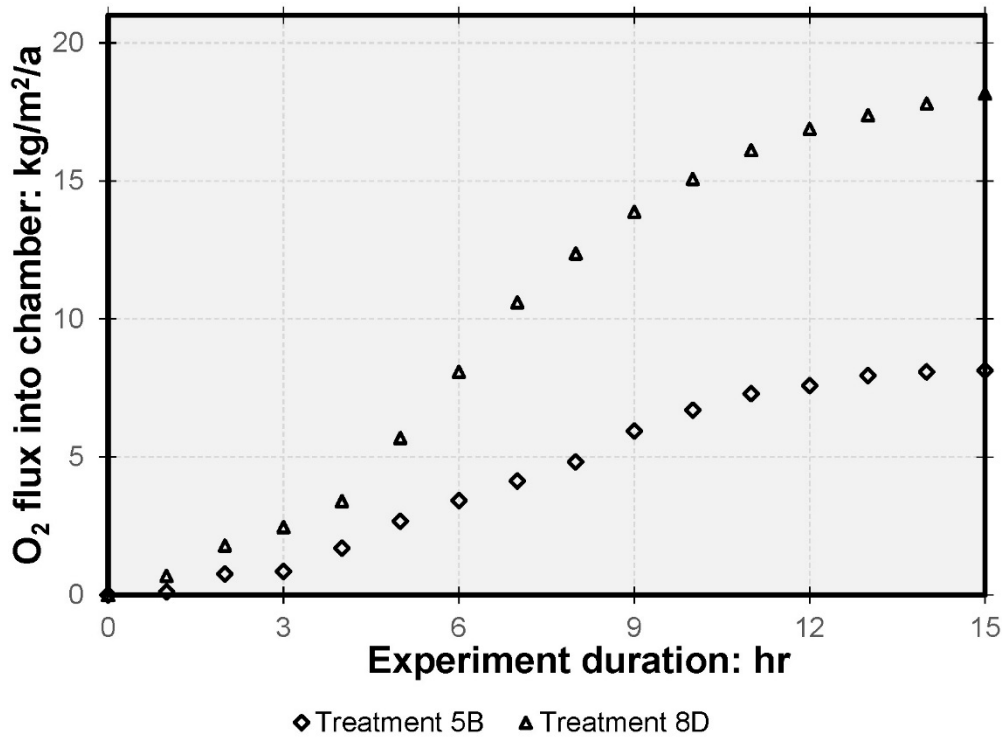

Figure 3.8 Geometric mean of all O_2 fluxes through Treatment 5B and Treatment 8D into the open compartments of the subsurface flux chambers modelled with non-linear curve fitting equations.

Geometric mean flux rates for CO_2 from the ground surface into the surface SFCs on Treatments 5B and 8D and the geometric mean flux rates for CO_2 from the LOS into the subsurface SFC on Treatment 8D are plotted in Figure 3.9. Mass flux of CO_2 into the chamber headspace commenced instantaneously after starting the purge tests. Flux rates of CO_2 increased for approximately 2.5 hours to a peak of 2.3 kg/m^2/a for Treatment 5B, 1.4 kg/m^2/a for LOS, and 0.6 kg/m^2/a for Treatment 8D.

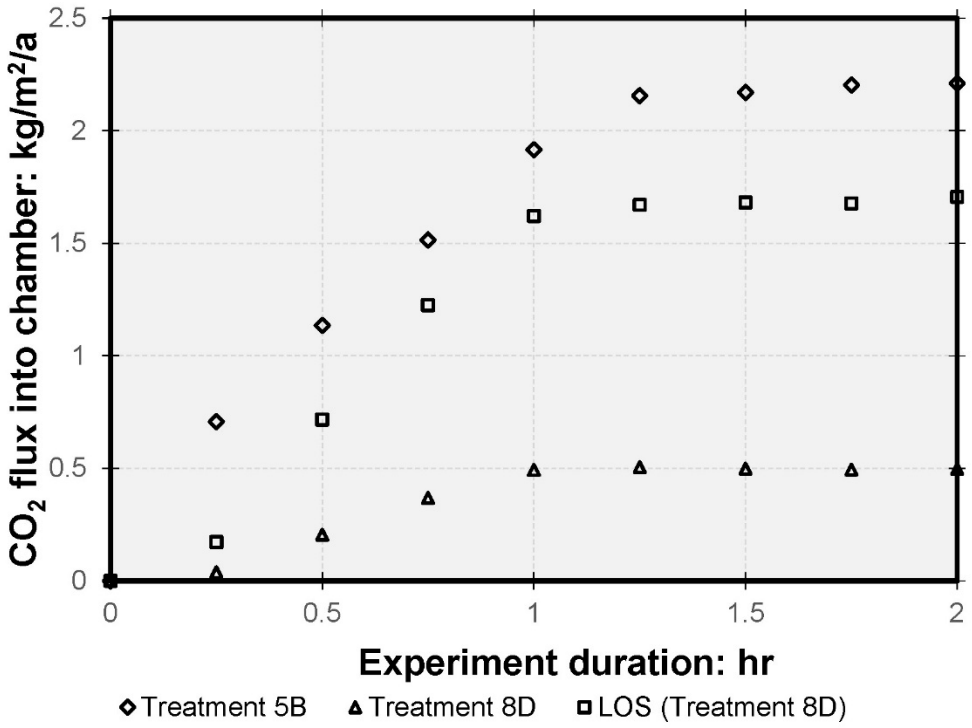

Figure 3.9 Geometric mean of all CO_2 fluxes through Treatment 5B and Treatment 8D into the surface flux chamber and through the LOS into the closed compartment of the subsurface flux chamber modelled with non-linear curve fitting equations.

3.4.2 Indirect flux measurements using pressures and concentrations measured at various depths in soil vapour probes

Concentrations of pore gasses and differential pressures were measured over the 2014-2015 field seasons in soil vapour probes installed at depths of 0.3-0.5, 0.5-1, 1-2, 2-3 and 3-4 m. At total of 165 to 215 measurements were taken from the SVP's at each of these depth ranges, except for the deepest (3-4 m), from which 43 measurements were made.

Using the various models described in Table 3.2, the relationship between the O_2 diffusion coefficient (D_p) and VWC was determined for each of the soil cover materials and LOS as presented in Figure 3.10. In general, the 6 models show a similar trend and at a higher water content generally predict similar values for the diffusion coefficient. Other than for LOS, which has similar predicted values over the full range of VWC, there is more scatter at lower water contents among the predicted values using the various models. In particular, Eberling (1993) generally predicts diffusion coefficients lower than that of the other models for peat and subsoil, while M-Q (1960) predicts diffusion coefficients higher than that of the other models for all soils and LOS.

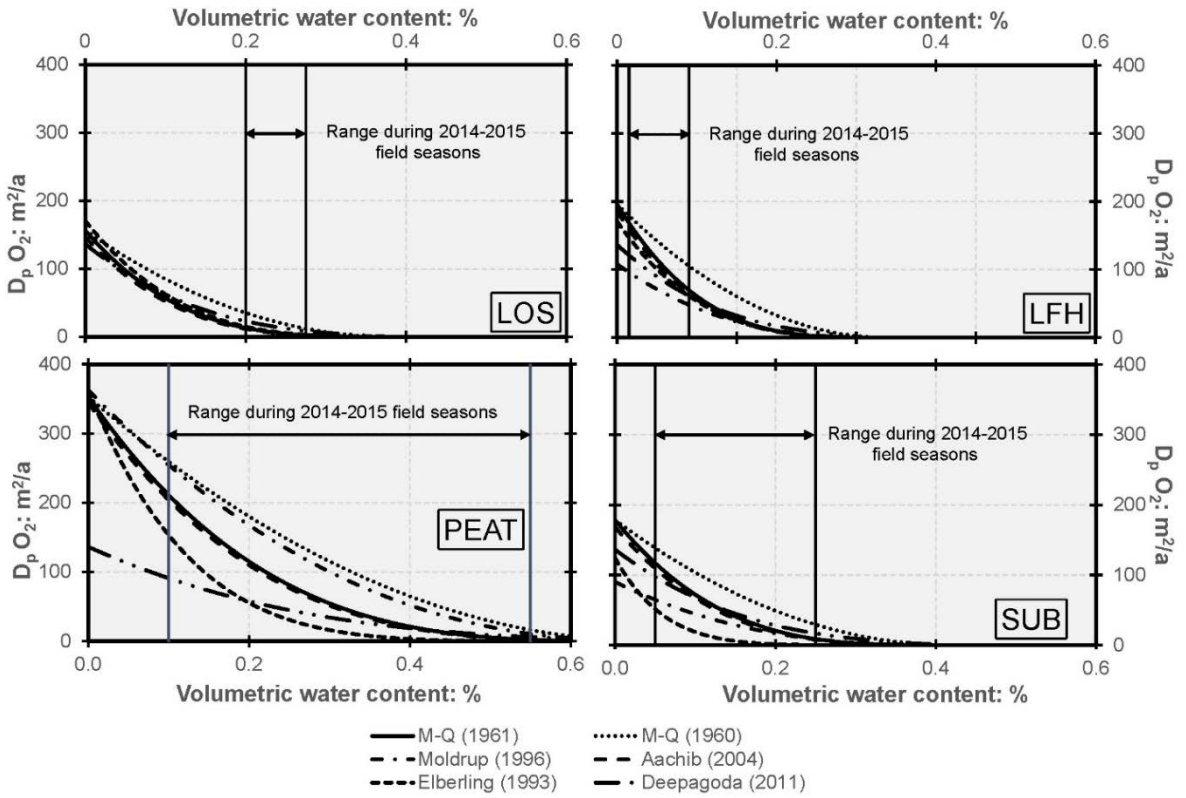

Figure 3.10 Range of values of O_2 diffusion coefficient for LFH, LOS, peat, and subsoil as a function of the volumetric water content of the soil for a selection of diffusion coefficient models. (Moldrup, 1996 was not used for LOS).

The modelled values of the diffusion coefficient may be combined with the vertical variation in material and water content to develop a relationship between diffusion coefficient and depth for each soil cover treatment over LOS. Figure 3.11 presents this variation of O_2 diffusion coefficient with depth for selected soil profiles. The geometric mean O_2 diffusion coefficient of the 6 models were calculated at various depth increments.

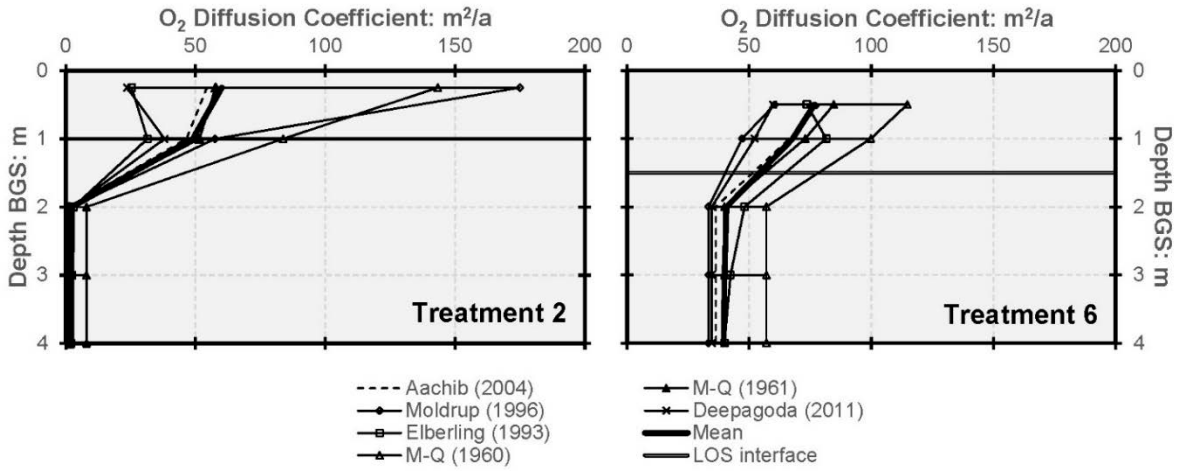

Figure 3.11 Variation of the oxygen diffusion coefficient with depth for selected soil profiles.

Mean O_2 and CO_2 pore-gas concentrations from all measured values are plotted in Figures 3.12 to 3.15. The measured gas concentrations may be evaluated in the context of conditions monitored at a nearby area of undisturbed natural boreal forest within the lease area wherein the soil was found to be well-aerated with O_2 concentrations close to 20% and CO_2 concentrations less than 0.3% to a depth in excess of 3 m (data not reported).The soil profile was similar in physical characteristics to the LFH and subsoil material in this study (e.g. PSD, SWCC, and proportion of oil), but did not have LOS type parent geologic material within the measured depth.

Pore-gasses within LFH, peat, and subsoil at depths ranging from 0.3-0.5 m were well-aerated with relatively low CO_2 concentrations of typically <1.5%. Within the subsoil at a depth of 1 m, O_2 concentrations were typically between 16-20%, but dropped to a minimum of 8.7% on Treatment 8A. CO_2 concentrations in the subsoil, while mostly between 0.5-3.5%, peaked at a maximum of 8.6% on Treatment 8A. The general trend was that median O_2 concentrations in LOS below the soil covers decreased with depth to less than 5% at 3-4 m. CO_2 generally followed the inverse trend, with median CO_2 concentrations increasing with depth to more than 8% at 3-4 m.

The distribution with depth of O_2 diffusion coefficients for the various soil cover systems was estimated for all treatments using the six diffusion coefficient models (Equations 3.1 to 3.6). The geometric mean O_2 diffusion coefficient of the six models was used to calculate diffusive O_2 fluxes from field measurements of pore-gas concentrations measured in the SVP's.

Group A soils are displayed in Figure 3.12. Due to steeper O_2 concentration gradients and lower VWC measured in Treatment 1A, diffusive fluxes increased in the LOS to a depth of 2 m BGS. Peak diffusive fluxes for Treatment 1B were in the upper peat layer due to the high diffusion coefficient and at 2 m BGS in the LOS due to the steep concentration gradient. For Treatment 2, on the other hand, highest diffusive fluxes occurred in the cover soils, but were restricted in the LOS.

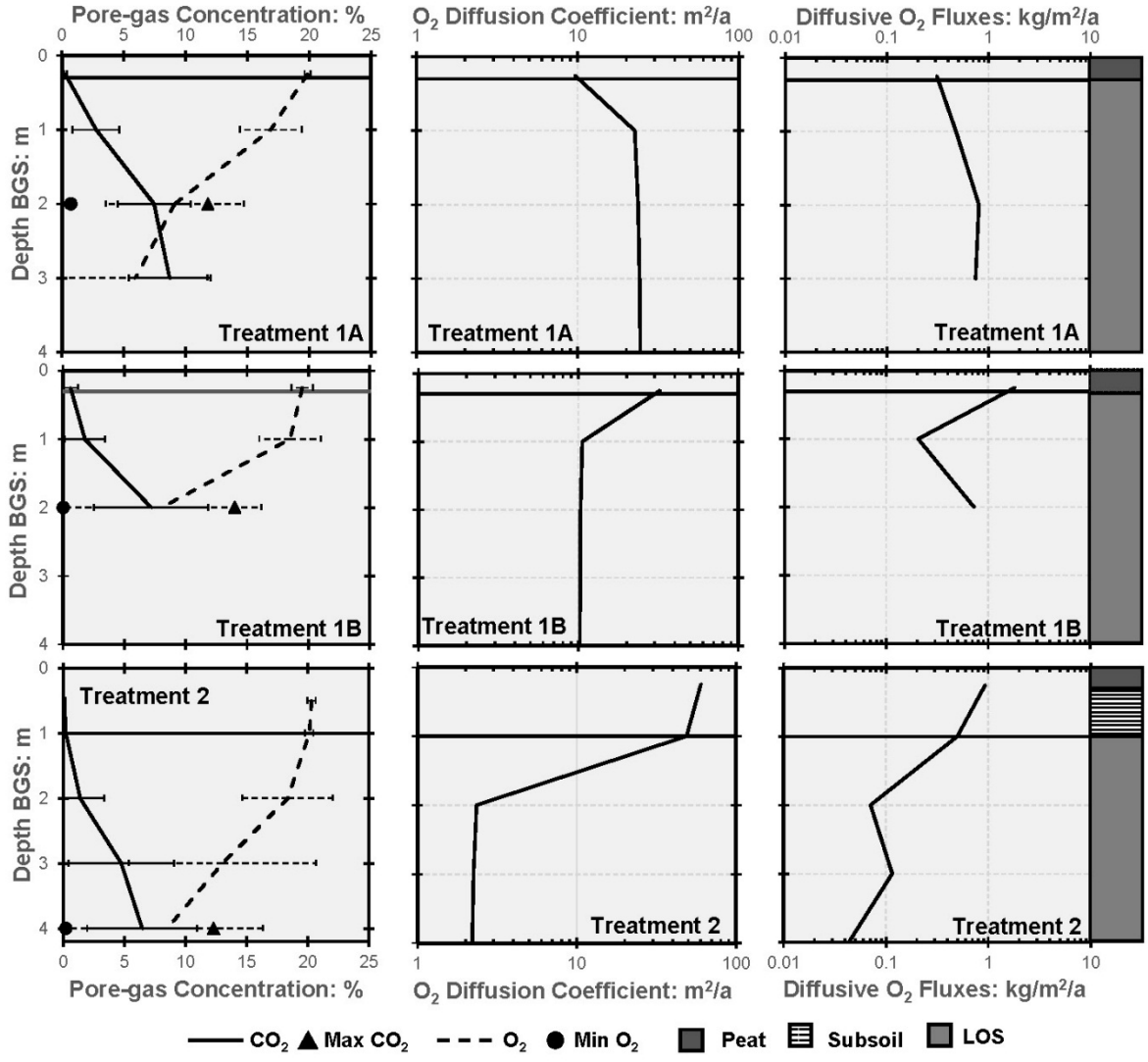

Figure 3.12 Range of O_2 pore-gas concentrations measured with soil vapour probes and diffusive fluxes calculated using the concentration gradient method during the 2014 and 2015 field seasons for Group A soils. Horizontal black lines signify the interface between the soil covers and LOS.

Diffusive fluxes for Group B soils are displayed in Figure 3.13. Diffusive fluxes were highest in the lower subsoil and upper LOS at 1-2 m BGS, however, fluxes at all other depths were similar in magnitude.

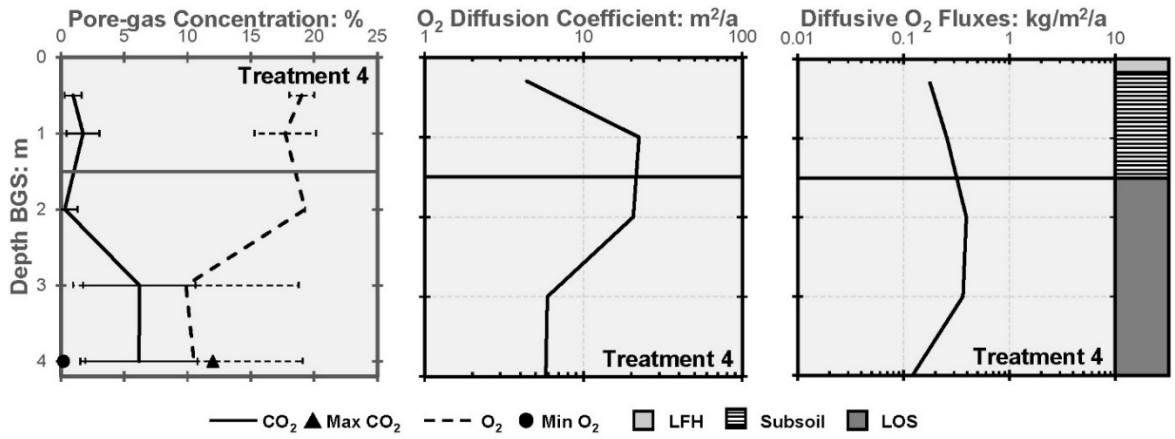

Figure 3.13 Range of O_2 pore-gas concentrations measured with soil vapour probes and diffusive fluxes calculated using the concentration gradient method during the 2014 and 2015 field seasons for Group B soils. Horizontal black lines signify the interface between the soil covers and LOS.

Diffusive fluxes for Group C soils are plotted in Figure 3.14. Treatment 6 with the LFH coversoil had the highest estimated diffusive fluxes of all treatments in the LFH layer at 0.3 m BGS and in the LOS between 1-3 m BGS due to steep concentration gradients and high diffusion coefficient estimation. Treatment 5A had high diffusive fluxes in the upper subsoil (0.3-0.5 m), but rates were restricted deeper into LOS. Diffusive fluxes for Treatment 7 were restricted in the upper LOS as a result of low O_2 concentration gradients and a low estimation of the diffusion coefficient.

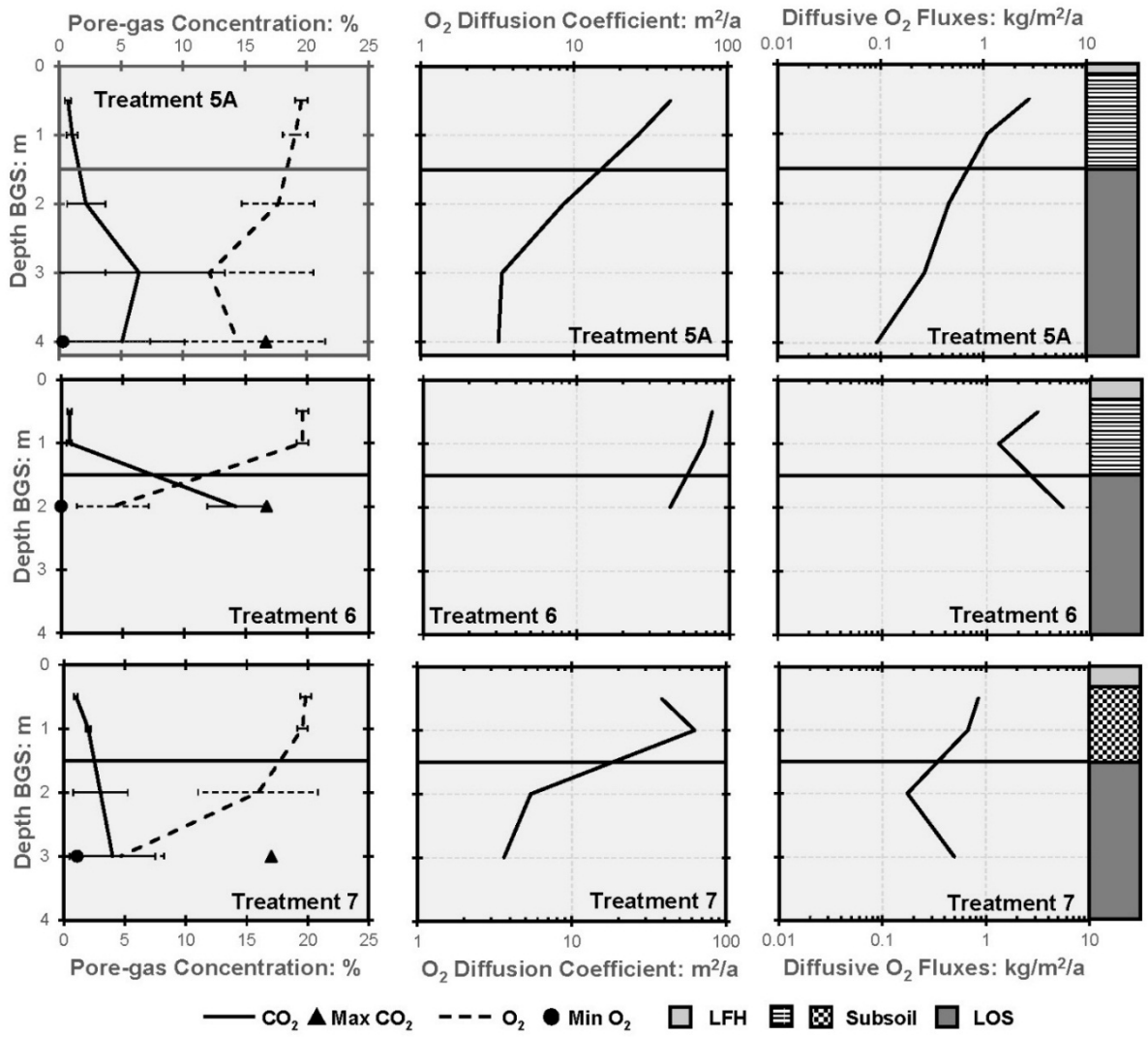

Figure 3.14 Range of O_2 pore-gas concentrations measured with soil vapour probes and diffusive fluxes calculated using the concentration gradient method during the 2014 and 2015 field seasons for Group C soils. Horizontal black lines signify the interface between the soil covers and LOS.

Diffusive fluxes for Group D soils are presented in Figure 3.15. All SVP measurements for Group D were within the same one hectare location. Location 8A and 8B had higher fluxes in the upper 0.3-0.5 m peat layer, but rates decreased with depth into the subsoil and LOS. Rates at Location 8C increased in the LOS at 3 m BGS due to steep concentration gradients.

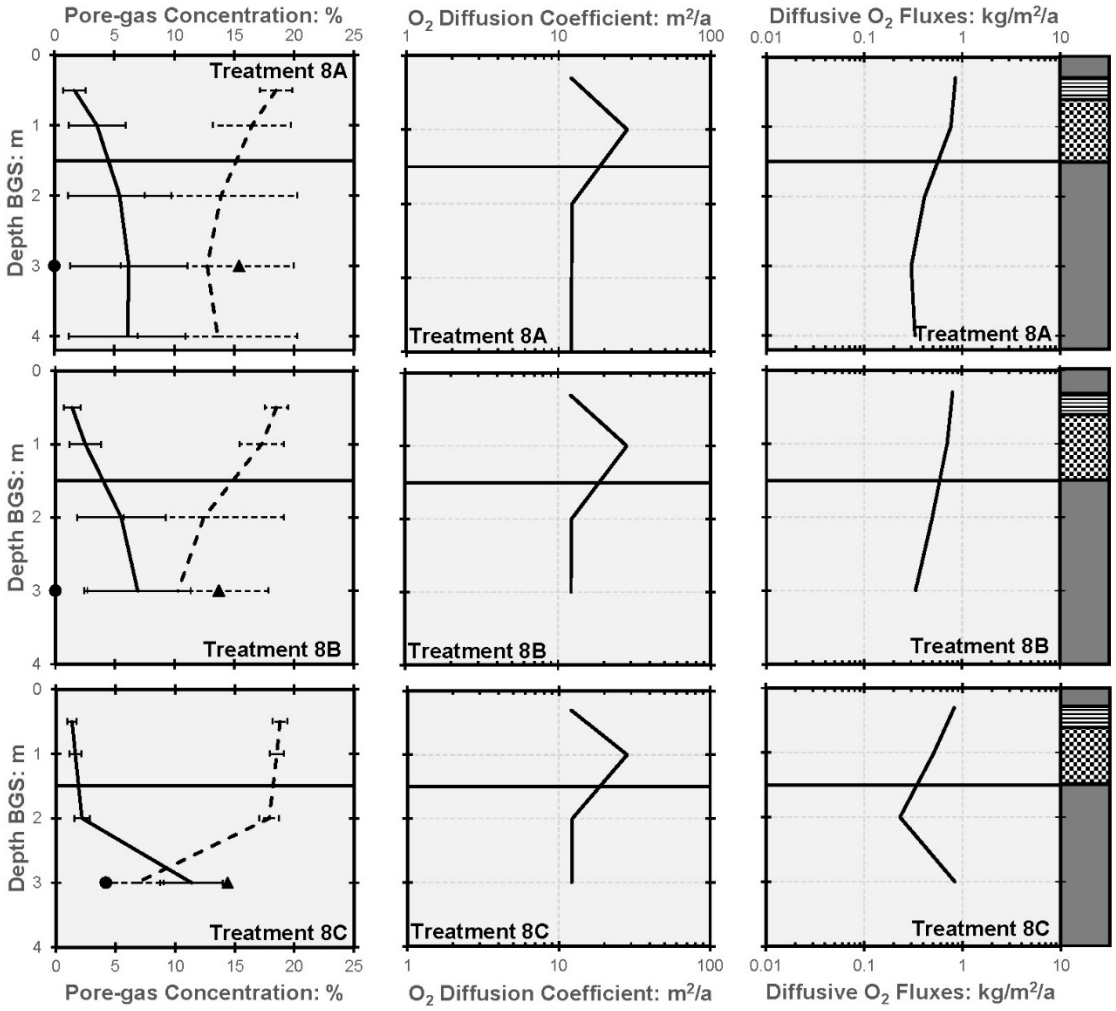

Figure 3.15 Range of O_2 pore-gas concentrations measured with soil vapour probes and diffusive fluxes calculated using the concentration gradient method during the 2014 and 2015 field seasons for Group D soils. Horizontal black lines signify the interface between the soil covers and LOS.

During the 2014 field season from May to November, high pore-gas CH_4 concentrations were measured in the SVP on Treatment 1B (0.3 m peat cover placed over LOS) relative to other locations at the ASCS, where CH_4 ranged from 0-1.7% (data not reported). Mean CH_4 concentrations on Treatment 1B of 24.8% and 18.8% were measured at 2 m and 3 m BGS, respectively, with individual measurements surpassing 35% at the beginning of the 2014 field season in May and decreasing to less than 10% at the end of the field season in November. During the same period, mean concentrations of O_2 were 8% in the LOS, with completely anaerobic (0%) concentrations detected on a number of sampling events. Note CH_4 concentration measurements on Treatment 1B were limited to the 2014 field season due to SVPs being found to be clogged at the beginning of the 2015 field season.

3.4.3 Relative importance of advection and diffusion

Figure 3.16 displays soil-atmosphere differential pressures measured during the 2015 field season. Differential pressures varied by location and with depth. In reality, the variable positive and negative pressure gradients with depth exhibited in most of the soil profiles actually represents a relatively constant pressure at depth with higher and lower barometric fluctuations. Thus for Treatments 1A and 8C, the lack of pressure gradient suggests highly air-permeable soils which respond quickly to fluctuations in barometric pressure. The general trend was that differential pressures increased in LOS with depth compared to the soil cover materials.

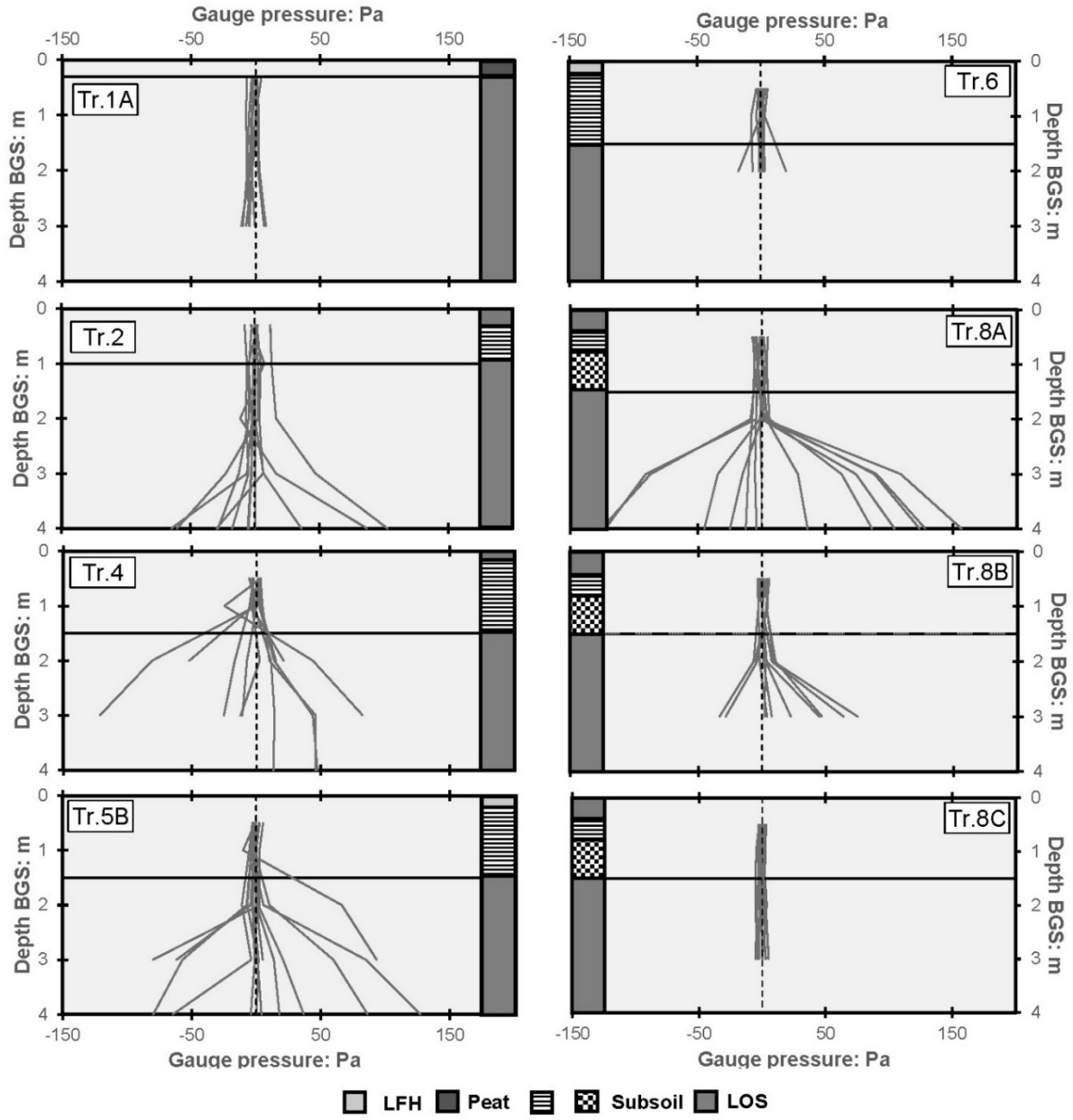

Figure 3.16 Differential pressure measurements during the 2015 field season at the ASCS.

Soil-atmosphere advective O_2 and CO_2 fluxes across the soil covers resulting from pressure-gradient driven advection were calculated using Darcy's Law based on differential pressures, in-situ air permeability, gas density, and gas concentrations at the base of the soil cover. Soil-atmosphere diffusive O_2 and CO_2 fluxes across the entire soil cover thickness resulting from diffusion were calculated with the geometric mean of the six different diffusion coefficient models (Equations 3.1-3.6).

The geometric mean of all diffusive and advective O_2 fluxes across the interface between the LOS and soil covers for the 2015 field season are presented in Table 3.3 along with the geometric standard deviation and the ratio of advective flux to diffusive flux. Treatment 1A (0.3 m Peat over LOS) and Treatment 2 (0.3 m Peat and 0.7 m subsoil over LOS) had the largest ratios of advection to diffusion. These high F_A/F_D may be misleading, however, since small differential pressures in the upper LOS directly below thinner covers can lead to large pressure gradients. Generally, advective fluxes decreased and diffusive fluxes increased with cover soil thickness. Comparing 1.5 m thick soil covers, F_A/F_D tended to be lower for Group D soil covers with 0.1-0.3 m peat caps, while the lowest F_A/F_D was for Treatment 6 (0.2 m LFH and 1.3 m subsoil), which had the lowest rates of advective fluxes and highest rates of diffusive fluxes.

Table 3.3 Mass flux of O_2 across interface between LOS and soil cover treatments by diffusion and advection.

O_2 Fluxes (kg/m^2/a)						
Treatment	**Cover thickness (m)**	**F_A – Advective Flux**	**Std. Dev.**	**F_D – Diffusive flux**	**Std. Dev.**	**Ratio F_A/F_D**
1A	0.3	82	80	0.31	0.46	265
2	1	122	166	0.50	0.26	244
4	1.5	41	48	0.32	0.41	128
5A	1.5	53	112	0.77	0.30	69
6	1.5	5	7	3.33	0.80	2
8A	1.5	19	16	0.59	0.45	32
8B	1.5	14	22	0.60	0.49	23
8C	1.5	16	12	0.37	0.30	43

Similarly, the geometric mean of all diffusive and advective CO_2 fluxes across the interface between the LOS and soil covers for the 2015 field season, geometric standard deviation from the mean, and the ratio of advection to diffusion are presented in Table 3.4. Treatment 4 (0.3 m peat and 1.2 m subsoil) and Treatment 5A (0.1 m LFH and 1.4 m subsoil) had the highest F_A/F_D. The lowest F_A/F_D was for Treatment 6 (0.2 m peat and 1.3 m subsoil), owing to having the lowest advective fluxes and highest diffusive fluxes. While the general trend was for diffusive fluxes to increase with increasing cover thickness, there was no clear trend for advective CO_2 fluxes and cover thickness.

Table 3.4 Mass efflux of CO_2 across interface between LOS and soil cover treatments by diffusion and advection.

CO_2 Fluxes (kg/m^2/a)						
Treatment	**Cover thickness (m)**	**F_A - Advection**	**Std. Dev.**	**F_D - Diffusion**	**Std. Dev.**	**Ratio F_A/F_D**
1A	0.3	0.9	1.1	0.10	0.16	9
2	1	1.2	1.6	0.15	0.08	8
4	1.5	6.1	14.6	0.21	0.30	29
5A	1.5	29.6	70.8	0.53	0.22	56
6	1.5	0.4	1.3	2.96	0.81	0.14
8A	1.5	2.0	4.2	0.50	0.40	4
8B	1.5	1.9	3.2	0.49	0.42	4
8C	1.5	1.5	1.2	0.32	0.27	5

3.5 Discussion of Results

3.5.1 Flux chambers

CO_2 flux rates from Treatment 8D (0.3 m peat and 1.2 m of subsoil) were lower than Treatment 5B (0.1 m LFH and 1.4 m subsoil). This may be attributed to the peat layer containing a greater saturated pore volume than the LFH to facilitate rapid dissolution of gaseous CO_2. The peat layer was thicker than the LFH, 0.30 m thick compared to the 0.10 m thick LFH layer, while the peat also had a higher total porosity of 78% compared to 42% for the LFH layer.

Conversely, O_2 flux rates through Treatment 8D were greater than through Treatment 5B. This is hypothesized to be due to steeper positive pressure gradients (atmospheric pressure > soil pressure) driving downwards gas flow from the atmosphere into the subsurface static flux chamber headspace during field tests.

3.5.2 Pore-gas characterization

Concentrations of pore-gas O_2 measured with SVPs installed in the upper 1.5 m of the various soil cover materials and LOS were found to be less than 10% O_2 on only two occasions, while CO_2 concentrations within the soil cover materials and LOS in the upper 1.5 m never exceeded 15%. Extreme increases in CO_2 and decreases in O_2 didn't appear until 2 m BGS (in the LOS), even in treatments with thinner covers such as Treatment 1A and 1B (0.3 m peat overlying LOS). Based on soil gas profiles, it appears that adequate soil-atmosphere gas exchange takes place in the upper 1.5 m regardless of whether LOS is present at that depth. Pore-gas

O_2 and CO_2 concentrations in the upper 1.5 m were within the range of values considered safe for reclamation vegetation and are not likely to pose a risk of O_2 deficiency or CO_2 toxicity for reclamation vegetation. Notwithstanding potential issues related to the transport and storage of moisture and penetrability to plant roots into the LOS, these findings hint at the possibility that a soil cover may not be needed to achieve adequate aeration in the upper 1.5 m.

Pore-gas concentrations in LOS at depths below approximately 1.5 m were frequently less than 10% for O_2 and greater than 15% for CO_2, which may reflect PHC degradation and CH_4 oxidation. It should be noted that PHC degradation and CH_4 oxidation may also be occurring at depths shallower than 1.5 m when LOS was present, however, sufficient soil-atmosphere gas exchange is likely replenishing O_2 in the pore space and preventing the buildup of CO_2. At a nearby undisturbed site with coarse-textured subsoil material, near atmospheric pore-gas O_2, low CO_2, and undetectable CH_4 appeared to indicate that soils within undisturbed boreal forests are likely to be well-aerated and exhibit negligible methane production or oxidation (data not reported). However, the natural site is not entirely like the reclamation study sites. The soil texture characteristics of the natural site are similar to the LFH and subsoil reclamation soil cover materials, but there is no finer textured and PHC containing material present within the depth investigated (4 m) like LOS. Finer textured soils have been characterised to have low concentrations of pore-gas O_2 (Bakker and Bronswijk 1993), however, due to the variable PHC content of the LOS it was not possible to directly compare O_2 and CO_2 pore-gas concentrations in the LOS to literature values.

The selection of soil cover material and placement thickness also plays an important role in soil-atmosphere gas exchange. During the 2014 field season, pore-gas CH_4 concentrations from 2-3 m BGS on Treatment 1B (0.3 m peat soil cover) averaged between 18.8-24.8% in the LOS, with individual measurements surpassing 35%. However, CH_4 was mostly removed at a depth of 1 m (0.70 m below the peat soil cover), which indicates CH_4 was produced deeper in the LOS (under near-anaerobic concentrations) and oxidized within the upper portion of the LOS (where O_2 concentrations are near-atmospheric). High CH_4 concentrations in the 0.3 m

peat soil cover treatment may be attributed to moisture in the peat layer remaining frozen until late-June (as inferred from sub-0˚C temperatures measured by temperature probes installed at 0.25 m BGS), which restricts soil-atmosphere gas exchange by acting as a barrier to gas movement. It appears that the CH_4 that had accumulated beneath the frozen peat layer and then was slowly released during the growing season after the peat layer thawed. This would explain the higher CH_4 concentrations in June and the gradual decrease to the end of October.

3.5.3 Diffusion and advection

Significant differences in diffusive fluxes were observed in the various soil cover treatments and LOS due to variations in soil-atmosphere concentration gradients and diffusion coefficient estimations. Spatial variations in O_2 and CO_2 soil-atmosphere concentration gradients may be indicative of localized zones of microbial degradation, methane oxidation and/or respiration. The range of diffusion coefficients estimated for each soil cover material and LOS varied as a result of differences in soil texture, moisture, and temperature. Advective fluxes varied significantly in the various soil cover treatments and LOS. These differences can be attributed to differential pressures and air permeability varying spatially by orders of magnitude.

The study found that advection dominated over diffusion in all treatments for O_2 and CO_2 except for Treatment 6 (0.2 m LFH and 1.3 m Subsoil), which had the lowest F_A/F_D for O_2 and was diffusion dominated for CO_2. Note that Treatment 6 had the lowest F_A/F_D for O_2 and CO_2 due to having the highest diffusive fluxes of all treatments (see Figure 3.14). These findings suggest that this location may have been either a localized zone of microbial degradation and methane oxidation, and/or the LOS was coarser-grained and quickly responded to barometric pressure fluctuations. However, it is more likely that Treatment 6 was coarser-grained since the LOS at this location had the lowest average bulk density based on a characterization of the bulk density of LOS at the ASCS in 2010 by AITF (2013) with the CPN® MC-1 DR-P Portaprobe Moisture/Density Gauge (CPN Inc., Concord, California, USA). The dominance of advective fluxes over diffusive fluxes for the other treatments may be partially explained by the cover soils being relatively coarse-textured and the ASCS lacking shelter from wind gusts

(which induce near-surface pressure changes). Ratios of O_2 advection to diffusion were highest in Group A soils with <1.5 m cover thickness (Treatment 1A and 1B – 0.3 m and Treatment 2 – 1.0 m). Soil gas profiles indicate that thinner soil covers had lower soil-atmosphere concentration gradients than thicker cover soils. These low concentration gradients, in combination with relatively higher air permeability values, resulted in 0.3 m soil covers being advection-dominated to a higher degree than the thicker soil covers. When comparing O_2 advective and diffusive fluxes in 1.5 m soil covers, Group D soils with 0.1-0.3 m peat or 1.4-1.2 m multi-layered subsoils tended to have low advective fluxes and F_A/F_D, which is possibly explained by the peat layer having a large air-filled pore volume capable of quickly responding to variations in barometric pressures.

3.5.4 Comparison of direct and indirect flux measurements

SFC measurements on Treatment 5B and SVP measurements on Treatment 5A were located roughly 300 m apart at different cells at the ASCS. The Treatment 8 SFC and the Treatments 8A, 8B, and 8C SVPs, however, were within the same one hectare cell. Comparison of O_2 and CO_2 flux rates determined from direct measurements (SFC) and indirect measurements (SVP) for Group C soils (Treatments 5A and 5B) and Group D soils (Treatments 8A, 8B, 8C, and 8D) are presented in Table 3.5.

Table 3.5 O_2 and CO_2 fluxes determined by direct (static flux chamber) and indirect (soil vapour probes) methods for Group D soils (0.3 m peat and 1.2 m multi-layered subsoil)

Group	Treatment[1]	Sampling technique[2]	O_2 fluxes ($kg/m^2/a$)	CO_2 fluxes ($kg/m^2/a$)
C	5A	SVP	6.0	0.93
	5B	**SFC**	**7.5**	**1.4**
D	8A	SVP	19.6	2.4
	8B	SVP	14.6	2.3
	8C	SVP	16.4	1.8
	8D	**SFC**	**18.0**	**2.3**

[1] Letters indicate replicate cells of treatments.
[2] SVP = soil vapour probe; SFC = static flux chamber.

For Group C soils located on different cells at the ASCS, gas fluxes of O_2 were 20% different and gas fluxes of CO_2 were 34% different between direct SFC measurements and indirect calculations made with pressure and concentration measurements in the SVP. For Group D

soils located within the same 1 hectare cell, O_2 fluxes were more comparable with 9-19% differences and CO_2 fluxes were also more comparable with 0-22% differences between direct and indirect methods. Both the direct and indirect methods worked well to quantify gas fluxes through soil covers and results from the two methodologies were reasonably close when taking into account spatiotemporal differences.

3.6 Conclusions

This objective of this paper was to develop an understanding of pore-gas dynamics in LOS and reclamation soil covers by i) characterising pore-gasses at various depths in the soil covers and LOS; ii) directly measuring O_2 ingress and CO_2 efflux using static flux chambers; iii) indirectly measuring O_2 fluxes by diffusion and advection; and iv) quantifying the importance of diffusion and advection to O_2 and CO_2 gas transport.

Soil-atmosphere gas exchange occurred at a sufficient rate to a depth of 1.5 m into the soil covers and uppermost LOS horizon such that pore-gas concentrations of O_2 and CO_2 were typically below the threshold that poses a risk to the growth and survivability of reclamation vegetation (>15% CO_2 and <10% O_2). Deeper into the LOS landform, however, pore-gas concentrations of O_2 and CO_2 frequently surpassed the threshold considered to pose a risk to plant growth and survivability. Pore-gas CH_4 within the LOS landform was typically detected at concentrations <1.7% other than one location where CH_4 concentrations peaked at >35%.

The novel subsurface flux chamber that was custom designed and fabricated for this study successfully enabled the direct measurement of O_2 ingress through multi-layered soil covers and CO_2 efflux from the LOS landform into the soil covers. Fluxes of O_2 and CO_2 directly measured with the subsurface chamber were comparable to fluxes of O_2 and CO_2 indirectly measured from concentration-gradient driven diffusion and pressure-gradient driven advection.

Transport of O_2 and CO_2 across the cover soils was dominated by advection for all treatments except for one location where the uppermost LOS horizon had been placed to a lower bulk density (1.45 Mg/m^3) and responded quickly to variations in barometric pressure.

Acknowledgements

Funding for this research was supported by COSIA (Canadian Oil Sands Innovation Alliance). We would like to thank staff at Syncrude Canada Ltd. in Edmonton, AB and Fort McMurray, AB and O'Kane Consultants for their assistance with the field work.

References

Aachib M, Mbonimpa M, and Aubertin M. 2004. **Measurement and Prediction of the Oxygen Diffusion Coefficient in Unsaturated Media, with Applications to Soil Covers**. Water, Air, and Soil Pollution, Volume (156): 163-194. DOI: 10.1023/B:WATE.0000036803.84061.e5

AITF (Alberta Innovates Technology Futures). 2013. **Bulk Density Characterization of Surface Reclamation Cover Soil for the Aurora Capping Study**. Prepared for Marty Yarmuch, Syncrude Canada, Ltd. by B. Drozdowski, A. Underwood, D. Degenhardt, and R. Faught.

Alberta Energy. 2016. **About Oil Sands: Facts and Statistics**. [Accessed October 2016] Available at: http://www.energy.alberta.ca/oilsands/791.asp

American Society for Testing and Materials (ASTM).2008. **D-6836-02**: **Standard Test Methods for Determination of the Soil Water Characteristic Curve for Desorption Using a Hanging Column, Pressure Extractor, Chilled Mirror Hygrometer, and/or Centrifuge**. Annual Book of ASTM Standards, Vol. 4.09. ASTM. Philadelphia, Pa. DOI: 10.1520/D6836-02R08E02

American Society for Testing and Materials (ASTM).2007. **D-422-63**: **Standard Test Method for Particle-Size Analysis of Soils**. ASTM. Philadelphia, Pa. DOI: 10.1520/D0422-63R07E02

Auer LH, Rosenberg ND, Birdsell KH, and Whitney EM. 1996. **The Effects of Barometric Pumping on Contaminant Transport**. Journal of Contaminant Hydrology. (24) 145-166. DOI: 10.1016/S0169-7722(96)00010-1

Bakker DM and Bronswijk JJB. 1993. **Heterogeneous oxygen concentrations in a structure clay soil**. Soil Science. (155): 309-315. DOI: 10.1097/00010694-199305000-00001

Barber LA, Bocksette J, Christensen DO, Tallon, LK, and Landhausser SM. 2015. **Effect of Soil Cover System Design on Cover System Performance and Early Tree Establishment**. Mine Closure 2015, Vancouver, Canada.

Bartholomeus RP, Witte JP, Bodegom PM, Van Dam JC, and Aerts R. 2008. **Critical Soil Conditions for Oxygen Stress to Plant Roots: Substituting the Feddes-function by a Process-based Model**. Journal of Hydrology (360): 147-165. DOI: 10.1016/j.jhydrol.2008.07.029

Buckingham E. 1904. **Contributions to our Knowledge of Aeration of Soils**. Bulletin 25. Bureau of Soils, U.S. Department of Agriculture, Washington, D.C.

CAPP (Canadian Association of Petroleum Producers). 2016. **Basic Statistics**. [Accessed October 2016] Available at: http://www.capp.ca/publications-and-statistics/statistics/basic-statistics

Chang HT and Loomis WE 1955. **Effect of carbon dioxide on absorption of water and nutrients by roots**. Plant Physiology. (30): 155-161.

Columbus Instruments. 2016. **User's Manual for Model 180C**.

Dane and Topp. 2002. **Water Retention and Storage. Pages 671-697 in Methods of Soil Analysis Part 4 – Physical Methods**. Soil Science Society of America Inc. Madison, Wisconsin.

Darcy H. 1856. **Les Fontaines Publiques de la Ville de Dijon**. Victor Dalmont, Paris, France. DOI: 10.1061/40683(2003)5

Davidson EA, Savage K, Verchot LV, and Navarro R. 2002. **Minimizing Artifacts and Biases in Chamber-based Measurements of Soil Respiration. Agricultural and Forest Meteorology**. (113): 21-37. DOI: 10.1016/S0168-1923(02)00100-4

Deepagoda T, Moldrup P, Schjonning P, Kawamoto K, and Komatsu T. 2011. **Density-Corrected Models for Gas Diffusivity and Air Permeability in Unsaturated Soil**. Vadose Zone Journal. (10): 226-238. DOI: 10.2136/vzj2009.0137.

Elberling B, Larsen F, Christensen S, and Postma D. 1998. **Gas Transport in a Confined Unsaturated Zone during Atmospheric Pressure Cycles**. Water Resources Research. (34): 2855-2862. DOI: 0043-1397/98/98WR-0237

Elberling B, Nicholson RV, and David DJ. 1993. **Field Evaluation of Sulphide Oxidation Rates**. Nordic Hydrology. (24): 323-338.

Fick A. 1855. **On liquid diffusion**. Ann. Phys. (170): 59–86. doi:10.1002/andp.18551700105. 94: 59

Flower, FB. 1981. **Landfill gas, what it does to trees and how its injurious effects may be prevented**. Journal of Arboriculture. (7): 43-52

Fukuda H. 1955. **Air and Vapor Movement in Soil Due to Wind Gustiness**. Soil Science (79): 249-256.

Geigenberger P. 2003. **Response of plant metabolism to too little oxygen**. Current Opinion in Plant Biology. (6): 247–256. *DOI*: 10.1016/S1369-5266(03)00038-4

Government of Alberta. 2007. **Alberta Environmental Protection and Enhancement Act of 2007**. Alberta Queen's Printer, Edmonton, Alberta.

Grischenkov, V. et. Al. 1999. **Degradation of Petroleum Hydrocarbons by Facultative Anaerobic Bacteria under Aerobic and Anaerobic Conditions**. Process Biochemistry. (35): 889-896. DOI: 10.1016/S0032-9592(99)00145-4

Heinemeyer A and McNamara NP. 2011. **Comparing the Closed Static versus the Closed Dynamic Chamber Flux Methodology: Implications for Soil Respiration Studies**. Plant Soil. (346): 145-151. DOI: 10.1007/s11104-011-0804-0

Hillel D. 2003. **Introduction to Environmental Soil Physics**. Academic Press.

Huang M, Barbour SL, and Rodger H. 2015. **An Evaluation of Air Permeability Measurements to Characterise the Saturated Hydraulic Conductivity of Soil Reclamation Covers**. Canadian Journal of Soil Science. (95): 15-26. DOI: 10.4141/CJSS-2014-072

Hutchinson GL, Livingston GP, Healy RW, and Striegl RG. 2000. **Chamber Measurement of Surface-atmosphere Trace Gas Exchange: Numerical Evaluation of Dependence on Soil, Interfacial Layer, and Source/sink Properties**. Journal of Geophysical Research. (105): 8865-8875. DOI: 1 0.1029/1999JD901204

Kim H and Benson CH. 2004. **Contributions of Advective and Diffusive Oxygen Transport through Multilayer Composite Caps over Mine Waste**. Journal of Contaminant Hydrology. (71): 193-218.DOI: 10.1016/j.jconhyd.2003.10.001

Kjeldsen P and Scheutz C. 2005. **Biodegradation of Trace Gasses in Simulated Landfill Soil. Journal of the Air & Waste Management Association**. (55): 878-885. DOI: 10.1080/10473289.2005.10464693.

Kozlowski T. 1985. **Soil aeration, flooding, and tree growth. Journal of Arboriculture**. (11:3).

Kroetsch DJ, Geng X, Chang SX, Saurette DD. 2011. **Organic Soils of Canada: Part 1: Wetland Organic Soils.** Canadian Journal of Soil Science. (91): 807-822 DOI: 10.4141/CJSS10043

Leone IA. Flower FB, Arthur JJ, and Gilman EF. 1977. **Damage to woody species by anaerobic landfill gasses**. Journal of Arboriculture.(3): 221-225

LandTEC. 2010. **GEM™2000 and GEM™2000 Plus Gas Analyser and Extraction Monitor Operation Manual**. LandTEC North America, Colton, California, USA.

Marshall TJ. 1959. **The Diffusion of Gasses through Porous Media**. Journal Soil Science. (10): 79-82.

Massman WJ. 2006. **Advective transport of CO2 in permeable media induced byatmospheric pressure fluctuations: 1 An analytical model**. Journal of Geophysical Research. (111). DOI: 10.1029/2006JG000163

Millington R and Quirk J. 1960. **Transport in Porous Media**. In Trans. 7th Intl. Congr. Soil. Sci. Vol. 1.

Millington R and Quirk J. 1961. **Permeability of Porous Solids**. Transactions of the Faraday Society. (57): 1200-1207. DOI: 10.1039/TF9615701200

Moldrup P, Olesen T, Gamst J, Schjonning P, Yamaguchi T, and Rolston DE. 2000. **Predicting the Gas Diffusion Coefficient in Repacked Soil.** Science Society of America Journal. (64): 1588-1594. DOI: 10.2136/sssaj2000.6451588x

Moldrup P, Olesen T, Rolston DE, and Yamaguchi T. 1997. **Moldeling Diffusion and Reaction in Soils: VII. Predicting Gas and Ion Diffusivity in Undisturbed and Sieved Soils**. Soil Science. (162): 632-640. DOI: 10.1097/00010694-199706000-00002

Molins S and Mayer KU. 2007. **Coupling between geochemical reactions and multicomponent gas and solute transport in unsaturated media: A reactive transport modeling study**. Water Resources Research. (43) DOI: 10.1029/2006WR005206

Nay SM, Mattson KG, and Bormann BT. 1994. **Biases of Chamber Methods for Measuring Soil CO2 Efflux Demonstrated with a Laboratory Apparatus.** Ecology. (75): 2460-2463.

Nilson RH, Peterson EW, Lie KH, Burkhard NR, and Hearst JR. 1991. **Atmospheric Pumping: A mechanism Causing Vertical Transport of Contaminated Gasses through Fractured Permeable Media**. Journal of Geophysical Research. (96): 933-948.

Penman HL. 1940. **Gas and Vapor Movement in Soil: The Diffusion of Vapors through Porous Solids**. Journal of Agricultural Science. (30): 437-462. DOI: 10.1017/S0021859600048164

Pernitsky T, Si B, Barbour SL, and Hu W. 2016. **Effects of Petroleum Hydrocarbon Concentration and Bulk Density on the Hydraulic Properties of Lean Oil Sand Overburden**. Canadian Journal of Soil Science. In Publication. DOI: 10.1139/CJSS-2015-0126

Pezeshki SR, Pardue JH, and Delaune RD. 1993. **The Influence of Soil Oxygen Deficiency on Alcohol Dehydrogenase Activity, Root Porosity, Ethylene Production and Photosynthesis in Spartina Patens.** Environmental and Experimental Botany. (33): 565-573.

Pihlatie MK, Christiansen JR, Aaltonen H, Korhonen JF, Nordbo A, Rasilo T, Benanti G. Giebels M, Helmy M, Sheehy J, Jones S, Juszczak R, Klefoth R, Lobo-do-Vale R, Rosa AP, Schreiber P, Serca D, Vicca S, Wolf B, and Pumpanen J. 2013. **Comparison of Static Chambers to Measure CH4 Emissions from Soils**. Agricultural and Forest Meteorology. (171-172): 124-136. DOI: 10.1016/j.agrformet.2012.11.008

Poulsen T, Christophersen M, Moldrup P, and Kjeldsen P. 2003. **Relating Landfill Gas Emissions to Atmospheric Pressure using Numerical Modelling and State-space Analysis**. Waste Management and Research. (21): 356-366. DOI: 10.1177/0734242X0302100408.

Pumpanen J, Kolari P, Ilvesniemi H, Minkkinen K, Vesala T, Niinistö S, Lohila A, Larmola T, Morero M, Pihlatie M, Janssens I, Yuste JC, Grünzweig JM, Reth S, Subke JA, Savage K, Kutsch W, Østreng G, Ziegler W, Anthoni P, Lindroth A, Hari P. 2004. **Comparison of Different Chamber Techniques for Measuring Soil CO2 Efflux**. Agricultural and Forest Meteorology. (123): 159-176. DOI: 10.1016/j.agrformet.2003.12.001

Redecker KR, Baird AJ, and The YA. 2015. **Quantifying Wind and Pressure Effects on Trace Gas Fluxes Across the Soil-Atmosphere Interface**. Biogeosciences. (12): 7423-7434. DOI: 10.5194/bg-12-7423-2015

Rowland SM. 2009. **Recreating a functioning forest soil in reclaimed oil sands in northern Alberta: an approach for measuring success in ecological restoration**. Journal of Environmental Quality. (4): 1580-1590. DOI: 10.2134/jeq2008.0317.

Salminen JM, Tuomi PM, Suortti A-M, and Jorgensen KS. 2004. **Potential for Aerobic and Anaerobic Biodegradation of Petroleum Hydrocarbons in Boreal Subsurface**. Biodegradation. (15): 29-39. DOI: 10.1023/B:BIOD.0000009954.21526.e8

Seely GE, Falta RW, and Hunt JR. 1994. **Buoyant Advection of Gasses in Unsaturated Soil. Journal of Environmental Engineering**. (120): 1230-1247. DOI: 10.1061/(ASCE)0733-9372(1994)120:5(1230)

Thorstenson DC and Pollock DW. 1989. **Gas Transport in Unsaturated Zones: Multicomponent Systems and the Adequacy of Fick's Laws**. Water Resources Research. (25): 477-507. DOI: 10.1029/WR025i003p00477

Wong MH. 1988. **Soil and plant characteristics of landfill sites near Merseyside, England**. Environmental Management. (12): 491-499

Whitton BA, Chan GYS, and Wong MH. 1991. **Effects of Landfill Gas on Subtropical Woody Plants**. Environmental Management. 15(3): 411-431.

Zettl J, Huang M, Barbour SL, Barber L. 2012. **Field Air Permeability Testing to Characterise the Hydraulic Conductivity of Coarse Textured Reclamation Covers over Uranium Mine Waste**. Geo Manitoba. Paper 320, p. 7-25.

4.0 SOIL COLUMN EXPERIMENTS TO QUANTIFY METHANE OXIDATION RATES IN OVERBURDEN AND RECLAMATION SOIL COVERS

Preface

Engineered soil cover systems are capable of passively removing gaseous methane with microbial reduction and oxidation reactions. Methane oxidation rates were quantified for peat, LFH, subsoil, and lean oil sand using batch soil column experiments. Loading rates of methane to the soil column were based on CO_2 fluxes that were characterised in a preliminary study to range from 0.1-7.1 kg $CH_4/m^2/a$; higher loading rates up to 30 $kg/m^2/a$ were also tested in the column experiments. Gas concentrations were measured with continuous, non-dispersive infrared gas analysers capable of measuring 0-30% CO_2 and CH_4 and a paramagnetic gas analyser capable of measuring 0-100% O_2. Variations in temperature were simulated by placing the soil columns in climate chambers at 4°C, 22°C, and >31°C. Reduced soil moisture was simulated by discontinuing the daily application of water to the multi-layered soil column for 45 days. Increased bulk density was simulated by running experiments with a column compacted to a dry bulk density of 1500 kg/m^3 and then de-constructing the column and re-packing to 1800 kg/m^3. This research is important to predict whether CH_4 produced by methanogenic biodegradation of petroleum hydrocarbon substrates will be passively consumed in the engineered soil cover systems overlying the lean oil sands and/ or the uppermost horizon of lean oil sands.

Reference: Scale KO and Fleming IR. 2017. **Soil Column Experiments to Quantify Methane Oxidation Rates in Overburden and Reclamation Soil Covers.** Submitted to International Journal of Mining, Reclamation and Environment, March 2017.

Abstract

Methane oxidation rates were quantified using soil column experiments for three reclamation soil cover materials in single and multi-layer configurations and for lean oil sands salvaged from an oil sands mine in Alberta, Canada. Methane fluxes from the lean oil sands were characterized in a previous study to range between 0.1-7.1 kg $CH_4/m^2/a$; however, lower and higher CH_4 loading rates were also tested in the column experiments to account for slow leaks and fugitive

emissions. The effects of variations in temperature, soil moisture, and bulk density were simulated. Oxidation rates were significantly higher for all soil materials and lean oil sands at temperatures >31˚C and were higher at 22˚C than 4˚C. Daily application of water for the multi-layered soil column was discontinued for 45 days and oxidation rates decreased from 80% efficiency to 38%. Dry bulk density for the sandy subsoil material was increased from 1500 to 1800 kg/m^3 and oxidation rates decreased by more than 35%. The transient soil column batch experiment method used in this study enabled oxidation rates to be quantified for expected CH_4 loads (0.5-1 kg/m^2/a) and for expected temperatures (≤22°C). At CH_4 loads >10 kg/m^2/a and at temperatures >31°C, however, the experiments were limited by the finite volume of O_2 in the columns.

4.1 Introduction

Reclaiming areas disturbed by open-pit mining to an “equivalent land capability” is a significant priority and challenge for the oilsands industry in Alberta, Canada. Large above-grade overburden landforms are amassed during the mine operation when LOS is trans-located to dedicated disposal areas in order to access underlying oil sand deposits. The overburden substrate consists of low-concentration “lean” oil sands (LOS) with a petroleum hydrocarbon (PHC) concentration up to the economical ore grade concentration of 7%.The placement of single and multi-layered soil cover systems above the LOS landform is an effective strategy for upland reclamation whilst taking into consideration soil material type, horizon configuration, and capping thickness to facilitate the growth of native boreal plant and tree species. The Aurora soil capping study (ASCS) is a field-scale soil cover testing program at the Syncrude Canada Ltd. Aurora North mine (57°20’ N, -111° 32’, Figure 4.1 below) that was constructed to evaluate the efficacy of various textural materials and capping thicknesses placed in single and multi-layer configurations.

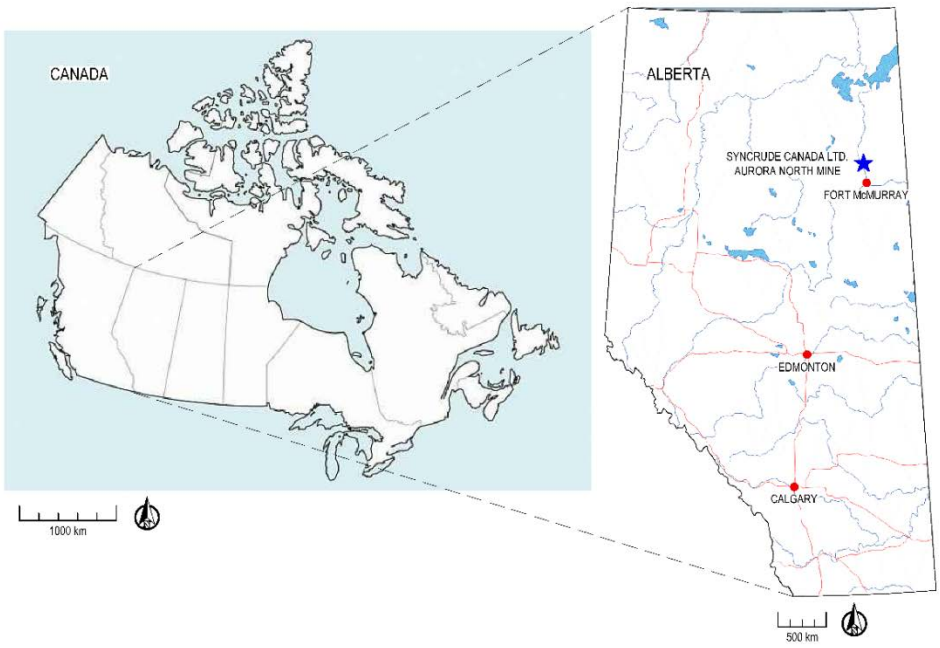

Figure 4.1 Map showing the location of Alberta in Canada (left). Map of Alberta showing the location of Syncrude's Aurora North mine (right)

The primary function of the soil covers is to provide moisture and nutrients to reclamation vegetation; however, since the soil covers are biologically active, they consume methane gas (CH_4) produced during the methanogenic degradation of the PHC component of LOS (under methanogenic conditions) in biochemical redox reactions (CH_4 oxidation). Soil covers are proven to be an effective and economically viable strategy for reducing CH_4 emissions from landfills (Huber and Lechner 1999), however, the consumption of plant available oxygen (O_2) in the aerobic zone of the soil covers could be problematic for the growth and metabolism of newly introduced reclamation vegetation (Bartholomeus et al 2008).

The laboratory study presented herein is intended to supplement the multi-disciplinary research conducted at the ASCS (see Barber et al 2015) by quantifying CH_4 oxidation rates in soil cover materials and LOS using transient “batch” soil column experiments. The materials characterised were locally-salvaged soils (peat, subsoil, LFH) and LOS. The soils and LOS were tested in single and multi-layered configurations over the expected range of CH_4 fluxes

that were characterised in preliminary gas sampling carried out by Korbas (2014). Effects of variations in temperature, moisture content, and bulk density were simulated.

4.2 Background

4.3 Preliminary pore-gas and gas flux characterization at the ASCS

The LOS at the ASCS was characterised for CO_2 fluxes and CH_4 pore-gas concentrations by Korbas (2014) prior to placement of soil covers. The methodology and results of the site characterization are described in detail in Korbas (2014) and Scale et al (2016). Pore-gas O_2 concentrations were found to decrease from 15% in the upper 2 m to near-anaerobic in the lower 4-5 m below ground surface (BGS). Key findings from gas sampling events conducted over a 2 year period were that soil-atmosphere CO_2 fluxes ranged from 0.1-7.1 kg/m^2/a (Scale et al 2016).

4.4 Theory

4.4.1 Factors affecting CH_4 oxidation

The relationship between soil moisture and CH_4 oxidation has been researched extensively for landfill cover soils and has been found to strongly correlate to CH_4 oxidation (Boeckx et al 1996; Czepiel et al 1996; Whalen and Reeburgh 1996, Bogner 1997; Christophersen 2001; Stein and Hettiaratchi 2001; Scheutz and Kjeldsen 2004; Zeiss 2005; Einola et al 2007; Gebert et al 2011a). The effects of soil moisture on CH_4 oxidation arise from restrictions in O_2 and CH_4 diffusivity at high moisture contents (Dorr et al 1993; Boeckx et al 1996; Moldrup 1996; Borjesson and Svensson 1997; De Visscher and Van Cleemput 2003; Aachib et al 2004; Molins et al 2008; Gebert et al 2011) and physiological stresses to microbial populations at low moisture contents (Whalen et al 1990; Boeckx et al 1996; King 1997; Borjesson 2004). The relationship between soil moisture and CH_4 oxidation therefore tends to be non-linear and parabolic, with oxidation rates being reduced at high and low moisture contents (Eionola et al 2007). Optimal ranges of gravimetric moisture contents to facilitate CH_4 oxidation depend on soil texture, but typically ranges from 11-28%, with upper and lower limits of ≤ 3-7% and ≥ 30-41% (Whalen et al 1990; Czepiel 1996; Boeckx 1996; Stein and Hettiaratchi 2001; Einola 2007).

The relationship between soil temperature and CH_4 oxidation has also been well-documented for landfill cover soils (Whalen 1991; Czepiel 1996; Humer and Lechner 1999; Christophersen 2001; Borjesson 2004; Einola 2007; Hettiaratchi 2011). It has been noted, however, that soil temperature is less influential to CH_4 oxidation rates than soil moisture content (King and Adamsen 1992; Adamsen and King 1993; Boeckx 1996). Similar to soil moisture, temperature affects CH_4 oxidation by altering both the diffusivity of CH_4 and O_2 and the physiology of microbial populations (De Visscher and Van Cleemput 2003; Borjesson et al 2004; Scheutz and Kjeldsen 2004; Mohanty et al 2007). Optimal soil temperatures to facilitate CH_4 oxidation typically range from approximately 20-38°C, with upper and lower limits of ≤ 5°C and ≥ 40°C (Whalen et al 1990; King and Adamsen 1992; Humer and Lechner 1999; Gebert et al 2003; Borjesson et al 2004; Scheutz and Kjeldsen 2004; Einola et al 2007; Mohanty et al 2007).

Bulk density is related to total soil porosity, which is related to air-filled porosity by soil moisture (Ball et al 1997; Hilel 2003). As previously stated, CH_4 oxidation rates are influenced by soil moisture and temperature due to restrictions in O_2 and CH_4 diffusivity (Dorr et al 1993; Boeckx et al 1996; Moldrup 1996; Borjesson and Svensson 1997; De Visscher and Van Cleemput 2003; Aachib et al 2004; Molins et al 2008; Gebert et al 2011a). Increasing bulk density, which may result from compaction during placement of a soil cover, can therefore lead to reductions in air-filled porosity and connectivity of the pores depending on the soil texture (Ball et al 1997; Gebert et al 2011a; Rachor et al 2011).

4.4.2 Guidelines for methane oxidation capacity of landfill soil covers

Estimated CH_4 oxidation rates for landfill soil covers vary significantly based on the texture of the soil as well as the field or laboratory testing methodology and (see Chanton 2009). Prior to 2013, CH_4 oxidation rates for landfill soil covers were mandated to be 10% of the CH_4 load by the US EPA greenhouse gas (GHG) reporting program (USEPA 1999). This 10% value was later revised to 10%, 25%, or 35% depending upon the field-specific conditions at the landfill (USEPA 2013). The problem with applying a fixed oxidation percentage is the

assumption that oxidation rates are a function of CH_4 loading and the capacity of the soil cover system to oxidize CH_4 scales indefinitely with CH_4 loads (Gebert et al 2011c).

An alternative criterion to assess the effectiveness of landfill cover soils is to compare oxidation rates to Austrian and German landfill guidelines, which recommend soil covers be capable of oxidizing CH_4 at a minimum rate of 3.1 kg/m^2/a (Stegmann 2006; Ritzkowski and Stegmann 2010; Gebert et al 2011c).

4.5 Materials & Methodology

4.5.1 Soil moisture probe

The Sentek® Diviner 2000™ capacitance moisture probe was used to measure water content profiles in soil columns over the duration of the soil column experiments (SenTek 1999). The Diviner 2000™ probe uses frequency domain reflectometry to determine the volumetric water content (VWC) within a zone projected radially into the soil approximately 0.01 m. Water content profiles were regularly measured in 0.05-0.1 m increments. The probe was calibrated for each soil prior to conducting the column experiments; the probe was re-calibrated for each soil after completing the column experiments.

4.5.2 Total alkalinity measurements

Total alkalinity measurements on samples of soil column leachate were conducted using the Mettler-Toledo® T50™ auto-titrator. Calibration of the pH meter was conducted on a weekly basis with laboratory-grade pH buffer solutions with pH values of 4, 7, and 10.

4.5.3 Design and construction of soil columns

Soil column experiments were conducted using custom-fabricated, stackable 1 m tall by 0.3048 m diameter Teflon-lined steel columns. Clean, washed gravel with a nominal particle size of 9 mm was placed to 0.1 m at the base of each column to serve as a drainage layer. The gravel was autoclaved using the Univclav® MJ-54™ to eliminate external microbial communities (Uniequip 2015). A 0.053 mm aperture size stainless steel mesh was placed between the gravel and soil materials to segregate soil materials while facilitating free drainage of water.

Soils were placed moist in the columns in thirty lifts of approximately 0.02 m with the goal to create a homogenous soil matrix and limit the formation of preferential flow paths. The Diviner 2000™ access tube was centred on the metal screen separating the gravel drainage layer and soils. Each lift was compacted using a custom-fabricated ram with curved outer and inner edges to facilitate compacting the circular outer perimeters of the column and Diviner 2000™ access tube. The upper 2-3 mm of each lift was manually scarified to promote hydraulic connectivity between layers (Plummer et al 2004).

Compaction was achieved to dry bulk density representative of field conditions as measured in a 2013 ASCS site survey that used a combination of CPN® MC-1 DR-P Portaprobe Moisture/Density Gauge and bulk density collar sampling techniques (AITF 2013). The dry bulk density levels achieved for each column are listed below:

- Peat = 700 kg/m^3; LFH = 1300 kg/m^3; LOS = 1500 kg/m^3; subsoil = 1500 kg/m^3 (initially); subsoil = 1800 kg/m^3 (re-compacted).

The multi-layered soil column (MLSC) setup is illustrated in Figure 4.2. Columns were sealed at the top to prevent intrusion of atmospheric gasses. The flowrate of CH_4 gas delivered to the column was measured using an Agilent ADM1000® placed in-line with gas flow. Flow rates were routinely verified by measuring the volume of exhaust gas collected over a known period of time at the top of the column using a Tedlar bag.

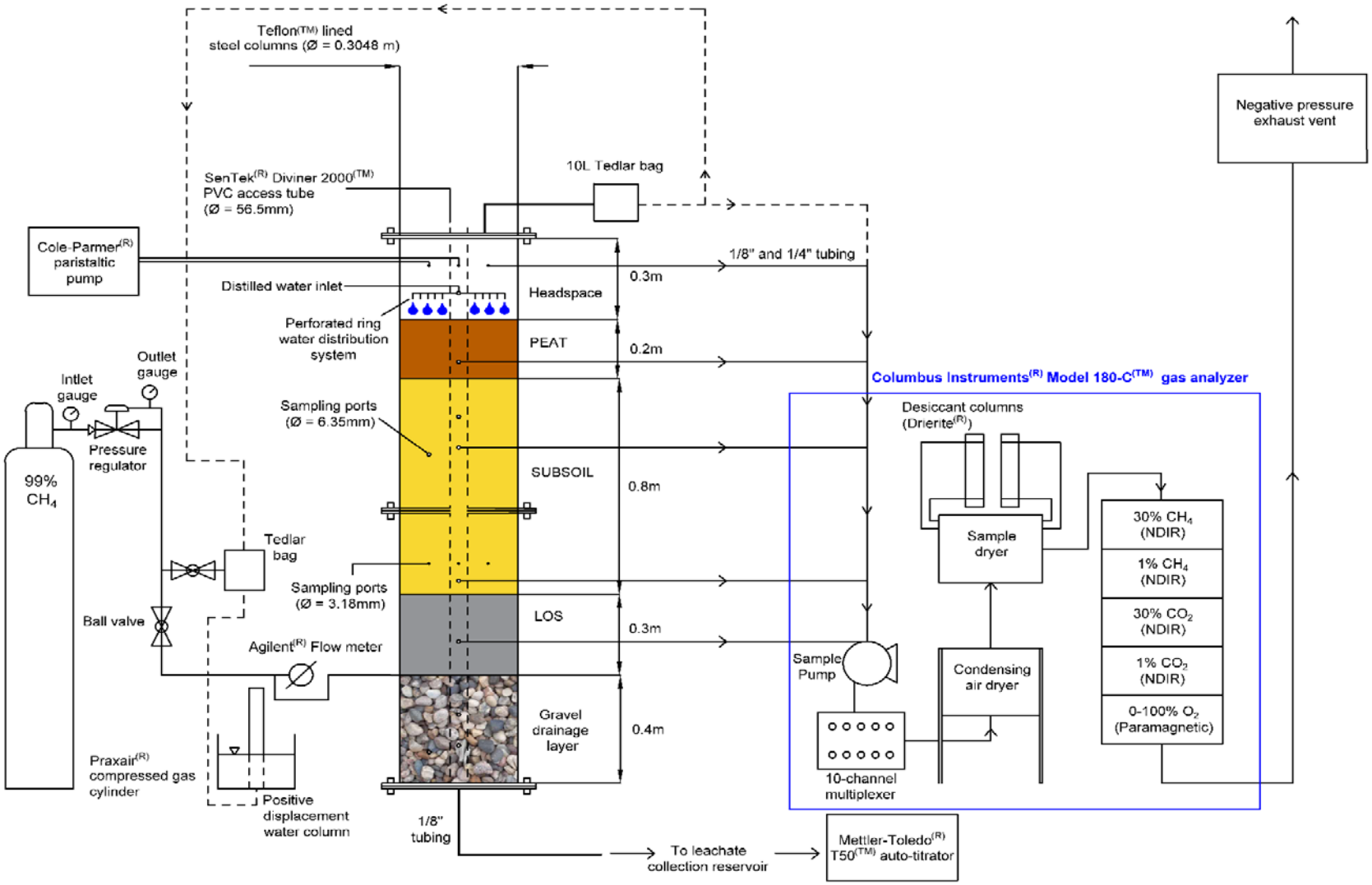

Figure 4.2 Illustration of the soil column setup used in the laboratory soil column experiments. (E.g. multi-layered column).

4.5.4 Soil column sampling procedure

The sampling procedure involved pumping 99.9% pure CH_4 (supplied by Praxair®) at known inlet rates into soil column(s) for periods of 22-48 hour whilst conducting initial and final mass balances on gasses in the soil column, headspace, and exhaust. Initial pore-gas concentrations, gas pressures, and temperatures were measured at 3-4 ports along the side of the column. Gas-tight Tedlar bags ranging in sizes of 0.001-0.01 m^3 (ESS 2015) were connected to a sampling port in the chamber headspace to mitigate buildup of pressures inside the headspace and enable the collection and monitoring of exhaust gasses.

At the end of each experiment, pore-gas concentrations in the column headspace and exhaust gasses were measured using the Columbus Instruments® Micro-Oxymax™ and Model 180C™ continuous O_2, CO_2, and CH_4 gas analysers (Columbus Instruments, Columbus, Ohio, USA). The pore-volume of gasses in the columns were approximated using air-filled porosity determined from regularly measured VWC profiles. A complete mass balance of gasses in the column before and after the experiment was conducted for each batch experiment. The stoichiometry of O_2 & CH_4 consumed and CO_2 produced was thusly determined for each experiment.

4.5.5 Column water addition and collection

Water dosage rates were calculated based on precipitation rates at the ASCS from May-November in 2014 and 2015 measured at an onsite MET station. The average rate of precipitation from May-November was 1.77 mm/day for 2014 and 1.19 mm/day for 2015. Dosage rates ranging from 45-90 mm/day were therefore applied to simulate the mean precipitation rate of 1.48 mm/day, whilst taking into account storage and evaporation in the overlying soil covers.

Pore-water samples were regularly collected from the bottom of the soil columns for measurement of pH and total alkalinity.

4.5.6 Loss on ignition

Loss on ignition (LOI) tests were conducted in a Thermo Scientific® BF51842PBC-1 Lindberg Blue M® Box Furnace to estimate the percentage of organic matter in the soil sample (Ball 1964). Organic matter starts to ignite when heated to approximately 200˚C and is completely depleted at 550˚C, the standard temperature at which LOI was correlated to the percentage of organic carbon determined using chromatography (Dean 1974).

4.6 Results

4.6.1 Percentage organic matter

LOI tests were conducted prior to constructing the soil columns in order to estimate the percentage of organic matter in the LFH, LOS, peat, and subsoil. Mean organic matter contents based on initial and final LOI testing were highest in peat (9.3%), followed by LOS (3.1%), LFH (1.6%), and lowest in subsoil (0.6%).

4.6.2 Diviner 2000™ VWC profiles

Mean VWC profiles measured with the Diviner 2000™ capacitance probe over the duration of the soil column experiments are presented in Figure 4.3. Minor variations in VWC were present in LFH, subsoil, and peat, which may indicate that the materials were not completely uniform. For the MLSC, peat retained more water than the subsoil or LOS. It appears that capillarity break effects occurred at the material interfaces, whilst a layering effect appears to have transpired in the middle of the subsoil at the height where the two columns were bolted together. The VWC profiles measured with the Diviner 2000™ appear to be lower on average than would be expected based on predictions from numerical solutions based on soil-water characteristic curves (Scale and Fleming (2016)). This discrepancy may be due to inadequate contact of soil particles with the Diviner 2000™ access tube or possibly due to density effects arising during packing the soil column or settling of particles over time.

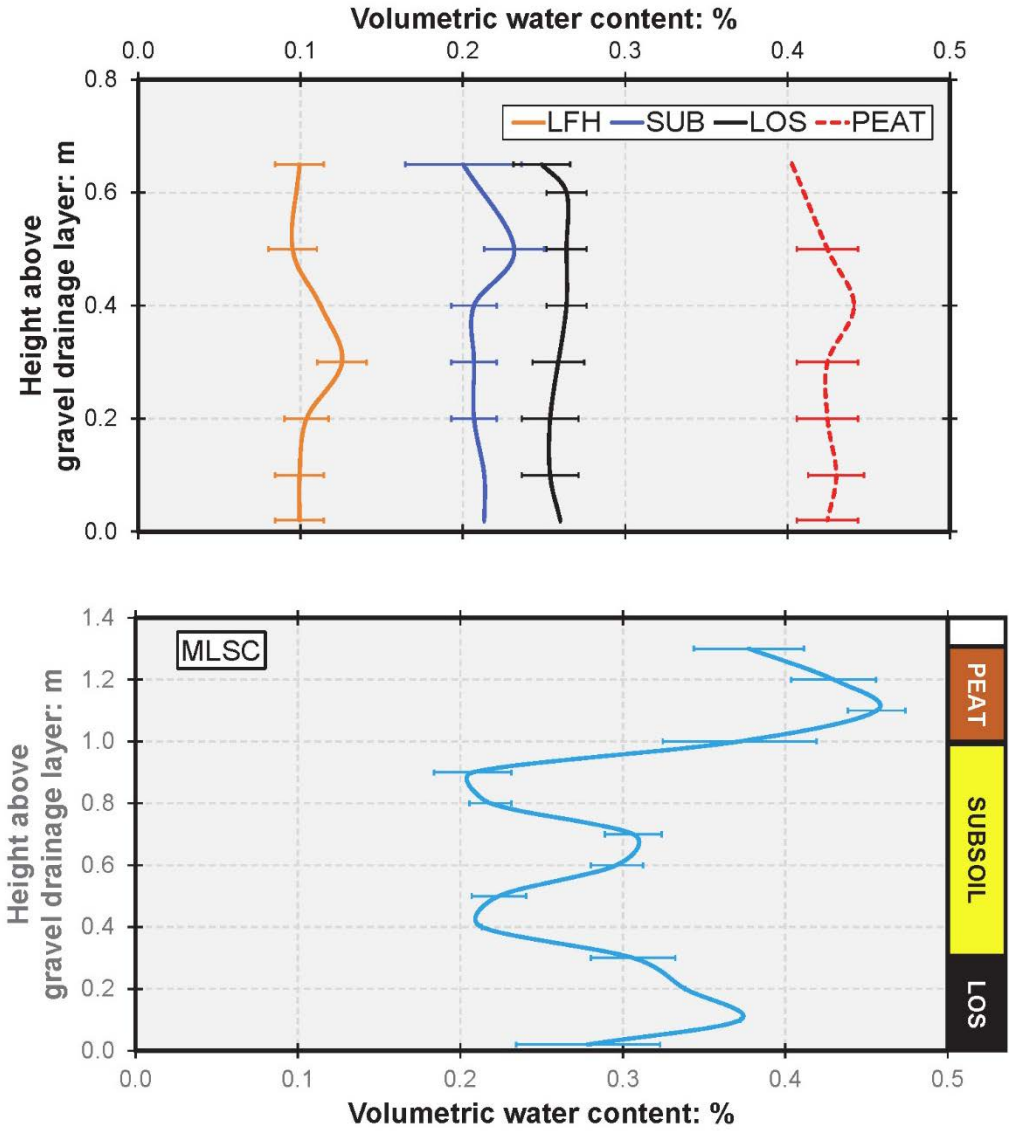

Figure 4.3 Mean volumetric water contents and standard deviations from the mean as measured in the individual soil columns and the multi-layered soil column over the course of the soil column experiments using the SenTek® Diviner 2000™ capacitance probe

4.6.3 Oxidation rates

Experimentally determined oxidation rates and efficiencies for the columns packed with individual soil cover materials (LFH, LOS, peat, and subsoil) and the MLSC column are presented in Table 4.1. Oxidation rates for the columns packed with individual soil cover materials (LFH, LOS, peat, and subsoil) are presented in Figure 4.4 below. Columns packed with LFH, LOS, and peat oxidized nearly 100% of the CH_4 added up to loading rates of 5 kg/m^2/a when placed in the climate chamber at temperatures >31°C. Columns at 22°C oxidized roughly 25-50% of the CH_4 added up to loading rates of 10 kg/m^2/a. At 4°C, however,

the soil columns were only capable of oxidizing 5-10% of the CH_4 added, which is equal to or less than the US EPA's minimum 10% CH_4 removal efficiency guidelines for a landfill cover soil (USEPA 2009). The subsoil column packed at a dry density of 1500 kg/m^3 at 22°C was deconstructed and re-compacted to a dry density of 1800 kg/m^3. At this higher dry density, however, oxidation rates were not able to be measured across CH_4 loads up to 30 kg/m^2/a. All soil cover materials and LOS surpassed the 3.1 kg/m^2/a oxidation rate recommended for German and Austrian landfill cover soils at temperatures >22°C (Stegmann 2006); however, none of the soil cover materials or LOS at 4°C were capable of oxidizing at 3.1 kg/m^2/a.

Table 4.1 Range of CH_4 removal rates and oxidation efficiencies for the MLSC, LFH, subsoil, peat, and LOS columns as determined with batch soil column experiments conducted at climate chamber temperatures of 4°C, 22°C, and >31°C. CH_4 removal rates and oxidation efficiencies for the subsoil column at a bulk density of 1800 kg/m^3 are not included.

			All tests		**4°C**		**22°C**		**31°C**	
			Min	**Max**	**Min**	**Max**	**Min**	**Max**	**Min**	**Max**
MLSC	CH_4 in	(kg/m^2/a)	0.3	14.1	N/A	N/A	0.3	14.1	N/A	N/A
	CH_4 rem.	(kg/m^2/a)	0.3	7.3	N/A	N/A	0.3	7.3	N/A	N/A
	Efficiency	(%)	38%	98%	N/A	N/A	38%	98%	N/A	N/A
LFH	CH_4 in	(kg/m^2/a)	0.1	22.8	0.2	13.8	0.1	3.8	0.2	3.4
	CH_4 rem.	(kg/m^2/a)	0.0	3.8	0.0	1.1	0.0	33.8	0.2	3.2
	Efficiency	(%)	4%	100%	4%	14%	19%	54%	95%	100%
SUB	CH_4 in	(kg/m^2/a)	0.1	33.8	0.1	23.7	0.2	4.6	N/A	N/A
	CH_4 rem.	(kg/m^2/a)	0.0	4.6	0.0	2.0	0.1	4.6	N/A	N/A
	Efficiency	(%)	5%	65%	6%	17%	14%	65%	N/A	N/A
PEAT	CH_4 in	(kg/m^2/a)	0.1	38.9	0.1	16.9	0.1	38.9	0.1	15.8
	CH_4 rem.	(kg/m^2/a)	0.0	9.1	0.0	1.1	0.1	6.3	0.1	9.1
	Efficiency	(%)	4%	100%	4%	12%	15%	51%	59%	100%
LOS	CH_4 in	(kg/m^2/a)	0.1	20.3	0.1	13.0	0.2	20.3	0.1	5.6
	CH_4 rem.	(kg/m^2/a)	0.0	4.6	0.0	1.3	0.1	4.3	0.1	4.6
	Efficiency	(%)	5%	99%	5%	12%	19%	54%	84%	99%

[1] N/A = not applicable

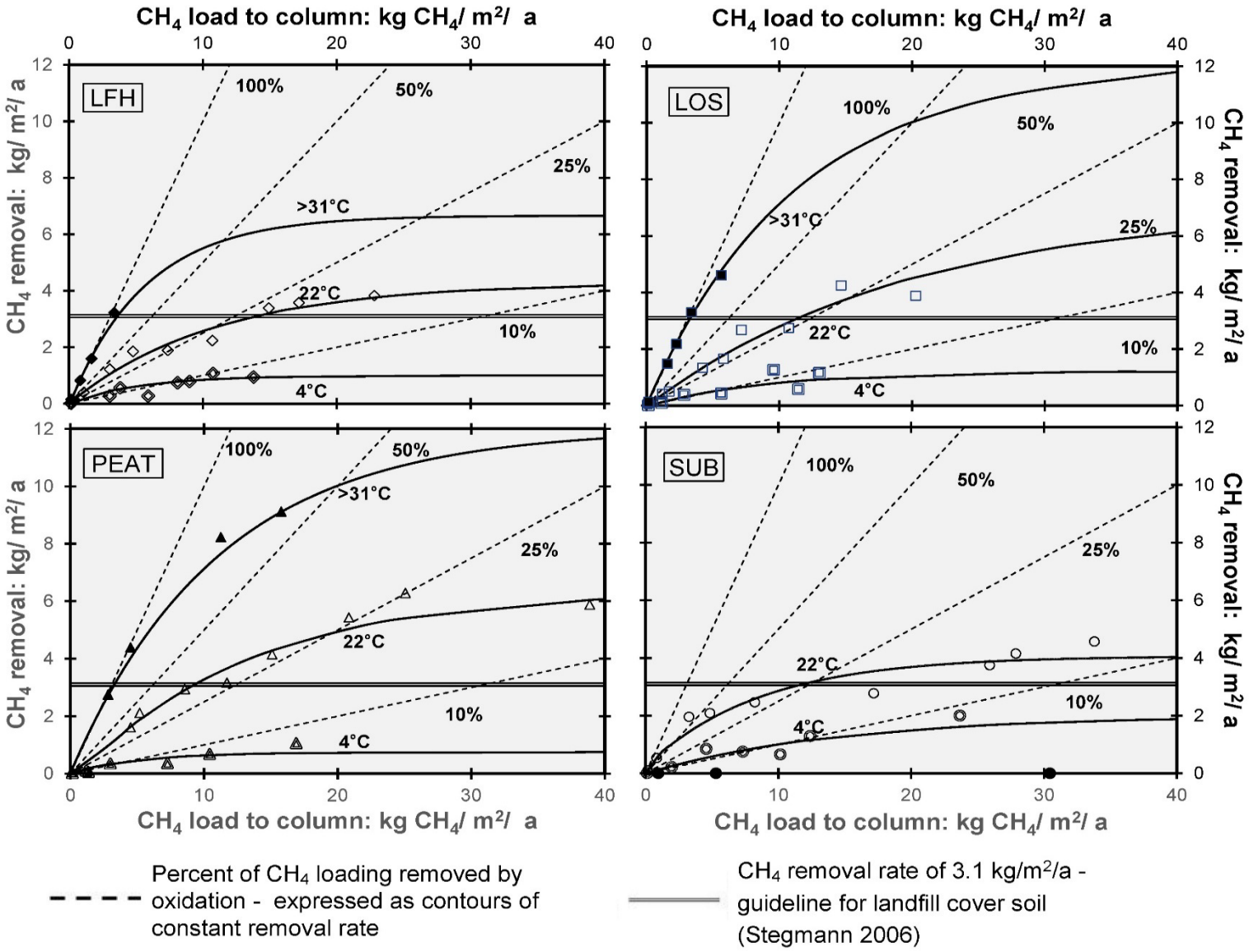

Figure 4.4 CH_4 removal rates for LFH, LOS, peat, and subsoil columns at climate chamber temperatures of 4°C, 22°C, and >31°C.

Experimentally determined oxidation rates for the MLSC column are presented in Figure 4.5. Tests were only conducted at 22°C due to space limitations in the temperature-controlled climate chambers. Oxidation rates surpassed 3.1 kg/m^2/a whilst regular column watering was conducted. After watering was discontinued, however, oxidation rates decreased over time to less than 3.1 kg/m^2/a (Stegmann 2006). After watering had been discontinued for 45 days, oxidation rates decreased from 80% efficiency to 38% efficiency at CH_4 loads of 6 kg/m^2/a.

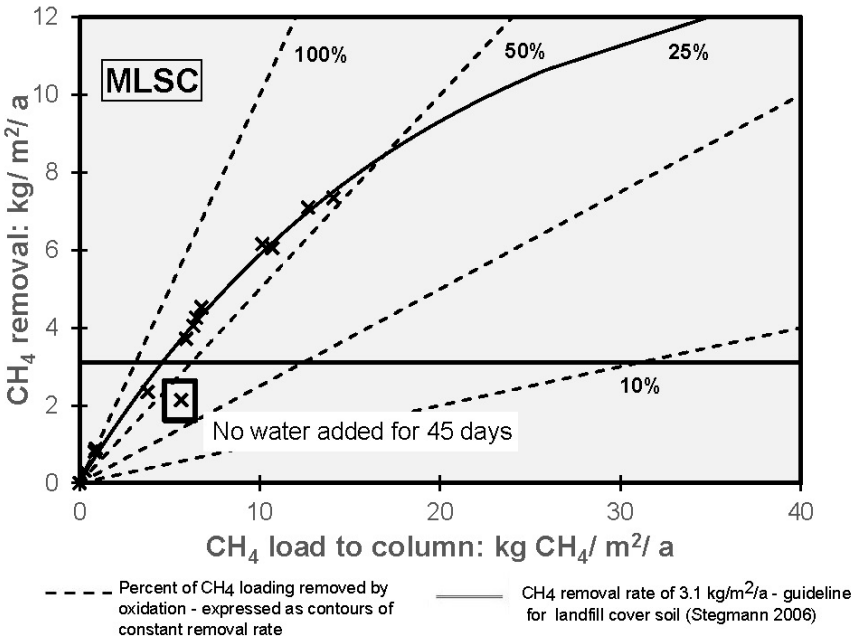

Figure 4.5 CH_4 removal rates for the multi-layered soil cover as determined with batch soil column experiments.

4.6.4 Respiration rates

Rates of microbial respiration were measured for the soil columns by using the same sampling procedure as the CH_4 oxidation experiments without adding CH_4 to the columns. Rates of CO_2 production resulting from respiration are presented in Table 4.2. The MLSC column had the highest respiration rates of any column at 22°C. For the individual soil materials, respiration rates were highest for peat, followed by LOS, and lastly LFH for the columns tested at temperatures of 4°C and >31°C. Rates of CO_2 production in the MLSC column were reduced by up to 90% after watering had been discontinued for 12 days.

Table 4.2 CO_2 production rates measured during soil column respiration experiments

CO_2 production rates [kg/a]			
Column	**4˚C**	**22˚C**	**>31˚C**
MLSC	--	• 0.29 - 0.48 • 0.023 at low VWC	--
LFH	0.0092	0.17	0.11
LOS	0.012	0.12	0.16
Peat	0.043	0.12	0.28
Subsoil	--	0.14	--

4.6.5 Leachate pH and total alkalinity

The range of pH values and total alkalinity for column leachate are compiled and presented in Table 4.3. Generally, leachate collected from the LOS column had the lowest pH, whilst having highest alkalinity levels. Leachate from subsoil, meanwhile, had the highest pH and lowest alkalinity levels. It should be noted that only two samples of subsoil leachate were able to be collected during the column experiments. Leachate collected from the MLSC column, LFH, and peat all had similar pH and total alkalinity levels when accounting for variations between tests.

Table 4.3 Range of pH values and total alkalinity measured on samples of column leachate with the Mettler-Toledo® T-50™

		Leachate pH				**Total alkalinity [mg/L $CaCO_3$]**			
Column	**# Tests**	**Max**	**Min**	**Mean**	**Std. Dev**	**Max**	**Min**	**Mean**	**Std. Dev**
MLSC	5	7.7	7.0	7.4	0.25	385	300	334	32
LFH	13	8.4	6.7	7.3	0.52	445	198	317	96
LOS	17	8.0	6.8	7.2	0.34	493	305	414	59
Peat	11	8.0	6.7	7.4	0.38	464	177	289	84
Subsoil	2	7.8	7.6	7.7	0.10	295	285	290	5

The mass balance for missing CO_2 in the CH_4 oxidation experiments was evaluated using the mass of CO_2 dissolved in the soil column pore-water calculated based on total alkalinity measurements and calculated based on Henry's law with CO_2 partial pressures. For two particular experiments, the mass balance for CO_2 was closed in this manner as discussed in the following section and annotated on Figure 4.6.

4.6.6 Stoichiometry

Rates of O_2 consumption and CO_2 production calculated as a function of CH_4 removal rate are plotted in Figure 4.6. Rates of O_2 consumption generally followed the 2:1 line, however, the trend was for rates to decrease below 2:1 at higher CH_4 loads.

There is significantly more scatter in rates of CO_2 production compared to O_2 consumption. CO_2 production rates tended to be higher at relatively lower CH_4 removal rates and lower at relatively higher CH_4 removal rates. For two particular tests (carried out at CH_4 loadings of 8 and 9.5 kg/m^2/a), the mass of CO_2 partitioned to pore-water (including water removed from the bottom of the column) was calculated based on total alkalinity measurements and Henry's law with CO_2 partial pressure as measured. Figure 6 shows that these approaches (particularly Henry's Law) account for much of the missing mass of CO_2, thus indicating a reasonable closure of mass balance up to the stoichiometric ratio for CH_4 oxidation of 1 mole CO_2 produced per 1 mole CH_4 consumed.

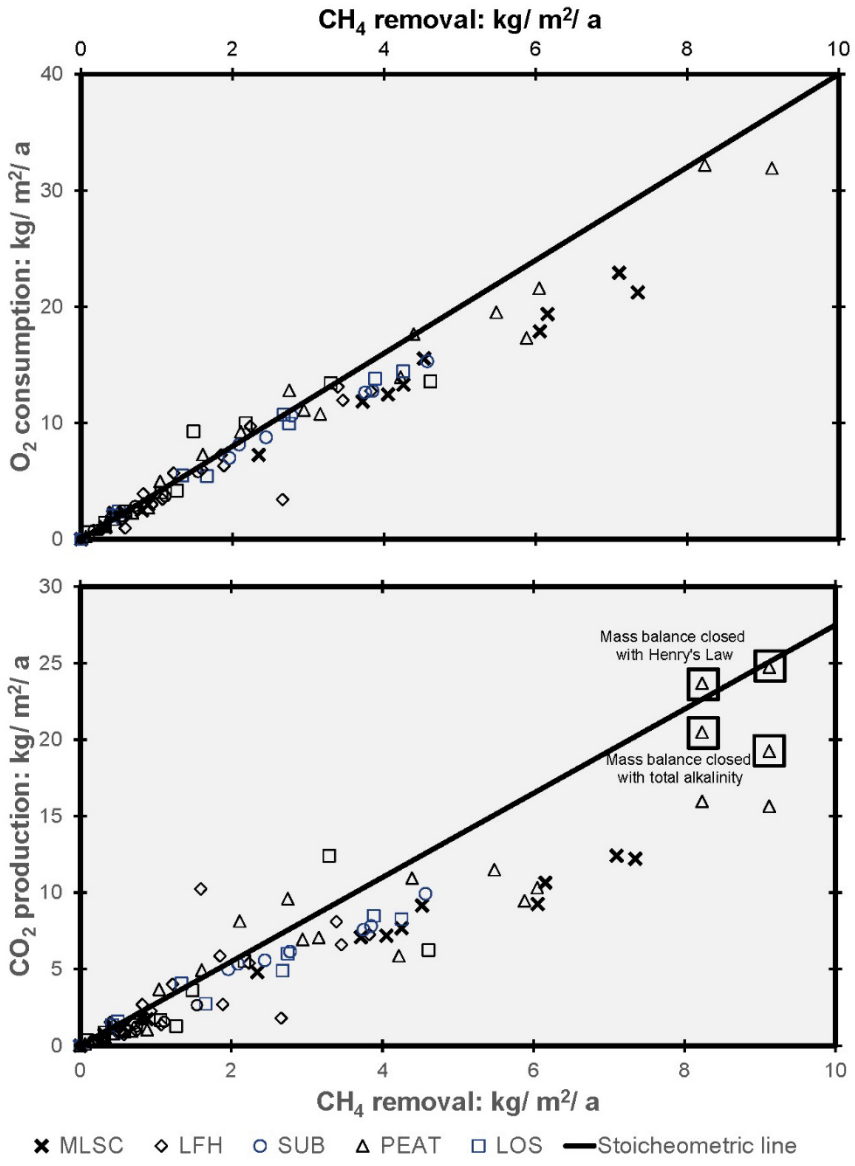

Figure 4.6 Rates of O_2 consumption and CO_2 production in the soil column experiments as a function of the rate of CH_4 removal.

Microbial CH_4 oxidation and microbial respiration are simultaneous processes contributing to the production of CO_2. The contribution of respiration decreases significantly with increasing rates of CH_4 oxidation (Gebert 2011b). Therefore, observations that O_2 consumption and CO_2 production were higher at lower rates of CH_4 oxidation are likely attributed to additional consumption of O_2 and production of CO_2 by microbial respiration.

4.6.7 Statistics

Single-factor ANOVA was conducted to compare oxidation rates at 4°C, 22°C, and 31°C for the LFH, LOS, and peat columns. There were significant differences in oxidation rates for all

columns at the different temperatures ($p < 0.01$). Post hoc T-tests with the Bonferonni correction were used to compare oxidation rates at the various temperatures in pairs (Dunn 1961). Oxidation rates for all columns were statistically higher at 31°C than at 22°C; oxidation rates at 22°C were statistically higher than at 4°C.

ANOVA was also conducted to compare oxidation rates for the subsoil column at 4°C and 22 °C (dry density of 1500 kg/m^3) and oxidation rates at 22°C (dry density of 1800 kg/m^3). There were significant differences for all three temperature and bulk density configurations. Based on post-hoc T-tests with the Bonferonni correction applied, oxidation rates were statistically higher at 22°C with a dry density of 1500 kg/m^3 than at 22°C with a dry density of 1800 kg/m^3. Furthermore, oxidation rates were statistically higher at 4°C with a dry density of 1500 kg/m^3 than at 22°C with a dry density of 1800 kg/m^3.

Oxidation rates at 4°C for LFH and LOS were not statistically different ($p > 0.05$), however, oxidation rates for the other columns compared in pairs were statistically different ($p < 0.05$). Subsoil had the highest oxidation rates at 4°C, followed by LOS and LFH, with peat having lowest oxidation rates. At 22°C, oxidation rates for peat were statistically higher than LFH ($p < 0.05$), although oxidation rates at 22°C for the other columns compared in pairs were not statistically different ($p > 0.05$). Lastly, oxidation rates at 31°C for peat and LOS were not statistically different ($p > 0.05$), but LFH was statistically lower at 31°C than both peat and LOS ($p < 0.01$).

4.7 Discussion

4.7.1 Oxidation rates

Based on a preliminary characterization of gas fluxes from uncovered LOS at the ASCS, CH_4 fluxes ranged from 0.1-7.1 kg/m^2/a, with the majority of fluxes ranging between 0.5-1 kg/m^2/a. Soil column experiments were conducted at lower and higher CH_4 loads in order to account for slow leaks and fugitive emissions.

Oxidation rates in the MLSC column were significantly higher than any of the columns packed with individual soil cover materials. This was anticipated, however, as the soil cover thickness for the MLSC was 1 m rather than 0.65 m, which results in a longer pore distance for the CH_4 to travel. Nearly all the CH_4 added to the MLSC column was removed over predicted CH_4 loads of 0.5-1 kg/m^2/a and roughly 70-80% removed at CH_4 loads up to 10 kg/m^2/a. The maximum thickness that soil covers could be tested in the laboratory was 1 m due to space requirements for a headspace, gravel drainage layer, and to facilitate access for the 1.6 m Diviner 2000™ capacitance probe. It should be noted that it is possible CH_4 removal rates may have attained near-100% efficiency over the range of CH_4 loads expected in the field had the thickness of the MLSC been increased by 0.5 m to re-create the 1.5 m placement thickness of many of the soil cover systems at the ASCS.

The US EPA's GHG reporting guidelines originally mandated a 10% oxidation efficiency for landfill soil covers (USEPA 2009) and later revised this guideline to mandate oxidation efficiencies to range from 10-35% (USEPA 2013). The individual soil cover materials tested in these column experiments surpassed the US EPA's highest specified efficiency of 35% at temperatures >22˚C. Oxidation rates at 4˚C, however, were equal to or less than the US EPA's minimum specified 10% CH_4 removal efficiency. All soils surpassed the 3.1 kg/m^2/a oxidation rate considered suitable for use as a landfill cover soil according to Austrian and German guidelines at temperatures >22˚C, however, none of the soils at 4˚C were capable of oxidizing at 3.1 kg/m^2/a (Stegmann 2006, Ritzkowski and Stegmann 2010, Gebert et al 2011c).

Based on field gas sampling at the ASCS, soil-atmosphere gas exchange sufficiently aerated the upper approximately 1 m of the LOS landform (data not reported). This 1 m thickness of LOS can therefore be considered an extension of the soil cover system for the practical purposes of removing CH_4 released from the LOS.

4.7.2 Effects of moisture, temperature and bulk density

Drought conditions were simulated for the MLSC column by discontinuing the daily application of water for 45 days. Reductions in VWC of the soil materials packed in the MLSC over the course of the drought simulation are indicated by VWC profiles measured with the Diviner 2000™ in Figure 4.7.

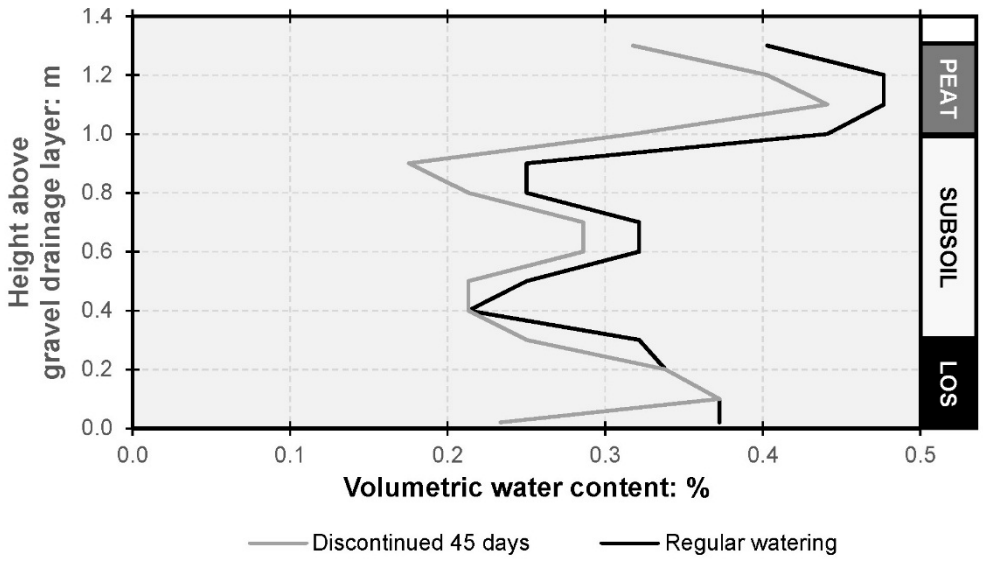

Figure 4.7 Volumetric water content profiles in the MLSC column measured with the Diviner 2000 capacitance probe during regular column watering and after watering had been discontinued for 45 days.

As the plot of CH_4 removal rate vs loading in Figure 4.5 clearly showed, the MLSC column maintained effective CH_4 oxidation for several weeks after watering was discontinued. For experiments conducted during the first 8-17 days after watering was discontinued, oxidation rates were reduced from 80-100% efficiency to roughly 50% efficiency. For the experiment conducted 45 days after watering was discontinued, however, the oxidation rate had reduced to 38% efficiency. The prolonged lack of water to a soil cover is therefore expected to eventually compromise oxidation efficiency.

Climate chamber temperatures were varied from 4-31˚C to simulate the temporal variations in soil temperature that are representative of field conditions at the ASCS. Soil temperatures were measured at the ASCS using Campbell Scientific® CS229™ Heat Dissipation Matric Potential Sensors installed at various depths in the soil materials and LOS and are presented

in Table 4.4 (Campbell Scientific 2009). Minimum temperatures in all soils and LOS were well below 0˚C and are thusly omitted from the table.

Table 4.4 Maximum and mean soil temperatures measured during 2014 and 2015 with Campbell Scientific® CS229™ Heat Dissipation Matric Potential sensors installed at various depths in the cover soils and LOS at the ASCS

		Soil temperatures [˚C]			
		LFH	**LOS**	**Peat**	**Subsoil**
Shallow (0-0.15m depths)	**Max**	42	14	26	29
	Mean	6	4.6	4	6.5
Deeper (0.15-1.4m depths)	**Max**	N/A	14	24	21
	Mean	N/A	4.6	3.5	5.2

Nearly all the CH_4 added to the columns was oxidized at temperatures >31˚C for the columns packed with LFH, LOS, and peat. This high temperature is near the peak of temperatures measured at the ASCS for the LFH, peat, and subsoil, however, it is significantly warmer than would be expected for covered LOS. While the columns were at 22˚C, the effectiveness of the soil covers to remove CH_4 was reduced to roughly 30-50%. Lastly, CH_4 removal rates remained low at 4˚C, with typically less than 10% of the CH_4 added being removed. This lower temperature is closer to the expected temperature at all depths for all soils. It should be noted, however, that CH_4 production rates will likely be reduced at lower temperatures since methanogens responsible for CH_4 are physiologically impacted by lower temperatures similar to methanotrophs (Anderson 1982). Moreover, reductions in CH_4 production from the LOS at lower temperatures was observed in the laboratory column study presented in Scale et al (2016).

The effect of increased density (i.e. by compaction) was simulated for a single experimental setup by removing the column contents (subsoil packed to a dry bulk density of 1500 kg/m^3) and re-compacting to a dry bulk density of 1800 kg/m^3. This value is at the high-end of measured densities at the ASCS, whereas 1500 kg/m^3 was closer to the mean for most of the soils tested (AITF 2013). The rate of methane removal was lower than could be measured for

the column compacted at this density. This suggests that careful planning may be necessary to avoid over-compaction during placement of reclamation cover soils.

4.7.3 Limitations of batch column experiments

The batch soil column experiments successfully enabled CH_4 oxidation rates to be quantified for expected CH_4 loads (0.5-1 kg/m^2/a) and for temperatures <31˚C. The limitations of batch experiments result from the finite volume of O_2 in the columns, which restricts CH_4 oxidation when the majority of O_2 is consumed. For tests with CH_4 loads less than 7.1 kg/m^2/a, which is the highest expected CH_4 load, there was typically 12-18% O_2 in the column pore spaces following the 22-48 hour experiments. At rates higher than 10 kg/m^2/a, however, O_2 in the pore space was often reduced to 5% or less. While oxidation rates were significantly higher at temperatures >31˚C, O_2 in the pore space was typically less than 5% after 22-24 hour for CH_4 loads less than 5 kg/m^2/a. For some experiments at temperatures >31˚C, all O_2 was completely consumed in the pore space leading to anaerobic conditions. As a result, oxidation rates at temperatures >31˚C were underestimated and experiments could not be conducted at CH_4 loads greater than 5 kg/m^2/a. Had sufficient O_2 been supplied to the soil columns, however, it is possible that oxidation rates at temperatures >31˚C would have maintained 90-100% efficiency to CH_4 loads in excess of 10 kg/m^2/a.

4.8 Conclusions

The objectives of this study were to quantify CH_4 oxidation rates in in single and multi-layered configurations of soil cover materials and LOS using transient “batch” soil column experiments whilst taking into consideration the effects of temperature, moisture content, and bulk density.

Oxidation was nearly 100% efficient at temperatures >31˚C across the range of CH_4 loading rates studied for the columns packed with LFH, LOS, and peat. Oxidation was roughly 30-50% efficient at 22˚C across the range of CH_4 loading rates studied for the columns packed with LFH, LOS, and peat. Oxidation was roughly 8-10% efficient at 4˚C across the range of CH_4 loading rates studied for the columns packed with LFH, LOS, and peat.

Increasing bulk density from 1500 kg/m^3 to 1800 kg/m^3 for subsoil at 22°C reduced the oxidation rate from roughly 50% efficiency over the range of expected CH_4 fluxes to virtually 0% efficiency. This is likely due to the significant reduction in air-filled porosity, which stifles CH_4 and O_2 diffusivity.

Moisture also had a significant effect on oxidation rates. However, it took 45 days without watering before oxidation rates were reduced from 80% efficiency to 38% efficiency over the range of expected CH_4 fluxes.

The multi-layered soil cover had significantly higher oxidation rates at temperatures tested compared to the single layer soil covers. This may simply reflect the greater thickness of cover, or possibly the effect of varying moisture content or other synergistic effects of the layered soil profile.

Batch soil column batch experiments enabled oxidation rates to be quantified for expected CH_4 loads (0.5-1 kg/m^2/a) and for the expected temperatures ≤ 22°C. However, at CH_4 loads >10 kg/m^2/a and at temperatures >31°C the experiments were limited by the finite volume of O_2 in the columns.

Acknowledgements

Funding for this research was supported by COSIA (Canadian Oil Sands Innovation Alliance). We would like to thank staff at Syncrude Canada Ltd. in Edmonton, AB and Fort McMurray, AB and O'Kane Consultants for their assistance with the field work.

References

Adamsen APS and King GM. 1993. **Methane Consumption in Temperate and Subarctic Forest Soils: Rates, Vertical Zonation, and Responses to Water and Nitrogen**. Applied and Environmental Microbiology. (59): 485-490

Anthony C. 1982. **The Biochemistry of Methylotrophs.** Academic Press, New York, 1982.

AITF (Alberta Innovates Technology Futures). 2013. **Bulk Density Characterization of Surface Reclamation Cover Soil for the Aurora Capping Study**. Prepared for Marty Yarmuch, Syncrude Canada, Ltd. by B. Drozdowski, A. Underwood, D. Degenhardt, and R. Faught.

Ball DF. 1964. **Loss-on-ignition as an Estimate of Organic Matter and Organic Carbon in Non-calcareous Soils**. Journal of Soil Science. (15): 84-92. DOI: 10.1111/j.1365-2389.1964.tb00247.xx

Barber LA, Bocksette J, Christensen DO, Tallon, LK, and Landhausser SM. 2015. **Effect of Soil Cover System Design on Cover System Performance and Early Tree Establishment**. Mine Closure 2015, Vancouver, Canada.

Bartholomeus RP, Witte JP, Bodegom PM, Van Dam JC, and Aerts R. 2008. **Critical Soil Conditions for Oxygen Stress to Plant Roots: Substituting the Feddes-function by a Process-based Model**. Journal of Hydrology (360): 147-165. DOI: 10.1016/j.jhydrol.2008.07.029

Ball BC, Dobbie E, and Parker JP. 1997. **The influence of gas transport and porosity on methane oxidation in soils**. Journal of Geophysical Research. (102): 301-308. DOI: 10.1029/97JD00870

Boeckx P, Van Cleemput O, and Villaralvo I. 1996. **Methane emission from a landfill and the methane oxidising capacity of its covering soil**. Soil Biology and Biochemistry. (28): 1397-1405. DOI: 10.1016/S0038-0717(96)00147-2

Bogner, J, Meadows M, Czepiel P. 1997. **Fluxes of methane between landfills and the atmosphere: natural and engineered controls**. Soil Use and Mangement. (13): 268-277. DOI: 10.1111/j.1475-2743.1997.tb00598.x

Borjesson G and Svensson B. 1997. **Effects of a Gas Extraction Interruption on Emissions of Methane and Carbon Dioxide from a Landfill, and on Methane Oxidation in the Cover Soil**. Journal of Environmental Quality. (26): 1182. DOI: 10.2134/jeq1997.00472425002600040034x

Borjesson G, Sundh I, and Svensson B. 2004. **Microbial oxidation of CH4 at different temperatures in landfill cover soils**. FEMS Microbiology Ecology. (48): 305-312. DOI: 10.1016/j.femsec.2004.02.006

Campbell Scientific. 2009. I**nstruction Manual for 229 Heat Dissipation Matric Water Potential Sensor**. Campbell Scientific Inc. Logan, Utah, USA.

Chanton JP, Powelson DK., and Green RB. 2009. Technical Report: **Methane Oxidation in Landfill Cover Soils, is a 10% Default Value Reasonable?** Atmospheric Pollutants

and Trace Gasses. DOI: 10.2134/jeq2008.0221

Christophersen M, Kjeldsen P, Holst H, and Chanton J. 2001. **Lateral gas transport in soil adjacent to an old landfill: Factors governing emissions and methane oxidation**. Waste Management Research. (19): 595-612. DOI: 10.1177/0734242X0101900616

Columbus Instruments. 2012. **User's Manual for Model 180-C**. Columbus Instruments, Columbus, Ohio, USA.

Columbus Instruments. 2002. **User's Manual for Micro-Oxymax**. Columbus Instruments, Columbus, Ohio, USA.

Czepiel PM, Mosher B, Crill PM, and Harriss RC. 1996. **Quantifying the effect of oxidation on landfill methane emissions**. Journal of Geophysical Research. (101): 721-759. DOI: 10.1029/96JD00222

De Visscher A and Van Cleemput O. 2003. **Simulation Model for Gas Diffusion and Methane Oxidation in Landfill Cover Soils**. Waste Management. (23): 581-591. DOI: 10.1016/S0956-053X(03)00096-5

Dean WE. 1974. **Determination of Carbonate and Organic Matter in Calcareous Sediments and Sedimentary Rocks by Loss on Ignition; Comparison with Other Methods**. Journal of Sedimentary Research. DOI: 10.1306/74D729D2-2B21-11D7-86480000102C1865D

Dorr H, Katruff L and Levin I. 1993. **Soil Texture Parameterization of the Methane Uptake in Aerated Soils**. Chemosphere. (26): 697-713. DOI: 10.1016/0045-6535(93)90454-D

Dunn OJ. 1961. **Multiple Comparisons among Means.** Journal of the American Statistical Association. (56): 52-64. DOI: 10.1080/01621459.1961.10482090
2011a

Einola JM, Kettunen RH, and Rintala J. 2007. **Responses of methane oxidation to temperature and water content in cover soil of a boreal landfill**. Soil Biology and Biochemistry. (39): 1156-1164. DOI: 10.1016/j.soilbio.2006.12.022

Gebert J, Groengroeft A, and Miehlich G. 2003. **Kinetics of Microbial Landfill Methane Oxidation in Blofilters**. Waste Management. (23): 609-619.

Gebert J, Rachor I, Grongroft A, and Pfeiffer EM. 2011a. **Temporal variability of soil gas composition in landfill covers**. Waste Management. (31): 935-945. DOI: 10.1016/j.wasman.2010.10.007

Gebert J, Rower IU, Scharff H, Roncato CDL, and Cabral AR. 2011b. **Can soil gas profiles be used to assess microbial CH4 oxidation in landfill covers?** Waste Management. (31): 987-994. DOI: 10.1016/j.wasman.2010.10.008

Gebert J, Huber-Humer M, Oonk H, and Scharff H. 2011c. **Methane Oxidation Tool: An Approach to Estimate Methane Oxidation on Landfills**. Methane Oxidation Tool –

Version 1.

Hettiarachchi VC, Hettiaratchi PJ, Mehrotra AK, and Kumar S. 2011. **Field-scale operation of methane biofiltration systems to mitigate point source methane emissions**. Environmental Pollution. (159) 1715-1720. DOI: 10.1016/j.envpol.2011.02.029

Hillel D. 2003. **Introduction to Environmental Soil Physics**. Elsevier Academic Press, Amsterdam.

Humer M and Lechner P. 1999. **Alternative Approach to the Elimination of Greenhouse Gasses from Old Landfills**. Waste Management Research. (7): 443-452. DOI: 10.1177/0734242X9901700607

King GM and Adamsen PS. 1992. **Effects of Temperature on Methane Consumption in a Forest Soil and in Pure Cultures of the Methanotroph Methylomonas rubra**. Applied and Environmental Microbiology. (58): 2758-2763.

Korbas. 2014**. Degradation and mobility of hydrocarbons in Oilsands waste at the Aurora Fort Hills disposal area**. M.Sc. Thesis, Department of Civil and Geological Engineering, University of Saskatchewan, Saskatoon, Saskatchewan, Canada.

Mohanty SR, Bodelier PLE, and Conrad R. 2007. **Effect of Temperature on Composition of the Methanotrophic Community in Rice Field and Forest Soil**. FEMS Microbiology Ecology. DOI: 10.1111/j.1574-6941.2007.00370.x

Molins S, Mayer KU, Scheutz C, and Kjeldsen P. 2008. **Transport and Reaction Processes Affecting the Attenuation of Landfill Gas in Cover Soils**. Journal of Environmental Quality. (37): 459-468. DOI: 10.2134/jeq2007.0250

Plummer M, Hull LC, and Fox DT. 2004. **Transport of Carbon-14 in a Large Unsaturated Soil Columns**. Vadose Zone Journal. (3): 109-121. DOI: 10.2113/3.1.109

Rachor I, Gebert J, Grongroft A, Pfeiffer EM. 2011. **Assessment of the methane oxidation capacity of compacted soils intended for use as landfill cover materials**. Waste Management. (31): 833-842. DOI: 10.1016/j.wasman.2010.10.006

Ritzkowski M and Stegmann R. 2010. **Generating CO_2 Credits through Landfill In-situ Aeration**. Waste Management. (30): 702-706. DOI: :10.1016/j.wasman.2009.11.014

Scale KO, Korbas T, and Fleming IR. 2016. **Degradation and Mobility of Petroleum Hydrocarbons in Oil Sand Waste**. Environmental Geotechnics. DOI: 10.1680/jenge.15.00035

Scheutz C and Kjeldsen P. 2004. **Environmental Factors Influencing Attenuation of Methane and Hydrochlorofluorocarbons in Landfill Cover Soils**. Journal of Environmental Quality. (33): 72-79. DOI: 10.2134/jeq2004.0072

SenTek. 2009. **Diviner 2000 User Guide Version 1.5**. Sentek Sensor Technologies, Stepney, South Australia.

Stegmann R, Heyer KU, Hupe K, Willand A. 2006. **Landfill care options, duration, costs and quantitative criteria for discharge from aftercare**. Technical Report 204 34

327. Environmental Research Plan of the Federal Ministry of Environment

Stein VB and Hettiaratchi JPA. 2001. **Methane Oxidation in Three Alberta Soils: Influence of Soil Parameters and Methane Flux Rates**. Environmental Technology. (22): 101-111. DOI: 10.1080/09593332208618315

Uniequip. 2016. **User's Manual for Univclav MJ 54 Vertical Autoclave**. Uniequip Laboratory Equipment and Sales, Planegg, Germany, 2016

USEPA (United States Environmental Protection Agency). 2009. Mandatory Greenhouse Gas Reporting. Code of Federal Regulations, Part 98, Title 40. Federal Registry, Vol 74, 56476.

USEPA (United States Environmental Protection Agency). 2013. Revisions to the Greenhouse Gas Reporting Rule and Final Confidentiality Determinations for New or Substantially Revised Data Elements; Final Rule. Code of Federal Regulations, Part 98, Title 40. Federal Registry. Vol 78, 71968.

Whalen SC, Reeburgh WS, and Sandbeck KA. 1990. **Rapid Methane Oxidation in a Landfill Cover Soil**. Applied and Environmental Microbiology. (56): 3405-3411.

Whalen SC and Reeburgh WS. 1996. **Moisture and Temperature Sensitivity of CH_4 Oxidation in Boreal Soils**. Soil Biology and Biochemistry. (28):1271-1281. DOI: 10.1016/S0038-0717(96)00139-3

5.0 THE ROLE OF PORE-GAS DYNAMICS IN GUIDING RECLAMATION PRACTICES

Preface

Understanding pore-gas dynamics within the soil covers and overburden landform can provide a basis to inform mine operators regarding practical issues involving the construction of overburden landforms, design of soil cover systems, and management of the reclamation site. In order to gain insight into the factors affecting the transportation of pore-gasses, finite difference numerical models were developed to simulate CO_2 flux from the LOS through multi-layered soil covers. In order to gain insight into the factors affecting the storage of pore-gasses, statistical procedures were conducted to examine correlations between pore-gasses and on-site conditions, measurable soil parameters, design of the soil covers, and characteristics of the overburden landform. The findings herein are used to provide practical recommendations to mine operators that can be implemented to facilitate the oxidation of methane within the soil covers and overburden whilst precluding the development of conditions that pose a risk to the growth and survivability of reclamation vegetation.

Reference: Scale KO and Fleming IR. 2017. **The Role of Pore-gas Dynamics in Guiding Reclamation Practices.** Submitted to Environmental Geotechnics, April 2017.

Abstract

The storage and transportation of pore-gasses in overburden and reclamation soil covers were evaluated using statistical analyses and finite difference numerical modelling in order to guide mine operators regarding practical issues involving the construction of overburden landforms, design of soil cover systems, and management of reclamation sites. Factors affecting gas transfer as a function of depth were soil moisture, soil temperature, gas pressures, and in-situ bulk density of the overburden landform. Furthermore, the construction of the overburden landform appears to be more impactful to pore-gas dynamics than the design of the soil covers. Based on these findings, practicable recommendations can be inferred to simultaneously facilitate CH_4 oxidation in the uppermost horizon of the overburden, while maintaining sufficient pore-gas O_2 in the plant-rooting zone of the soil covers to facilitate growth and survivability

of reclamation vegetation. It is recommended that overburden be placed to <1.5 Mg/m^3 (at a relatively lower void ratio) for soil covers thicker than 1m and placed to 1.6-1.8 Mg/m^3 (at a relatively higher void ratio) for soil covers thinner than 1m. Mine operators should also recognize and manage extreme moisture conditions in the soil covers and uppermost overburden to mitigate restrictions in gas exchange and CH_4 oxidation.

5.1 Introduction

Single and multi-layered soil cover systems are adopted for oil sands mine reclamation in Northern Alberta, Canada to transform above-grade overburden landforms amassed during oil sands mine operations into reclaimed boreal forest landscapes. Placing soil covers is a coordinated effort that involves salvaging (and potentially stockpiling) soil cover materials and hauling to active reclamation areas for placement using mechanical shovels, haul trucks and dozers. The design of the soil covers (i.e. capping thickness and configuration) thus has economic ramifications to mine operators by dictating the volume of soil that needs to be excavated, hauled, and placed. Moreover, the soil cover design has practical ramifications to reclamation efforts by altering the exchange rates of gasses between the atmosphere, soil cover, and underlying overburden landform (Scale and Fleming 2017a). These altered gas exchange rates may restrict concentrations of oxygen (O_2) in the plant-rooting zone of the soil covers to levels that pose a risk to the growth and survivability of reclamation vegetation (Flower 1981; Whitton et al 1991).

Various soil cover designs are being tested on a field-scale at the Aurora Soil Capping Study (ASCS) on Syncrude's Aurora North mine in Alberta, Canada (57°20' N, -111°32'). The ASCS is a 36 hectare subsection of an above-grade overburden landform that is subdivided into 36 one hectare study cells. Each cell is covered with one of twelve different configurations of soil cover materials and placement thickness. The landform substrate is predominantly lean oil sand (LOS), which ranges in texture from approximately sandy loam to loamy sand and may contain petroleum hydrocarbons (PHC) up to the economical ore grade of 7%. Characterisation of pore-gasses at the ASCS prior to placement of soil covers is presented in

Korbas (2014) and Scale et al (2016); characterisation of pore-gasses following placement of soil covers is presented in Scale and Fleming (2017a).

The objective of this paper is to understand the factors that affect the transport and storage of O_2 and carbon dioxide (CO_2) pore-gasses in LOS and reclamation soil covers. To understand the factors affecting the transportation of pore-gasses, a finite difference numerical model is developed that simulates steady-state diffusive and advective-diffusive CO_2 flux from the LOS through multi-layered soil covers. To understand the factors affecting the storage of pore-gasses, analysis of variance (ANOVA), multivariate regression, and t-tests with the Bonferonni correction are conducted to examine correlations between CO_2 and O_2 pore-gasses and the following factors:

- on-site conditions, specifically ambient temperature and barometric pressure;
- measurable soil parameters, such as soil temperature and soil moisture;
- soil cover design, including cover thickness and cover material; and
- characteristics of the LOS landform, such as in-situ bulk density.

Understanding the factors that affect the storage and transport of pore-gasses is intended to inform mine operators regarding practical issues involving the construction of LOS landforms, design of soil cover systems, and management of the reclamation site.

5.2 Background

5.2.1 Biodegradation of petroleum hydrocarbons

Microbial biodegradation of PHCs (e.g. the oil component of the LOS) is a biochemical process whereby microorganisms transform PHCs into CO_2 and water under aerobic conditions or into CO_2 and methane (CH_4) under anaerobic conditions (Zengler 1999; Townsend et al 2003; Salminen et al 2004). In practicality, the biodegradation of LOS has been demonstrated to be a source of CO_2 and CH_4 in laboratory column experiments and in field studies at the ASCS (Korbas 2014; Scale et al 2016; Scale and Fleming 2017). White these efforts represent a thorough characterization of pore-gasses and rates of gas flux at the ASCS, an in-depth

analysis was required to understand the factors affecting the storage and transport of pore-gasses.

5.2.2 Significance of soil moisture and temperature to gas transfer

The relationships between pore-gasses and soil temperature and soil moisture have been extensively reported in the literature (Whalen and Reeburgh 1996; Bowden et al 1998; Davidson et al 1998; Risk et al 2002; Hashimoto and Komatsu 2006; Kettunen et al 2006; Bekele et al 2007; Gebert et al 2010). Microorganisms require a sufficiently well-aerated pore-space for root and microbial respiration and the corresponding flux of O_2 and CO_2 to transpire. At higher water contents, less O_2 is available to facilitate root and microbial respiration due to restrictions in diffusion and gas permeability (Hillel 2003). At lower water contents, on the other hand, more O_2 is available and diffusion is less restricted, but insufficient water may be available for plants to carry out metabolic functioning (Dorr et al 1993; Boeckx et al 1996; Einola et al 2007; Gebert et al 2010). This leads to a non-linear relationship between soil moisture and the flux of O_2 and CO_2, with reductions in flux rates at both higher and lower water contents (Bekele et al 2007). The effect of temperature on microbial respiration is similarly non-linear. Root and microbial activity are impeded at extreme low and high temperatures, which leads to restrictions in the corresponding flux of O_2 and CO_2 (Bunt and Rovira 1955; Bekele et al 2007).

5.3 Materials & Methodology

5.3.1 Field sampling locations

Pore-gas concentrations and rates of gas flux were measured at the ASCS from 2013-2015 at the sampling locations presented in Figure 5.1. Further details regarding of the gas sampling procedures and results thereof are available in Scale and Fleming (2017a).

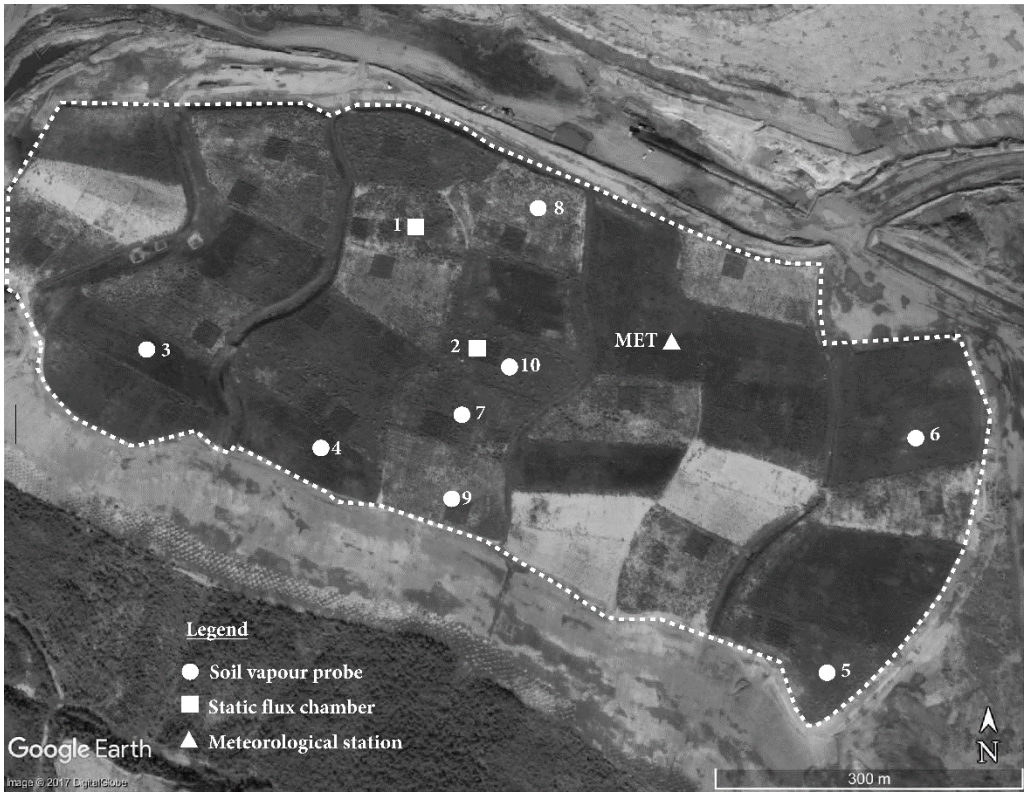

Figure 5.1 Gas sampling locations at the ASCS that were investigated from 2013-2015.

Details of the soil cover designs investigated in this research at each gas sampling location are presented in Table 5.1.

Table 5.1 Soil cover designs and associated in-situ bulk density in the upper 0.5 m of the LOS

Location	1	2	3	4	5	6	7	8	9	10,11,12
Treatment	5	8	1	2	3	4	5	6	7	8
Sampling method[1]	SFC	SFC	SVP	SVP	SVP	SVP	SVP	SVP	SVP	SVP
Bulk density[2] **(Mg/m^3)**	1.59	1.61	1.57	1.98	1.64	1.63	1.56	1.45	1.61	1.61
0-0.5 m BGS	0.1m LFH	0.3m Peat	0.3m Peat	0.3m Peat	0.1m Peat	0.3m Peat	0.1m LFH	0.2m LFH	0.2m LFH	0.3m Peat
0.5 m BGS	Sub	Sub	LOS	Sub	Sub	Sub	Sub	Sub	Sub	Sub
1 m BGS	Sub	Sub	LOS	Sub	Sub	Sub	Sub	Sub	Sub	Sub
1.5 m BGS	Sub	Sub	LOS	LOS	Sub	Sub	Sub	Sub	Sub	Sub
2 m BGS	LOS	LOS	LOS	LOS	LOS	LOS	LOS	LOS	LOS	LOS
3 m BGS	LOS	LOS	LOS	LOS	LOS	LOS	LOS	LOS	LOS	LOS
4 m BGS	LOS	LOS	LOS	LOS	LOS	LOS	LOS	LOS	LOS	LOS

[1] SFC = static flux chamber; SVP = soil vapour probe
[2] Average dry bulk density of the upper 0.5 m of the LOS landform

All soil cover materials were salvaged from within the mine footprint and directly placed or temporarily stockpiled. Peat is a sand-textured material that is intended to provide organic carbon, nutrients, and

improve water holding capacity. LFH and subsoil are also predominantly sand-textured; however, they both contain a greater proportion of silt than the peat. The LFH is considered an upland surface soil and contains surface litter such as twigs, stems, and seeds. A more detailed description of the soil cover materials, particle-size distributions, and soil water characteristic curves are provided in Scale and Fleming (2017a).

5.3.2 Field conditions

The meteorological station at the ASCS (shown in Figure 5.1) recorded air temperature and precipitation throughout the 2013 to 2015 field seasons. The air temperature ranged from -37°C to +33°C, with an arithmetic average air temperature of 2.5°C. Annual cumulative rainfall was 372 mm in 2013, 344 mm in 2014, and 248 mm in 2015.

Each cell at the ASCS was instrumented with Campbell Scientific® CS616™ Water Content Reflectometers for measurement of volumetric water content (VWC) and Campbell Scientific® CS229™ Heat Dissipation Matric Potential Sensors for measurement of soil temperature (Campbell Scientific 2009, 2016). The probes were installed at various depths into the soil covers and underlying LOS.

Profiles of arithmetic mean soil temperatures and standard deviations measured at the various gas sampling locations are presented in Figure 5.2. Mean temperatures in the soil cover materials and LOS tended to range from 3-7°C, with exposed surficial layers of peat and LFH varying more than intermediary layers of subsoil. The temperatures in the LOS, on the other hand, varied over a narrower range than the soil cover materials due to the LOS being better insulated from temporal variations in ambient temperature and solar radiation.

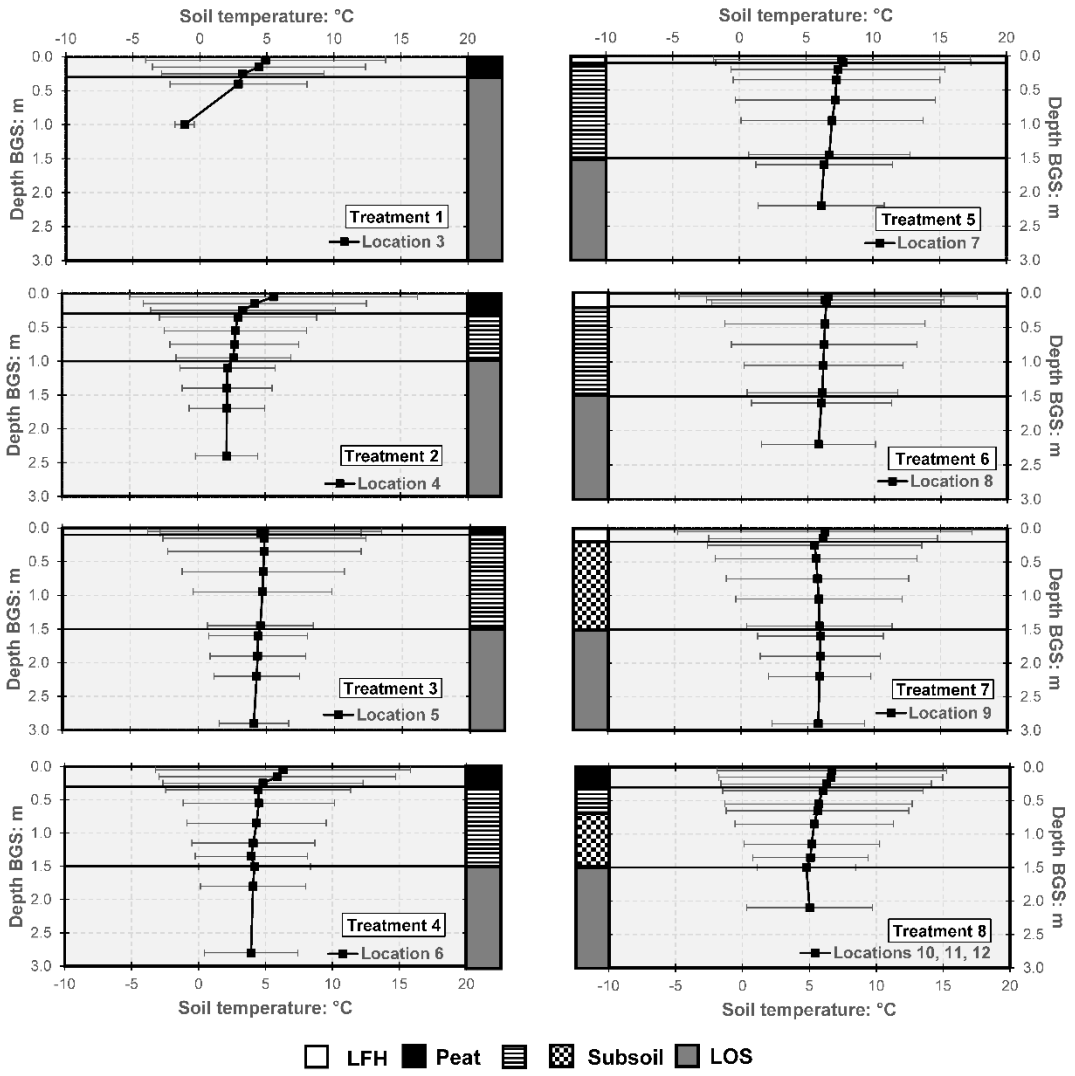

Figure 5.2 Arithmetic mean soil temperature measurements and standard deviations at all sampling locations from January 1, 2015 to December 31, 2015. Horizontal lines indicate the depth of the soil layers and the interface of the soil cover material and LOS.

Profiles of the arithmetic mean VWC and standard deviations measured at the various gas sampling locations are presented in Figure 5.3. The VWC of LFH and subsoil were similarly low in the near subsurface. VWC for LOS and peat, on the other hand, tended to be higher, with peat varying over a wider range than any other soil cover material or LOS. Interestingly, the VWC often tended to increase sharply at the interface between the soil cover materials and LOS.

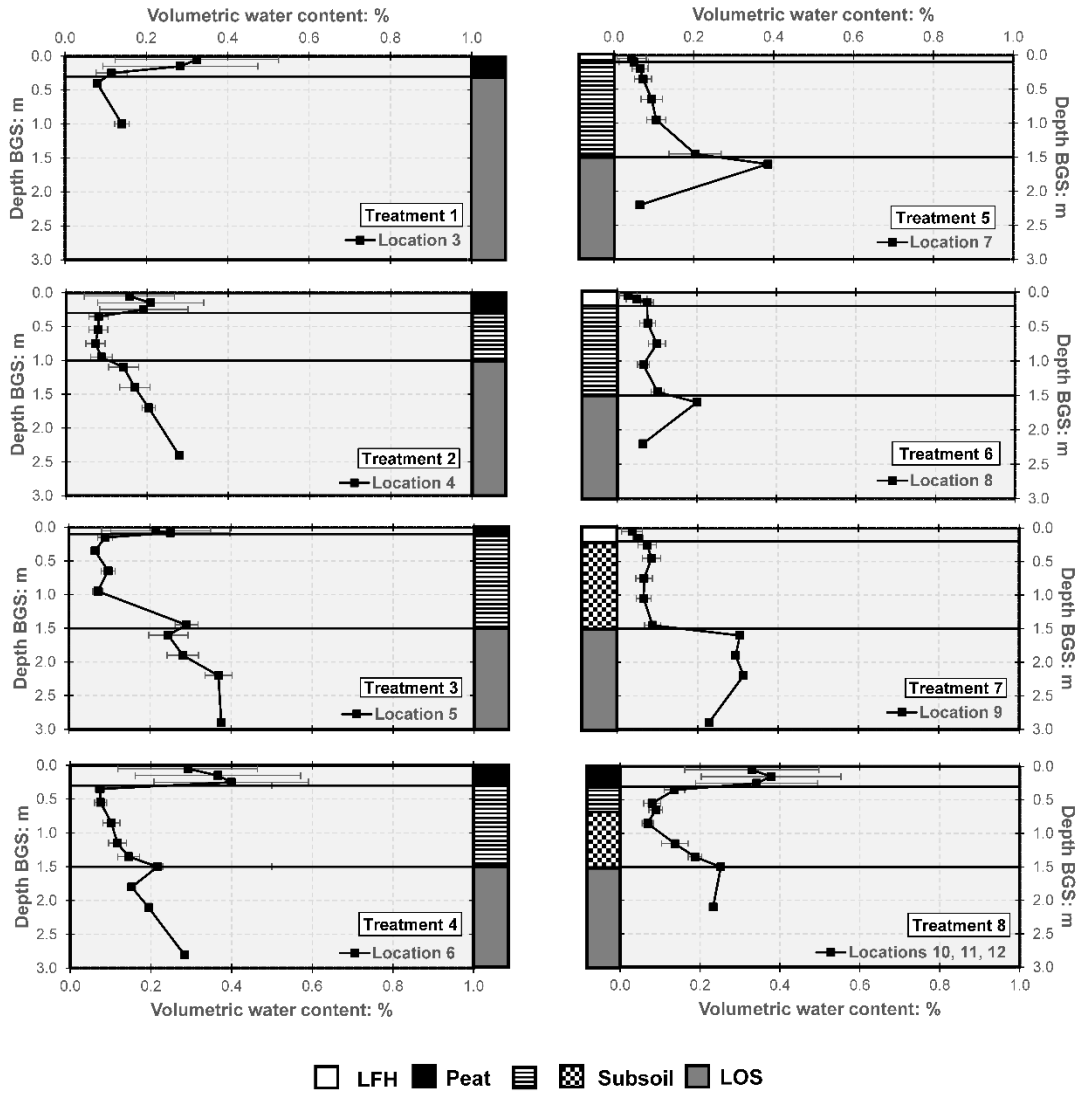

Figure 5.3 Arithmetic mean volumetric water content measurements and standard deviations at all sampling locations from January 1, 2015 to December 31, 2015. Horizontal lines indicate the depth of the soil layers and the interface of the soil cover material and LOS.

5.3.3 Characterisation of pore-gasses

Concentrations of pore-gasses and rates of gas flux were characterised at the ASCS during the 2013-2015 field seasons. Two methodologies were used at field scale as described by Scale and Fleming (2017a). In the first method, an automated multiplexing gas analyser (Columbus Instruments 2016) was used to directly measure gas fluxes in static flux chambers. A second methodology involved using the LandTec® GEM 2000™ (LandTec 2010) portable landfill gas analyzer to measure gas pressures and pore-gas O_2, CO_2, and CH_4 concentrations in single-point AMS® soil vapour probes (SVP). The characterisation of O_2 and CO_2 pore-

gasses in the soil covers and LOS during the 2014-2015 field seasons is presented in Figure 5.4. Pore-gas concentrations of O_2 and CO_2 within the soil covers and within the upper (approximately) 1 m of the LOS landform were typically >10% O_2 and <15% CO_2. Pore-gasses deeper within the LOS landform, on the other hand, fell to 0% for O_2 and rose to >16% for CO_2.

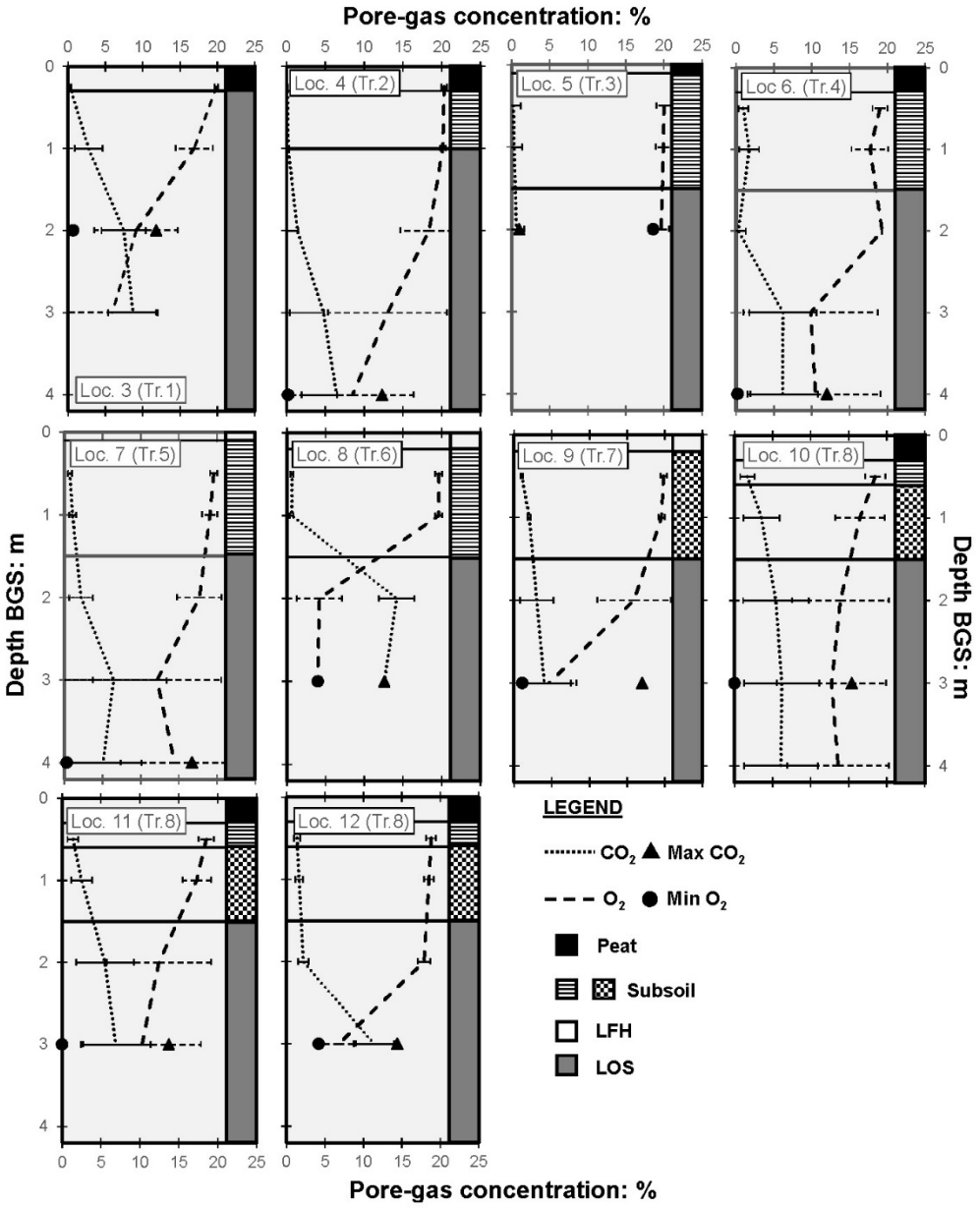

Figure 5.4 Pore-gas O2 and CO2 concentrations measured at the ASCS during the 2014 and 2015 field seasons. (Loc. = location; Tr. = treatment #).

5.3.4 Bulk density of the LOS landform

Spatial variability of the in-situ bulk density of the LOS landform was characterised at the ASCS in 2010 by AITF (2013) prior to placement of soil cover systems using the CPN® MC-1 DR-P Portaprobe Moisture/Density Gauge (CPN Inc., Concord, California, USA). Of the gas sampling locations in Figure 1, the lowest bulk density was 1.45 Mg/m^3 at location 8 (Treatment 6) and the highest bulk density was 1.98 Mg/m^3 at location 4 (Treatment 2). The bulk density at all other sampling locations ranged from 1.56-1.61 Mg/m^3. Bulk density of the LOS can be practicably controlled by mine operators during the construction of the LOS landform; as a result, the relationship between pore-gasses and bulk density of the LOS was evaluated.

5.3.5 Development of the numerical model

A numerical model was developed using MATLAB® that simulates CO_2 fluxes driven by concentration gradients (diffusion) and pressure gradients (advection) through 1.5 m thick multi-layered soil covers into the headspace of static flux chambers (Fick 1855; Darcy 1856; MathWorks 2016; Scale and Fleming 2017a). The model was calibrated using results from the static flux chamber tests described in Scale and Fleming (2017a). The model does not consider CH_4 transport, the transformation of CH_4, nor the corresponding flux and consumption of O_2. The model is a simplification of field conditions in that it considers CO_2 flux to be steady-state; hence the dissolution of CO_2 in pore-water is assumed to be in carbonate equilibrium.

The finite difference approximation uses a block-centred grid that solves for concentration values at nodes and flux values to midpoints. The spatial discretization grid was specified in increments of 0.1 m, except for the flux chamber, which was uniquely specified as 0.3048 m (based on the physical dimensions of the flux chamber). The time discretization grid was specified in increments of 0.01 hour. The effect of grid size was evaluated by conducting a sensitivity analysis on discretization grid sizes. The model was calibrated based on flux chamber data presented in Scale and Fleming (2017).

Using vertical VWC profiles measured at the ASCS, the model calculates the corresponding position-dependent CO_2 diffusion coefficient using the dual-phase Aachib et al (2004) formulation presented in Equation 5.1.

$$D_e = \frac{1}{\theta_T{}^2}\left[D_a^0\ \theta_a^{\ P} + HD_w^0\ \theta_w^{\ P}\right] \qquad [5.1]$$

Where θ_T is total porosity [L^3L^{-3}], Da_0 is diffusion coefficient in free air [L^2T^{-1}], θ_a is air-filled porosity [L^3L^{-3}], H is Henry's law equilibrium coefficient for a solution of gas in water, Dw_0 is diffusion coefficient in water [L^2T^{-1}], θ_w is volumetric water content [L^3L^{-3}], and P is an empirical curve-fitting parameter.

A constant CO_2 concentration boundary condition (BC) is applied at the depth corresponding to the material interface between the LOS and soil covers. This constant CO_2 concentration BC thus enables CO_2 fluxes to be simulated from the LOS into the soil covers. In practicality, however, this is a simplification of field conditions in that it does not consider CO_2 production resulting from the biodegradation of PHCs nor from CH_4 oxidation. The constant CO_2 BC was selected to be 1%, which is roughly the median value of all CO_2 measurements at a depth of 1.5 m.

The mass balance (continuity) equation for compressible, non-reactive, dual-phase, one-dimensional diffusive-advective flow through this representative elementary volume is presented in Equation 5.2.

$$\theta_a \frac{\partial C_g}{\partial t} = D_e \frac{\partial^2 C_g}{\partial z^2} - \frac{\nu\, C_g}{\delta z} - \theta_w \frac{\partial C_w}{\partial t} \qquad [5.2]$$

Where, C_g is the CO_2 concentration in the gaseous phase [ML^{-3}]; C_w is the CO_2 concentration in the aqueous phase [ML^{-3}]; ν is pore-gas velocity [LT^{-1}]; and dz is the space step in the vertical direction [L].

The total gas flux due to advection and diffusion (F_{AD}) is the sum of advective gas flux (F_A) and diffusive gas flux (F_D) as expressed in Equation 5.3.

$$F_{AD} = F_A + F_D = -D_e \frac{\partial C}{\partial z} + \nu C \quad [5.3]$$

Where, F_{AD} is advective-diffusive gas flux [$ML^{-2}T^{-1}$]; F_A is advective gas flux [$ML^{-2}T^{-1}$]; F_D is diffusive gas flux [$ML^{-2}T^{-1}$]; D_e is the effective diffusion coefficient [L^2T^{-1}]; C is gas concentration [ML^{-3}]; $\frac{\partial C}{\partial z}$ is the vertical pore-gas concentration gradient [ML^{-4}]; v is pore-gas velocity [LT^{-1}].

5.4 Results

5.4.1 Numerical modelling to simulate advective and diffusive gas fluxes in the soil covers

The CO_2 transport model was applied to two soil cover treatments, specifically location 1 – 0.1 m LFH and 1.4 m subsoil and location 2 – 0.3 m peat and 1.2 m subsoil. Input parameters and variables for the model were constrained to field measurements of CO_2 pore-gas concentrations, soil moisture, and soil-atmosphere pressure gradients calculated with a digital monometer connected to soil vapour probes (see Scale and Fleming 2017).

To verify the model output, simulations of diffusive and advective-diffusive CO_2 fluxes were compared to CO_2 concentration increases in the static flux chamber headspace measured during field tests conducted in 2013-2015 (see Scale and Fleming, 2017a). The numerical model successfully simulated CO_2 fluxes with advective-diffusive transport; however, field results could not be simulated with diffusive-only transport. The advective component of the CO_2 flux is based on an initial pressure gradient of 10 Pa between the soil and static flux chamber; this is a reasonable value in the context of field measurements of soil-atmosphere differential pressures (Scale and Fleming 2017a), which varied in magnitude from roughly 0-20 Pa at the soil cover/ LOS interface at 1.5 m. Presented in Figure 5.5 are results of the numerical model simulations and the geometric mean increases in CO_2 concentrations measured in the chamber headspace during flux chamber tests conducted at location 1 (Treatment 5) and location 2 (Treatment 8).

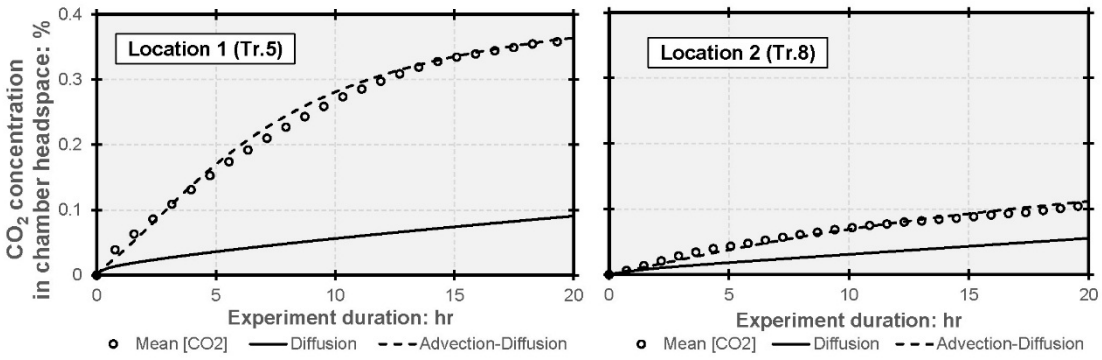

Figure 5.5 Diffusion-only and advection-diffusion simulations of CO_2 fluxes and CO_2 increases in the static flux chamber headspace during purge tests conducted on locations 1 and 2 at the ASCS during the 2013-2015 field seasons.

5.4.2 Effects of ambient temperature, soil temperature, water content, and differential pressures on O_2 and CO_2 pore-gasses

Statistical analyses including single and multi-variable regression were conducted to identify whether independent variables such as air temperature, soil temperature, soil moisture, and soil-atmosphere differential pressures were explicative of variations in O_2 and CO_2 pore-gasses at various depths in the soil covers and LOS. Note that air temperatures were only compared to O_2 and CO_2 at a depth of 0.5 m BGS.

The coefficient of determination, R^2, is an indicator of how well a regression model approximates measured values when one independent variable is being evaluated (Montgomery and Runger 2014). The adjusted R^2 value is an indicator of how well a multi-variable regression model approximates measured values when more than one independent vairable an is being evaluated (Montgomery and Runger 2014). R^2 values from the single variable regression analyses are summarized in Table 5.2 for each depth increment.

Table 5.2 Significance of air temperature, differential pressure, soil temperature, and volumetric water content on variations in O_2 and CO_2 pore-gas concentrations

Depth BGS [m]	Independent variables			
	Air temperature	**Differential Pressure**	**Volumetric water content**	**Soil temperature**
0.5	NS	NS	R^2 = 0.09 O_2 (-) R^2 = 0.16 CO_2 (+)	R^2 = 0.26 O_2 (-) R^2 = 0.21 CO_2 (+)
1	-	NS	R^2 = 0.13 O_2 (-) R^2 = 0.18 CO_2 (+)	NS
2	-	NS	R^2 = 0.65 O_2 (+) R^2 = 0.53 CO_2 (-)	NS
3	-	R^2 = 0.34 O_2 (+) R^2 = 0.24 CO_2 (-)	NS	NS
4	-	R^2 = 0.54 O_2 (+) R^2 = 0.53 CO_2 (-)	NS	NS

Note: NS = Not significant; (+) = positively correlated; (-) = negatively correlated

Differential gas pressures between the soil and the atmosphere were measured in 2015 at the ASCS using a high-precision digital manometer connected to soil vapour probes installed at various depths into the soil covers and LOS to a maximum depth of 4 m (Scale and Fleming 2017a). The differential pressures at 4 m varied from approximately -150 Pa to +150 Pa. To evaluate whether these extreme differential pressures had an effect on O_2 and CO_2 pore-gas concentrations, the relationship between the differential pressures and pore-gasses was investigated and concentration gradients of O_2 and CO_2 were found to be strongly related to differential pressures. The soil-atmosphere pressure gradients and the corresponding O_2 and CO_2 soil-atmosphere concentration gradients at 4 m BGS for sampling locations 4, 6, 7, and 9 are plotted in Figure 5.6. Note that these locations were the only locations with soil vapour probes installed at the maximum depth of 4 m.

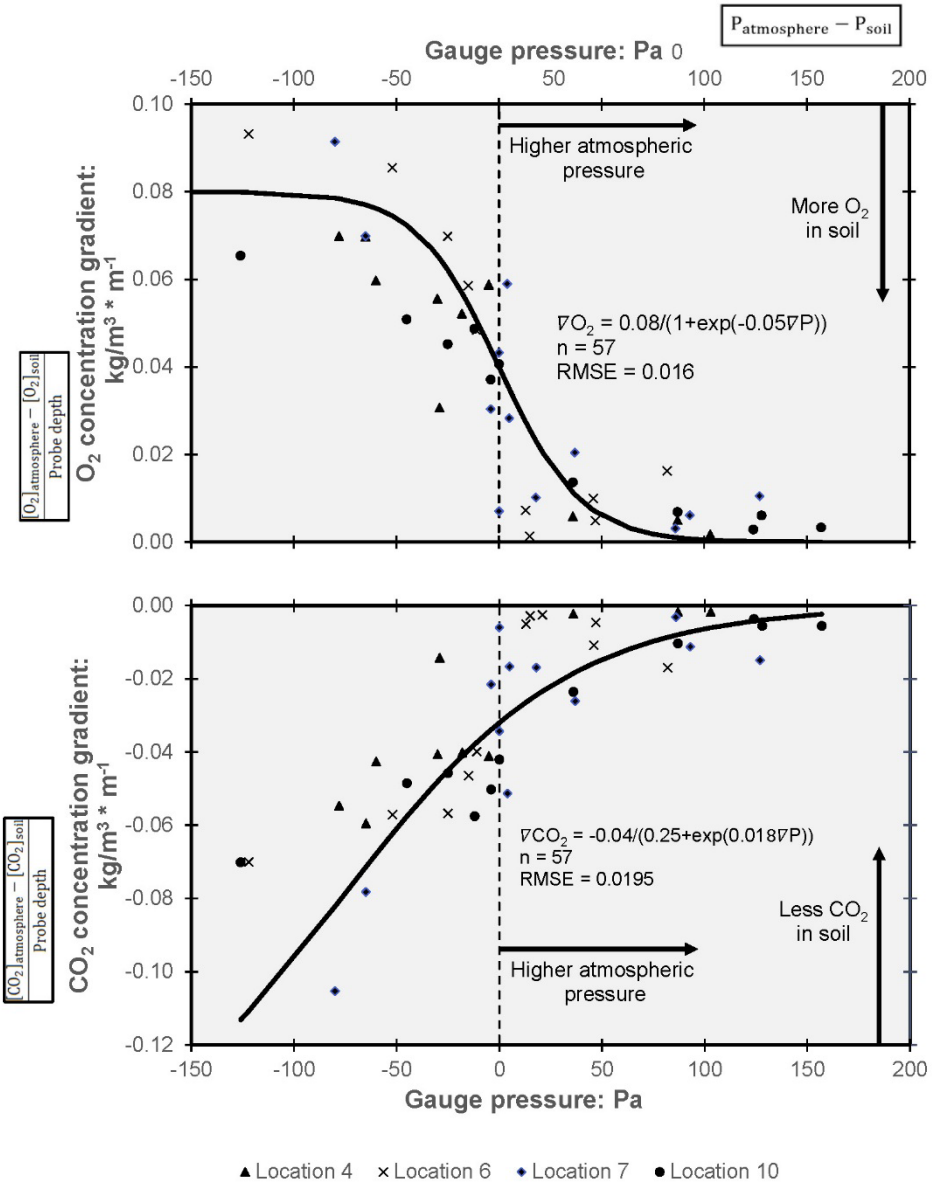

Figure 5.6 Soil-atmosphere pressure gradients and O_2 and CO_2 concentration gradients in the LOS at 4 m BGS

5.4.3 Effects of soil cover design on O_2 penetration

ANOVA and t-tests with Bonferonni corrections were conducted to investigate whether O_2 concentrations in the plant-rooting zone at 0.5 m BGS were impacted by the design of the soil covers in the upper 0.1-0.3 m BGS (as presented in Table 5.1). Findings from the statistical analyses of O_2 pore-gasses in subsoil and LOS at 0.5 m BGS underlying 0.1-0.2 m LFH and 0.1-0.3 m peat are presented in Table 5.3.

Table 5.3 Results from statistical analysis of O_2 pore-gas concentrations in the LOS and subsoil at 0.5 m BGS below 0.1 or 0.2 m LFH and 0.1 or 0.3 m Peat

Location	3	4	5	6	7	8	9	10	11	12
Treatment	1	2	3	4	5	6	7	8	8	8
0-0.5 m BGS	0.3m Peat	0.3m Peat	0.1m Peat	0.3m Peat	0.1m LFH	0.2m LFH	0.2m LFH	0.3m Peat	0.3m Peat	0.3m Peat
0.5 m BGS	LOS	Sub	Sub	Sub	Sub	Sub	Sub	Sub	Sub	Sub
Statistical Test	NSD	High	High	NSD	NSD	NSD	NSD	NSD	NSD	NSD

[1] NSD = no significant difference

No significant differences in O_2 concentrations were found in the subsoil below LFH, however, significant differences were present in the subsoil below peat. Locations 4 and 5, with 0.3 m and 0.1 m peat covers respectively, had statistically higher O_2 than in the subsoil or LOS at any of the other locations. Not considering locations 4 and 5, however, O_2 was not statistically different in the subsoil below LFH or peat; furthermore, O_2 was not statistically different in the LOS below peat (location 3) and in the subsoil below LFH or peat.

5.4.4 Effect of LOS bulk density on O_2 and CO_2 pore-gasses

The average in-situ bulk density in the uppermost 0.5 m of the LOS at each gas sampling location is presented in Table 1. The uppermost LOS horizon at location 4 (Treatment 2) had the highest average bulk density (1.98 Mg/m^3) and the lowest CO_2 and highest O_2 of all locations sampled. Further, at location 8 (Treatment 6), the uppermost LOS horizon had the lowest average bulk density (1.45 Mg/m^3) and the highest CO_2 and lowest O_2 of all locations sampled. The bulk density of the LOS for the other locations sampled ranged from 1.56-1.61 Mg/m^3 and the pore-gas concentrations of O_2 and CO_2 associated with these locations were intermediary.

5.5 Discussion

5.5.1 Numerical model

The transport of CO_2 through multi-layered soil covers into static flux chambers was measured during the 2013-2015 field seasons on location 1 (Treatment 5 – 0.1 m LFH and 1.4 m subsoil) and location 2 (Treatment 8 – 0.3 m peat and 1.2 m subsoil) as described in Scale and Fleming (2017a). The numerical model simulation of these static flux chamber experiments simulated field results by considering advective-diffusive CO_2 flux, but not CO_2 flux by diffusion alone.

Based on field results and numerical model simulations, CO_2 fluxes were higher on location 1 than location 2. In practicality, the peat layer contained a larger saturated pore-volume to facilitate the rapid dissolution of highly-soluble CO_2. It should be noted, however, that the steady-state numerical model did not consider the dissolution of CO_2. In the numerical model, CO_2 fluxes were higher through location 1 than through location 2 due to location 1 having a lower VWC in the upper 0.3 m (as presented in Figure 5.7) and thus a larger air porosity.

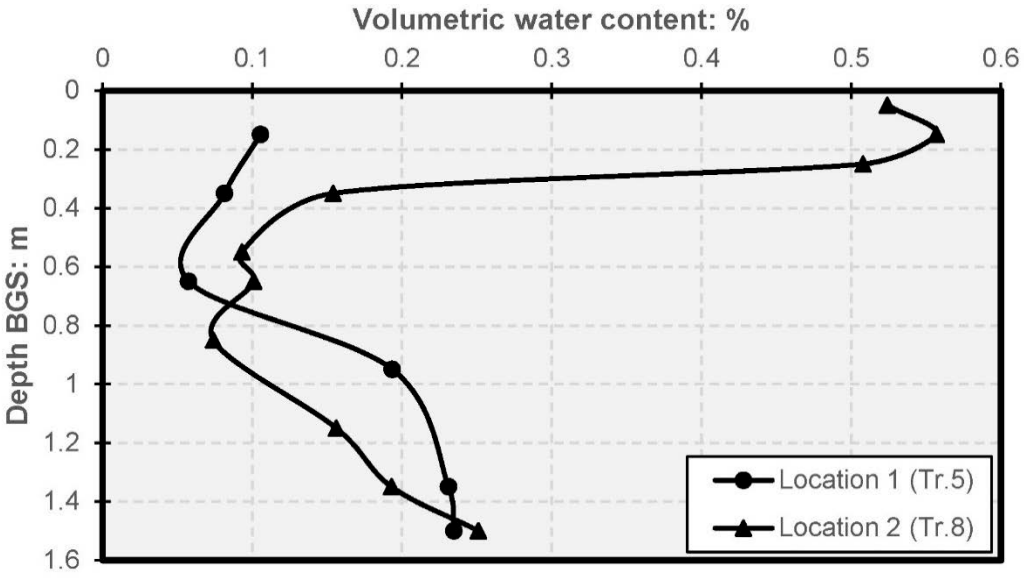

Figure 5.7 Average volumetric water contents measured in the subsurface with static flux chamber tests conducted on locations 1 and 2 at the ASCS during the 2013-2015 field seasons. (Tr. = treatment)

5.5.2 Response of O_2 and CO_2 pore-gasses to changes in ambient temperature, soil temperature, water content, and differential pressures

Air temperature was only evaluated in the upper 0.3-0.5 m and was not significant to either O_2 or CO_2 pore-gasses. This may be attributed to the thermal insulation provided by the soil covers (Figure 2). Soil temperatures and VWC in the upper 0.3-0.5 m, on the other hand, were highly significant and accounted for more than 38% of the variations in O_2 and CO_2 based on the adjusted R^2. This may be attributed to capacity for microbial communities to carry out respiration being sensitive to variations in temperature and moisture.

At depths ranging from 1-2 m BGS, which represents the interface between the soil covers and LOS, VWC was found to have the strongest influence on O_2 and CO_2 and explained up

to 53% of the variation in O_2 and 65% of the variation in CO_2 (at 2 m BGS). This may be attributed to the sharp increase in VWC at the interface between the coarser-textured cover soils and the finer-textured LOS that is clearly visible in the VWC profiles in Figure 5.3. This sharp increase in VWC likely restricted the capacity of microorganisms to carry out respiration due to the reduction in air porosity and corresponding reduction in O_2.

Deeper in the LOS at depths of 4 m BGS, differential pressures accounted for up to 54% of the variations in O_2 and 53% of the variations in CO_2. Increasing soil-atmosphere pressure gradients (atmospheric pressure > soil pressure) suggest that the downwards movement of atmospheric air was penetrating deep into the LOS and aerating the soil pores with atmospheric concentrations of O_2 of CO_2. This was indicated by higher pore-gas O_2 concentrations (lower O_2 concentration gradients) and lower pore-gas CO_2 concentrations (higher CO_2 concentration gradients). Conversely, decreasing soil-atmosphere pressure gradients (soil pressure > atmospheric pressure) suggest that pore-gasses within the LOS were rising upwards to the atmosphere and exhausting the finite volume of O_2 supplied by the atmosphere and drawing up CO_2 generated deeper in the LOS landform. This was indicated by lower pore-gas O_2 concentrations (higher O_2 concentration gradients) and higher pore-gas CO_2 (lower CO_2 concentration gradients). This phenomenon is denoted in the literature as the "barometric pumping effect" and has been observed to influence rates and direction of soil-atmosphere gas exchange (Czepiel et al. 1996; Christophersen et al. 2001; Massman 2006).

5.5.3 Soil cover design and O_2 penetration

Incorporating either 0.1-0.2 m LFH or 0.1-0.3 m peat into the design of a single or multi-layered soil cover did not have a significant impact on O_2 pore-gas concentrations in the plant-rooting zone at 0.5 m BGS in the shallow subsurface. Interestingly, there was no statistical difference in O_2 whether the material was intermediary subsoil or LOS. This corroborates the potential for a reduction of the soil cover design capping thickness (initially postulated in Scale and Fleming, 2017a).

5.5.4 Bulk density of the LOS and O_2 and CO_2 pore-gasses

In-situ bulk density of the LOS landform impacted O_2 and CO_2 pore-gasses near the interface between the soil covers and LOS. Location 8, which had the lowest bulk density of 1.45 Mg/m^3, had the lowest O_2 and highest CO_2 pore-gas concentrations. Location 4, which had the highest bulk density of 1.98 Mg/m^3, had the highest O_2 and lowest CO_2 pore-gas concentrations. These findings suggest that the 1) CH_4 oxidation capacity of the LOS is restricted at higher bulk density (lower void ratio), likely due to reductions in air porosity and the corresponding availability of O_2; and 2) the CH_4 oxidation capacity of the LOS is enhanced at the lower bulk density (higher void ratio), possibly due the increased air porosity and greater availability of O_2.

These relationships are supported by findings in Scale and Fleming (2017a) that rates of advective gas transport across the soil cover/LOS interface were significantly higher for location 4 than location 8, while rates of diffusive transport were significantly lower for location 4 than location 8. There are also two relevant findings in the soil column experiments conducted in Scale and Fleming (2017b) that should be noted: 1) LOS is capable of oxidizing CH_4 at rates comparable to soil cover materials; and 2) increasing bulk density by 0.3 Mg/m^3 significantly reduced methane oxidation rates.

Moreover, the maximum concentration of unreacted pore-gas CH_4 measured in SVP at the soil cover/LOS interface on location 4 was 0.7%, while on location 8 it was only 0.1%. On location 4 there was also an accumulation of unreacted pore-gas CH_4 from 0.9-1.2% at depths from 2-4 m BGS that was not present on location 8. It is unlikely that rates of petroleum hydrocarbon degradation at location 4 were greater than location 8 due to both locations containing a maximum 1.2% petroleum hydrocarbon content in the uppermost 0.1 m LOS horizon (as determined in a preliminary site characterisation). This unreacted pore-gas CH_4 at the soil cover/ LOS interface on location is further evidence that placing LOS to a higher bulk density (and lower void ratio) can lead to restrictions in rates of CH_4 oxidation.

5.5.5 Implications to operational practices

Notwithstanding highly relevant considerations such as moisture and nutrient dynamics, the efficacy of a soil cover system can be evaluated (albeit from a limited perspective) in terms of a) facilitating soil-atmosphere gas exchange to supply sufficient pore-gas O_2 to the plant-rooting zone; and b) functioning to passively remove pore-gas CH_4 with microbial oxidation reactions.

a) Passively removing pore-gas CH_4 with microbial oxidation reactions

Compaction of soil materials to a higher bulk density (and thus low void ratio) was found to restrict CH_4 oxidation based on findings in the soil column experiments in Scale and Fleming (2017b). It is therefore recommended that operators exercise care during the placement of LOS in order to minimize the bulk density of the LOS (and thus maximize the void ratio) during construction the LOS landform, including limiting traffic of heavy equipment during placement of soil covers. It is important to note that at higher void ratios the LOS will be more compressible and susceptible to wetting collapse if the subsequently placed soil covers are anticipated to be trafficable (even to light vehicles) in the future.

The LOS at location 8 had the lowest bulk density (relatively highest void ratio) of all gas sampling locations; it is likely that this low bulk density facilitated the rapid oxidation of CH_4 based on the pore-gas CO_2 concentrations being highest and O_2 being lowest of all the gas sampling locations. Note that soil-atmosphere gas exchange sufficiently aerated the soil covers on location 8 despite the rapid oxidation of CH_4 occurring in the uppermost LOS (and corresponding consumption and flux of O_2). In regards to management practices, it is recommended that mine operators be cognisant that rates of CH_4 oxidation may be restricted at elevated moisture conditions for the LOS. Pore-gas concentrations of O_2 and CO_2 were found to be strongly related to VWC in the uppermost LOS, with more O_2 and less CO_2 present at higher VWC. This suggests that rates of CH_4 oxidation were restricted by the additional moisture, possibly due to reductions in air porosity. In Scale and Fleming (2017b), a prolonged drought simulation reduced CH_4 oxidation rates by more than 50% after 45 days; it is therefore

likely that in-situ CH_4 oxidation rates may also be restricted under reduced moisture conditions. For this specific study, the extremes of VWC for the LOS that were found to restrict rates of CH_4 oxidation were >24% and <17%. It should be noted, however, that due to the limited number of areas that were sampled in this study it is not clear whether it can be extrapolated that rates of CH_4 oxidation will be restricted beyond these VWC extremes for the entire ASCS.

b) Supplying adequate pore-gas O_2 to the plant-rooting zone

While oxidizing CH_4 is an important function of soil covers for mitigating atmospheric carbon-loading, it is also necessary for the soil covers to maintain sufficient pore-gas O_2 to support reclamation vegetation. Compaction of the LOS during construction of the LOS landform did not inhibit pore-gas O_2 in the plant-rooting zone. The LOS on location 4 had the highest bulk density (and lowest void ratio) of all gas sampling locations and sufficient pore-gas O_2 was still supplied to the soil covers and LOS to a depth of roughly 3 m BGS. In this case, the soil cover and LOS were well-aerated due to the soil cover being thinner (1 m), the cover being relatively free-draining, and possibly also due to barometric “pumping” of atmospheric O_2 deeper into the LOS landform. The design of the soil cover was relatively less important to pore-gas O_2 than the characteristics of the LOS based on pore-gas O_2 concentrations in the plant-rooting zone at 0.5 m BGS in the LOS or intermediary subsoil being unaffected by the uppermost soil cover design. Pore-gas O_2 concentrations were weakly correlated ($R^2 \leq 13\%$) to VWC in the soil covers; it is therefore unlikely that seasonal variations in VWC in the soil covers will reduce pore-gas O_2 concentrations to levels considered a risk for the growth and survivability of reclamation vegetation.

The appropriate balance of facilitating oxidation of CH_4 in the uppermost horizon of LOS and maintaining sufficient pore-gas O_2 concentrations in the plant-rooting zone depends upon the placement thickness of the soil cover system. This study found with the soil reclamation and LOS materials at ASCS that an appropriate balance could be established with a LOS bulk

density <1.5 Mg/m^3; however, the thinner soil covers (≤1 m) will require a LOS bulk density ranging from 1.6-1.8 Mg/m^3.

5.6 Conclusions

The objective of this paper was to understand the factors affecting the transportation and storage of soil gasses in LOS and reclamation soil covers in order to inform mine operators regarding practical issues involving the construction of LOS landforms, design of soil cover systems, and management of the reclamation site.

To understand the factors affecting the transportation of soil gasses, a numerical model was developed to simulate steady-state diffusive and advective-diffusive CO_2 flux from the LOS through multi-layered soil covers. The results of the numerical model were calibrated based on static flux chamber tests conducted in the field during the 2013-2015 field seasons. Advective-diffusive transport simulated results from static flux chamber tests; however, diffusive-only transport was not capable of simulating results from static flux chamber tests. Elevated moisture contents in the soil covers restricted gas transport in the model.

To understand the factors affecting the storage of soil gasses, statistical analyses were conducted to examine correlations between CO_2 and O_2 pore-gasses and on-site conditions, measurable soil parameters, the design of the soil covers, and in-situ bulk density of the LOS landform in the upper 0.5 m.

Air temperature was not significant to O_2 and CO_2 pore-gasses in the upper 0.3-0.5 m; however, VWC and soil temperature at this depth accounted for more than 37% of the variations in O_2 and CO_2 (based on the adjusted R^2 value). Near the interface between the soil covers and LOS at depths of 1-2 m, VWC accounted for up to 52% of the variations in O_2 and 65% of the variations in CO_2. Deeper into the LOS at depths of 3-4 m BGS, differential pressures accounted for more than 52% of the variations in O_2 and CO_2.

The design of the soil covers in the uppermost 0.1-0.3 m did not significantly alter the O_2 pore-gas concentration in the intermediary layer of subsoil or in the LOS at a depth of 0.5 m BGS.

Bulk density was found to be correlated to O_2 and CO_2 pore-gasses in the uppermost horizon of LOS. Rates of CH_4 oxidation appear to have been elevated at lower LOS bulk density based on reduced pore-gas concentrations of O_2 and elevated pore-gas concentrations of CO_2. On the other hand, rates of CH_4 oxidation appear to have been restricted at higher LOS bulk density based on elevated pore-gas concentrations of O_2 and reduced pore-gas concentrations of CO_2.

If a thicker cover (≥1 m) is placed over the LOS, it is recommended that mine operators place LOS at a bulk density <1.5 Mg/m^3 in order to maintain sufficient pore-gas O_2 concentrations in the plant-rooting zone of the soil covers while allowing sufficient oxidation of CH_4 in the uppermost horizon of the LOS. If a thinner soil cover (≤1 m) is placed, it is recommended that mine operators place LOS at a bulk density ranging from 1.5-1.8 Mg/m^3 in order to maintain sufficient pore-gas O_2 concentrations in the plant-rooting zone of the soil covers while allowing sufficient oxidation of CH_4 in the uppermost horizon of the LOS. Mine operators may also want to recognize that the capability of the LOS to oxidize pore-gas CH_4 may be limited when the VWC of the LOS is approximately less than 15% or greater than 24%.

Based on these findings, the design of the construction of the LOS landform appears to be more impactful to pore-gas dynamics than the design of the soil covers.

Acknowledgements

Funding for this research was provided by Canadian Natural Resources Ltd., Imperial Oil Resources Ltd., Shell Canada, Suncor Energy, Syncrude Canada Ltd and Total E&P Canada Ltd. through the Canadian Oilsands Innovation Alliance (COSIA). We would like to thank staff at Syncrude Canada Ltd. in Edmonton, AB and Fort McMurray, AB and the staff at O'Kane Consultants for their supporting, assisting, and accommodating this research.

References

Anderson R and Lovely D. 2000. **Hexadecane Decay by Methanogenesis**. Nature. (404): 722-723. DOI: 10.1038/35008145

Bekele A, Kellman L, and Beltrami H. 2007. **Soil Profile CO_2 Concentrations in Forested and Clear Cut Sites in Nova Scotia, Canada**. Forest Ecology and Management. (242:2-3): 587-597. DOI: 10.1016/j.foreco.2007.01.088

Boeckx P, Van Cleemput O, and Villaralvo I. 1996. **Methane emission from a landfill and the methane oxidising capacity of its covering soil.** Soil Biology and Biochemistry. (28:10-11): 1397-1405. DOI: 10.1016/s0038-0717(96)00147-2

Bowden RD, Newkirk KM, and Rullo GM. 1998. **Carbon Dioxide and Methane Fluxes by a Forest Soil under Laboratory-controlled Moisture and Temperature Conditions**. Soil Biology and Biochemistry. (30:12): 1591-1597. DOI: 10.1016/S0038-0717(97)00228-9

Bunt JS and Rovira AD. 1955. **Effect of Temperature and Heat Treatment on Soil Metabolism**. Journal of Soil Science. (6:1): 129-136. DOI: 10.1111/j.1365-2389.1955.tb00837.x

Campbell Scientific. 2009. **Instruction Manual for 229 Heat Dissipation Matric Water Potential Sensor**. Campbell Scientific Inc. Logan, Utah, USA.

Campbell Scientific. 2016. **Instruction Manual for CS616 and CS625 Water Content Reflectometers**. Campbell Scientific Inc. Logan, Utah, USA.

Columbus Instruments. 2016. **User's Manual for Model 180C**. Columbus Instruments, Columbus, Ohio, USA.

Christophersen M, Kjeldsen P, Holst H, and Chanton J. 2001. **Lateral gas transport in soil adjacent to an old landfill: Factors governing emissions and methane oxidation**. Waste Management Research. (19): 595-612. DOI: 10.1177/0734242X0101900616

Czepiel PM, Mosher B, Crill PM, and Harriss RC. 1996. **Quantifying the effect of oxidation on landfill methane emissions**. Journal of Geophysical Research. (101): 721-759. DOI: 10.1029/96JD00222

Darcy H. 1856. **Les Fontaines Publiques de la Ville de Dijon. Victor Dalmont, Paris, France**. DOI: 10.1061/40683(2003)5

Davidson EA, Belk E, and Boone RD. 1998. **Soil Water Content and Temperature as Independent or Confounded Factors Controlling Soil Respiration in a Temperate Mixed Hardwood Forest**. Global Change Biology. (4): 217-227. DOI: 10.1046/j.1365-2486.1998.00128.x

Dorr H, Katruff L, and Levin I. 1993. **Soil texture parameterization of the methane uptake in aerated soils**. Chemosphere. (26): 697-713. DOI: 10.1016/0045-6535(93)90454D

Einola JM, Kettunen RH, and Rintala J. 2007. **Responses of methane oxidation to temperature and water content in cover soil of a boreal landfill**. Soil Biology and Biochemistry. (39): 1156-1164. DOI: 10.1016/j.soilbio.2006.12.022

Fick A. 1855. **On liquid diffusion**. Ann. Phys. (170): 59–86. DOI: 10.1002/andp.18551700105. 94:59

Fleming M, Fleming IR, Headley J, Du Jinglong, Peru K. 2012. **Surficial Bitumen in the Athabasca Oil Sands Region.** International Journal of Mining, Reclamation and Environment. (26:2): 134-147. DOI: 10.1080/17480930.2011.570098

Flower FB. 1981. **Landfill gas, what it does to trees and how its injurious effects may be prevented.** Journal of Arboriculture. (7): 43-52

Gebert J, Rachor IM, Grongroft A, Pfeiffer EM. 2010. **Temporal variability of soil gas composition in landfill covers**. Waste Management. (31:5): 935-945. DOI: 10.1016/j.wasman.2010.10.007

Gebert J, Rower IU, Scharff H, Roncato CDL, and Cabral AR. 2011. **Can soil gas profiles be used to assess microbial CH4 oxidation in landfill covers?** Waste Management. (31): 987-994. DOI: 10.1016/j.wasman.2010.10.008

Hashimoto S and Komatsu H. 2006. **Relationships between Soil CO_2 Concentration and CO_2 Production, Temperature, Water Content, and Gas Diffusivity: Implications for Field Studies through Sensitivity Analyses.** Journal of Forest Research. (11:1): 41-50. DOI: 10.1007/s10310-005-0185-4

Hillel D. 2003. **Introduction to Environmental Soil Physics**. Academic Press.

Kettunen RH, Eionola JM, and Rintala JA. 2006. **Landfill Methane Oxidation in Engineered Soil Columns at Low Temperature.** Water, Air and Soil Pollution (177:1): 313-334. DOI: 10.1007/s11270-006-9176-0

Korbas T. 2014. **Degradation and mobility of hydrocarbons in Oilsands waste at the Aurora Fort Hills disposal area**. M.Sc. Thesis, Department of Civil and Geological Engineering, University of Saskatchewan, Saskatoon, Saskatchewan, Canada.

LandTEC. 2010. **GEM™2000 and GEM™2000 Plus Gas Analyzer and Extraction Monitor Operation Manual**. LandTEC North America, Colton, California, USA.

Mathworks. 2016. **MATLAB and Statistics Toolbox Release 2016a**. The MathWorks, Inc., Natick, Massachusetts, United States.

Montgomery DC and Runger GC. 2014. **Applied Statistics and Probability for Engineers** 6th Edition. Wiley.

Risk D, Kellman L, and Beltrami H. 2002. **Carbon Dioxide in Soil Profiles: Production and Temperature Dependence**. Geophysical Research Letters. (29:6): 11-1-11-4 DOI: 10.1029/2001GL014002

Salminen JM, Tuomi PM, Suortti A-M, and Jorgensen KS. 2004. **Potential for Aerobic and Anaerobic Biodegradation of Petroleum Hydrocarbons in Boreal Subsurface**. Biodegradation. (15:1): 29-39. DOI: 10.1023/B:BIOD.0000009954.21526.e8

Scale KO, Korbas TK and Fleming IR. 2016. **Degradation and Mobility of Petroleum Hydrocarbons in Oil Sand Waste**. Environmental Geotechnics, DOI: 10.1680/jenge.15.00035

Scale KO and Fleming IR. 2017a. **Pore-gases Dynamics in Overburden and Reclamation Soil Covers.** Environmental Geotechnics. Accepted June 2017.

Scale KO and Fleming IR. 2017b. **Soil Column Experiments to Quantify Methane Oxidation Rates in Overburden and Reclamation Soil Covers**. Submitted to International Journal of Mining, Reclamation and Environment. Pending peer review.

Siddique T, Fedorak PM, Fought JM. 2006. **Biodegradation of Short-Chain n-Alkanes in Oil Sands Tailings under Methanogenic Conditions**. Environmental Science and Technology. (40:17): 5459-5464. DOI: 10.1021/es060993m

Townsend GT, Prince RC, and Suflita JM. 2003. **Anaerobic Oxidation of Crude Oil Hydrocarbons by the Resident Microorganisms of a Contaminated Anoxic Aquifer**. Environmental Science and Technology. (37:22): 5213-5218. DOI: 10.1021/es0264495

Visser S. 2008. **Petroleum Hydrocarbons (PHCs) in Lean Oil Sand (LOS): Degradation Potential and Toxicity to Ecological Receptors**. Prepared for Cumulative Environmental Management Association (CEMA) Reclamation Working Group.

Whalen SC and Reeburgh WS. 1996. **Moisture and Temperature Sensitivity of CH4 Oxidation in Boreal Soils**. Soil Biology and Biochemistry. (28:10/11):1271-1281. DOI: 10.1016/S0038-0717(96)00139-3

Whitton BA, Chan GYS, and Wong MH. 1991. **Effects of Landfill Gas on Subtropical Woody Plants**. Environmental Management. **(15:3)**: 411-431. DOI: 10.1007/BF02393888

Zengler K. 1999. **Methane formation from long-chain alkanes by anaerobic microorganisms**. Nature. **(401)**: 266-269. DOI: 10.1038/45777

6.0 SUMMARY OF CONCLUSIONS

6.1 Characterization of F1-F4 petroleum hydrocarbons fractions in lean oil sands

- Petroleum hydrocarbons (PHC) in the lean oil sands (LOS) material collected from ASCS and used in the column study consisted predominantly of heavier F3 (47%) and F4 (45%) fractions. The remaining PHC fractions consisted of smaller amounts of lighter F1 (0.1% excluding undetectable BTEX) and F2 (8.3%) fractions.
- The F1 fraction (including BTEX) was undetectable in the column leachate. The F2 fraction marginally exceeded clean water guidelines on a few occasions at temperatures ≥22°C. At lower temperatures, ≤4°C, the concentration of F2 hydrocarbons was near the 0.1 mg/L detection limit. F3 hydrocarbons were present at low concentrations, however, the F3 fractions are not currently regulated for groundwater in Alberta.

6.2 Pore-gasses and gas flux rates from uncovered LOS

- CO_2 effluxes from LOS landform typically ranged from 0.1-1.5 kg/m^2/a with peaks of 7.1 kg/m^2/a.
- Pore-gas concentrations in the LOS typically ranged from 0-2% for O_2, 3-9% for CO_2, and 0-4% for CH_4, with peaks of 18% for O_2, 21% for CO_2, and 12% for CH_4.
- Based on laboratory soil column experiments, rates of PHC degradation for the LOS from respiration were 60 g/a at 22°C and 15 g/a at temperatures ranging from 2-14°C. Rates of PHC volatilization for the LOS were 0.3 g/a.
- The effect of temperature on PHC degradation and CO_2 production was clearly observed from 4-22°C, with rates of CO_2 flux ranging from 0.1 kg/m^2/a at 4°C to 2.3 kg/m^2/a at 22°C.
- Rates of CO_2 flux quantified under laboratory conditions were comparable with flux rates measured with static flux chambers in the field (wherein LOS was exposed to atmospheric air temperatures and precipitation). This suggests that the column study

could be useful to produce meaningful and low cost estimates of in-situ PHC degradation.

6.3 Pore-gas concentrations in LOS and soil covers

- Pore-gas O_2, CO_2, and CH_4 concentrations were characterized in the soil covers and LOS following the placement of single and multi-layered soil covers. Concentrations of O_2 and CO_2 within the soil covers and within the uppermost approximately 1 m of LOS were generally at levels considered safe for plant growth (e.g. >10% O_2 and <15% CO_2). Pore-gasses deeper than 1 m within the LOS, however, surpassed the threshold considered safe for plant growth. Minimum O_2 concentrations were measured at 0%, peak CO_2 at 16%, and peak CH_4 at 36%.
- Frozen pore-water in a thin 0.3 m layer of peat overlying LOS remained frozen until late-June. This frozen layer blocked soil-atmosphere gas exchange and led to pore-gas CH_4 accumulating to concentrations greater than 36% deeper than 2 m in the LOS.

6.4 Gas fluxes through soil cover systems

- CO_2 effluxes from the soil covers were directly measured with static flux chambers. CO_2 effluxes from the LOS into the soil covers and O_2 ingress through the soil covers was measured using custom-designed and fabricated subsurface static flux chambers. The subsurface flux chambers were installed at a depth of 1.5 m below ground surface at two locations: one with 1.4 m subsoil covered by 0.1 m LFH and the other with 1.2 m subsoil covered by 0.3 m peat. Gasses were sampled with an automated multiplexing gas analyzer equipped to measure 0-100% O_2, 0-30% CO_2, and 0-30% CH_4. Rates of O_2 ingress peaked at 18 kg/m^2/a. Rates of CO_2 efflux peaked at 2.2 kg/m^2/a from the soil covers and 1.8 kg/m^2/a from the LOS.
- CO_2 effluxes were lower from the multi-layered soil cover with a 0.3 m peat layer than from the multi-layered soil cover with a 0.1 m LFH layer. These lower CO_2 effluxes are possibly due to the peat layer storing a greater volume of pore-water than the LFH to facilitate the rapid dissolution of CO_2.

6.5 Relative contribution of advection and diffusion to soil gas transport

- Rates of gas flux by concentration-gradient driven diffusion were indirectly measured from soil gas profiles using the concentration-gradient method and by estimating diffusion coefficients from vertical profiles of soil moisture and soil temperature. Rates of gas flux by pressure-gradient driven advection were indirectly measured from differential pressures and in-situ measurements of air conductivity. Diffusive fluxes ranged from 0.31-3.33 kg/m^2/a for O_2 and 0.10-2.96 kg/m^2/a for CO_2. Advective fluxes ranged from 5-122 kg/m^2/a for O_2 and 0.40-29.6 kg/m^2/a for CO_2.
- Rates of gas flux quantified using the direct and indirect methodologies varied by 0-34% in magnitude at comparable locations. These variations are reasonable when taking into consideration spatiotemporal differences and assumptions that soil characteristics are similar for locations within a 1 hectare study cell.
- Diffusion differed over a wide range of values due to spatial and material variability in soil moisture contents. Advection differed over a wide range of values due to spatial variability in air conductivity. Advection dominated over diffusion in all single and multi-layered soil covers except for one location wherein the LOS was placed at low in-situ bulk density (1.45 Mg/m^3) and thus responded quickly to variations in atmospheric pressure.

6.6 Methane oxidation rates in soil cover materials and lean oil sand

- CH_4 oxidation rates for LFH, peat, and subsoil reclamation soil cover materials and LOS were quantified using batch soil column experiments in single and multi-layered configurations. Based on CO_2 flux rates measured from the uncovered LOS, predicted rates of CH_4 flux were estimated to range from 0.1-7.1 kg/m^2/a; however, higher CH_4 fluxes up to 30 kg/m^2/a were tested in the soil column experiments. Variations in temperature, soil moisture, and bulk density were simulated.

- To simulate the effects of changing temperature, soil columns were placed in a climate chamber and tested at 4°C, 22°C, and >31°C. Oxidation rates were significantly higher for all soil materials and LOS at warmer temperatures.
- To simulate drought conditions, the daily application of water for the multi-layered soil column was discontinued for 45 days and oxidation rates decreased from approximately 80% to 38%.
- To simulate the effect of increasing bulk density, the column consisting of sandy subsoil was initially compacted to a dry density of 1500 kg/m^3 and was later disassembled and re-compacted to 1800 kg/m^3. Oxidation rates at the higher bulk density fell from approximately 50% to levels that were below detection limits.
- The batch soil column experiments used in this laboratory study enabled oxidation rates to be measured over the range of expected CH_4 fluxes (0.1-7.1 kg/m^2/a) and for expected soil temperatures (≤22°C). At higher CH_4 fluxes (>10 kg/m^2/a) and at higher soil temperatures (>31°C), however, the experiments were limited by the finite volume of O_2 in the columns and likely underestimated oxidation rates.

6.7 The role of the storage and transportation in guiding reclamation practices

- Soil moisture and soil temperature were weakly correlated to O_2 and CO_2 pore-gasses in the uppermost 1 m BGS (soil covers and LOS) and strongly correlated to O_2 and CO_2 pore-gasses to a depth of 2 m BGS (LOS). Deeper than 3 m BGS, O_2 and CO_2 pore-gasses were strongly correlated to differential pressure.
- Pore-gas concentrations of O_2 at 0.5 m BGS within intermediary layers of subsoil and LOS were unaffected by the design of the soil cover in the upper 0.1-0.3 m.
- Pore-gasses within the uppermost horizon of LOS were found to be related to the associated bulk density of the LOS in the upper horizon. Based on reduced pore-gas concentrations of O_2 and elevated CO_2, it appears that rates of CH_4 oxidation were elevated at lower LOS bulk density. At higher LOS bulk density, on the other hand,

rates of CH_4 oxidation appear to have been restricted based on elevated pore-gas concentrations of O_2 and reduced CO_2.

- The steady-state transport of CO_2 through two multi-layered soil covers was simulated with finite difference numerical modelling by considering flux by both advection and diffusion, but was not simulated by considering flux by diffusion alone. Elevated soil moisture conditions in the numerical model restricted CO_2 transport due to associated reductions in air porosity. In practicality, the restriction in CO_2 transport at elevated soil moisture conditions would be due to the additional dissolution of CO_2 in the larger volume of pore-water as well as the reduction in air porosity.

7.0 IMPLICATIONS TO MINE RECLAMATION USING SOIL COVERS

This purpose of this thesis was to develop a scientific basis for the site-specific estimation of the risk of gas-related toxicity to plant growth during the re-vegetation phase of the reclamation of lean oil sands LOS landforms. Based on this research, several general implications can be widely applied to practical issues involving the construction of LOS landforms, design of soil cover systems, and management of the reclamation site.

- While native boreal plants and tree species are sensitive to low O_2 or high CO_2/CH_4 pore-gas concentrations, the characterisation of pore-gasses in this study found that pore-gasses within the single and multi-layer covers were below the threshold that is considered a risk to growth and survivability of reclamation plant and tree species.
- Since pore-gasses within the 0.3 m soil covers and in the uppermost LOS horizon did not surpass the threshold that is considered to pose a risk to plant growth and survivability, the thickness of soil covers can likely be reduced from the 1.2-1.5 m thickness currently used by mine operators to 0.3 m without risking the development of conditions of low-O_2 stress or high-CO_2 toxicity. Furthermore, based on these findings, the uppermost LOS horizon can likely be incorporated into the design of the soil cover system. Note that this recommendation does not consider other important factors like moisture and nutrient dynamics or root penetrability.
- Pore-gas concentrations of CH_4 within the soil covers and the uppermost LOS horizon were typically undetectable or present at low concentrations (<1%). This indicates that the soil covers and uppermost LOS horizon are passively oxidizing CH_4 in-situ. The use of peat as a soil cover material may be inadvertently problematic, however, since pore-water within a 0.3 m peat layer at one sampling location remained frozen until late-June and acted as a barrier to gas exchange, thus leading to CH_4 accumulating to >35% deeper in the LOS.

- Soil cover placement thickness was positively related to CH_4 removal efficiency. Placing a thinner soil cover system is more economical since less soil is required to be hauled from the stockpiling location to the active reclamation site for placement. Placing a thicker soil cover system, while less economical, will have greater CH_4 removal efficiency and correspondingly lower CH_4 emissions.
- Oxidation rates were positively related to soil temperature, with higher oxidation rates measured at warmer soil temperatures. This suggests that the soil covers will oxidize CH_4 more effectively during the warmer months from June to August and oxidize CH_4 less effectively during the cooler months from September to May.
- Oxidation rates decreased significantly under reduced moisture conditions. This suggests that the capability of the soil covers to effectively oxidize CH_4 could be hindered by extended periods of low-precipitation or drought.
- Oxidation rates were reduced to below detectable levels when bulk density of the sandy subsoil was increased from 1.5 Mg/m^3 to 1.8 Mg/m^3. Moreover, concentrations of pore-gas O_2 were lower and concentrations of pore-gas CO_2 were higher in the uppermost horizon of LOS at a bulk density of 1.45 Mg/m^3 than at a bulk density of 1.98 Mg/m^3. These results suggest that CH_4 oxidation will likely be reduced at higher bulk densities.
- In regards to the placement of a thicker soil cover (≥1 m), operators should carefully place the LOS with the intention to minimize the in-situ bulk density of the LOS landform. By placing LOS at a bulk density <1.5 Mg/m^3, oxidation of CH_4 in the uppermost horizon of the LOS should take place rapidly, while the thicker soil cover will ensure that pore-gas O_2 is maintained at concentrations that do not pose a risk to the growth and survivability of reclamation vegetation.
- In regards to placing a thinner soil cover (≤1 m), operators should place the LOS to a bulk density ranging from 1.6-1.8 Mg/m^3 in order to limit rates of CH_4 oxidation in the uppermost LOS horizon and reduce the associated consumption and flux of pore-gas

O_2. This will maintain O_2 pore-gas at concentrations that do not pose a risk to the growth and survivability of reclamation vegetation.

- Mine operators should be aware that extreme soil moisture conditions can restrict gas exchange in the soil covers and oxidation of CH_4 in the uppermost LOS horizon.

8.0 RECOMMENDATIONS FOR FUTURE WORK

8.1 Recommendations for Field Work

- Characterization of pore-gasses could be conducted during winter when there is snowpack and soil temperatures are sub-zero in order to develop a more thorough understanding of the temporal variability in pore-gasses in soil covers and LOS. The measurement of pore-gasses beneath snowpack was unsuccessfully attempted in early-April 2014 using soil vapor probes that had been installed in late-2013. The probes were found to be plugged, likely due to water vapour condensing in the tubing and expanding upon freezing. New probes would therefore need to be installed in the soil underlying the snowpack and pore-gasses measured shortly thereafter.
- Additional soil vapour probes could be installed over a wider range of in-situ LOS bulk densities to develop a better understand the relationship between rates of O_2 ingress, CO_2 efflux and the in-situ bulk density of the LOS.
- No probes were installed in the various low and high-density tree plots due to site restrictions. Installing additional probes within the various tree plots would enable the effect of expanding tree root networks to pore-gasses and rates of gas flux to be evaluated.
- Measuring the diffusion coefficient (D_p) in-situ would enable diffusive fluxes to be calculated with greater accuracy than by estimating D_p based on measurements of soil moisture and temperature.
- The Dean and Stark measurements of oil content should be conducted to depths greater than 0.10 m to account for heterogeneities in the oil content of the lean oil sand with depth.

8.2 Recommendations for laboratory testing

- Soil moisture sensors with data-logging capabilities installed within the soil columns would enable more frequent and accurate water content measurements than using the Diviner 2000™ capacitance probe.

- The effect of bulk density to rates of CH_4 oxidation could be further investigated by compacting soil materials in smaller increments. For example, soil column experiments could be conducted on materials compacted to dry densities ranging from 1000 kg/m^3 to 2000 kg/m^3 in increments of 100 kg/m^3.
- Accelerated rates of CH_4 oxidation could be evaluated by incorporating layers of compost, bio-solids, or bio-char into the composite multi-layered soil covers tested in the batch soil column experiments.
- Isotope fractionation of the soil column headspace gasses could be measured as a secondary means of verifying that oxidation was occurring and that CH_4 wasn't being lost in storage within the column.
- Lean oil sands with petroleum hydrocarbon contents ranging from <1% to >7% could be incrementally tested to quantify the effects of petroleum hydrocarbon content to CH_4 oxidation rates.

9.0 APPENDICES

Appendix A: Calculating dissolved CO_2 using total alkalinity

The following calculations steps were used to estimate the CO_2 dissolved in the pore-water from total alkalinity measurements:

Step 1: Convert total alkalinity from units of mg/L $CaCO_3$ to mol/L H^+

Step 2: Relate HCO_3 and CO_3 using ka_2

$$[\mathrm{Alk}]_{\mathrm{Total}} = [\mathrm{HCO_3^-}] + 2[\mathrm{CO_3^-}] + [\mathrm{OH^-}] \quad \text{[A.1]}$$

$$\mathrm{HCO_3^-} \leftrightarrow \mathrm{H^+} + \mathrm{CO_3^{2-}} \quad \text{[A.2]}$$

$$\mathrm{ka_2} = [\mathrm{H^+}][\mathrm{CO_3^{2-}}]/[\mathrm{HCO_3^-}] \therefore [\mathrm{HCO_3^-}] = [\mathrm{H^+}][\mathrm{CO_3^{2-}}]/\mathrm{ka_2} \quad \text{[A.3]}$$

Step 3: Re-write TA in terms of CO_3^{2-} and solve for CO_3^{2-}

$$[Alk]_{Total} - [OH^-] = \frac{[\mathrm{H^+}][\mathrm{CO_3^{2-}}]}{ka_2} + [CO_3^{2-}] \quad \text{[A.4]}$$

Step 4: Solve for $[CO_2(aq)]$ using ka_1

$$CO_2(aq) + H_2O \leftrightarrow H^+ + HCO_3^- \quad \text{[A.5]}$$

$$ka_1 = \frac{[H^+][HCO_3^-]}{[CO_2(aq)]} \therefore [CO_2(aq)] = \frac{[H^+][HCO_3^-]}{ka_1} \quad \text{[A.6]}$$

Step 5: Solve for $[CO_2(aq)]_{Total}$ using the relationship for DIC

$$\mathrm{DIC} = [\mathrm{CO_2(aq)}] + [\mathrm{H_2CO_3^0}] + [\mathrm{HCO_3^-}] + [\mathrm{CO_3^{2-}}] \quad \text{[A.7]}$$

Appendix B: Calculating dissolved CO2 using Henry's Law

An alternative procedure was used to estimate the CO_2 dissolved in pore-water based on Henry's law and partial pressures of CO_2 in the column pores. The relationship for estimating the aqueous concentration of CO_2 using Henry's law is expressed below:

$$[CO_2(aq)] = \frac{(K_H)_{CO_2}}{P_{CO_2}} \qquad \text{[B.1]}$$

Where, K_H is Henry's law equilibrium coefficient for a solution of gas in water [$L^4\ T^2\ M^{-1}\ mol^{-1}$], P_{CO2} is the partial pressure of CO_2 [$M\ L^{-1}\ T^{-2}$], and [CO_2(aq)] is the aqueous concentration of CO_2 [$mol\ L^{-3}$].

The temperature dependence of Henry's law coefficients was considered in the procedure by including the following relationship (Sander 1999):

$$\mathrm{H(T)} = \mathrm{H^{\circ}} * \exp\left[-\frac{\Delta_{\mathrm{sol}}\mathrm{H}}{\mathrm{R}}\left(\frac{1}{\mathrm{T}} - \frac{1}{\mathrm{T^{\circ}}}\right)\right] \qquad \text{[B.2]}$$

Appendix C: Calibration of Diviner 2000™

Preliminary calibration of the Diviner 2000™ capacitance moisture probe involved first normalizing the sensor by recording raw air and raw water counts (SenTek 2009). The next step involved inserting the access tubes into 0.02 m^3 pails containing soil compacted to a specific dry bulk density. A hand-auger was used to remove a cylinder of soil and facilitate inserting the 0.056 m diameter access tubes. The Diviner 2000™ probe was inserted into the access tubes and the scaled frequency was recorded at incremental depths. The access tube was then removed. Soil samples were obtained from the pail at corresponding depths and the gravimetric water content of the samples was determined by placing the samples in the oven at 105˚C for 24 hours. The volumetric water content was determined by the following relationship:

$$\mathrm{VWC} = \mathrm{MC} * \frac{\rho_d}{\rho_w} \qquad [C.1]$$

Where, MC is the gravimetric water content [MM^{-1}], ρ_d is the dry bulk density [ML^{-3}], and ρ_w is the density of water [ML^{-3}].

A calibration equation was formulated relating the volumetric water content values and scaled frequencies in the form:

$$\mathrm{VWC} = \sqrt[b]{\left(\frac{\mathrm{SF}}{a}\right)} \qquad [C.2]$$

A final water content profile was measured for each soil column after completing the soil column experiments, whereupon the columns were deconstructed, samples obtained at incremental depths, and gravimetric water contents subsequently measured. Volumetric water contents and formulation of a calibration equation was determined similar to the preliminary

calibration. The final calibration was used for the following VWC profiles. The calibration results for the Diviner 2000™ sensor are shown in Figure C.1:

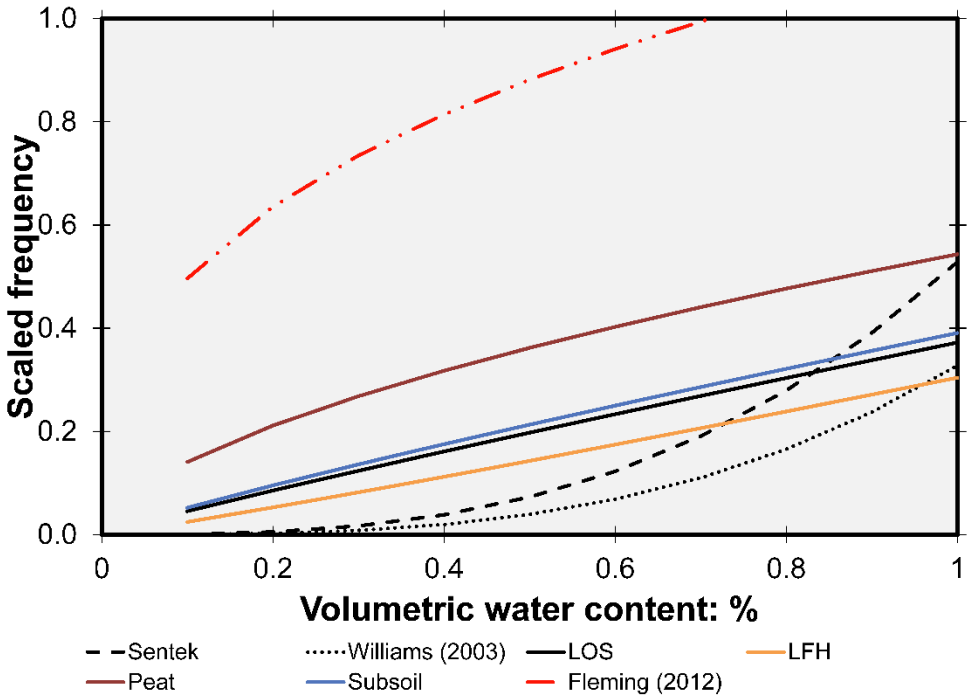

Figure C.1 Diviner 2000® calibration relationships for various soil materials.

The corresponding calibration coefficients, soil type, and researcher are presented in table C.1 below:

Table C.1 Calibration coefficient for Diviner 2000 for different soil materials

	Calibration coefficients		
Material	**a**	**b**	**Source**
N/A	1.25	0.35	SenTek (2009)
Topsoil	1.44	0.33	Williams (2003)
Sand with PHC	0.71	2.80	Fleming (2012)
LFH	2.98	0.92	*Current study*
LOS	2.95	1.09	*Current study*
Peat	2.83	1.71	*Current study*
Subsoil	2.93	1.14	*Current study*

Note that the calibration coefficients determined in this study are relatively large compared to the calibration equations in the previous study (not including Fleming, 2012). The reason for this is because the other coefficients were developed to simulate a large range of

VWC values for each soil. Whereas, with this current study, the coefficients were formulated to simulate a much narrower range of VWC values; thus, the coefficients determined result in more accurate VWC estimates over the range of scaled frequencies measured in the laboratory.

Appendix D: Technical description of Columbus Instruments® Microoxymax™ and Model 180C™

Gas analyses for the peat, LOS, and LFH soil columns were conducted using the Columbus Instruments® Micro-Oxymax™ modular gas analyser. Gas analysis for the double-stacked column, on the other hand, was conducted using the Columbus Instruments® Model 180-C™ gas analyser.

The two gas analysers are similar and the modular sensor are inter-changeable. The main difference is that the Micro-Oxymax™ has more sophisticated software and is designed to facilitate conducting fully-automated respiration experiments by refreshing the chamber headspace at set thresholds, compensating for pressure and temperature changes, and accurately calculating the headspace volume, incremental and cumulative rates, and respiratory quotients (Columbus Instruments 2002). It should be noted, however, that these sophisticated capabilities were not utilized for the soil column experiments. The Model 180-C™ can be considered to be a stripped-down version of the Micro-Oxymax™ that is capable of being equipped with various configurations of gas sensors with varying ranges of sensitivity (Columbus Instruments 2016). Both the Micro-Oxymax® and the Model 180-C® were equipped with condensing air drier units and a sample drier (with Ca_2SO_4 columns) to remove moisture from the gasses, 10 channel multiplexers to facilitate sequential sampling of numerous locations, and were both equipped with O_2, CO_2 and CH_4 sensors.

For the Micro-Oxymax™, the O_2 sensor was a 0-100% paramagnetic unit, the CO_2 was a 0-10% non-dispersive infrared (NDIR) unit (note that a 0-100% extended range NDIR unit was available, but not needed), and lastly, the CH_4 sensor was a 0-100% NDIR unit. For the Model 180-C™, the O_2 sensor was also a 0-100% paramagnetic unit, while CO_2 sensors were 0-1% and 0-30% NDIR units, and the CH_4 sensors were 0-1% and 0-30% NDIR units.

Appendix E: Calibration of Columbus Instruments® Micro-Oxymax™ and Model 180C™

Calibration of the CO_2 and CH_4 sensors for both gas analysers was conducted on a weekly basis using the following gas mixtures:

- 0.9% CO_2/ 99.1% N_2
- 25% CO_2/ 75% N_2
- 0.9% CH_4/ 99.1% N_2
- 25% CO_2/ 75% N2

As was discussed previously, the chambers were purged with “Extra-dry air”, supplied by Praxair®, which is approximately 20% O_2. Calibration of the O_2 sensors was done using the extra-dry air and was re-calibrated whenever a new gas cylinder was used, which happened approximately twice per week.

Appendix F: Governing equations

The following equation describes general transport by advection and diffusion:

$$J_{AD} = -D_e \frac{\partial C}{\partial z} + \nu C = -D_e \frac{\partial C}{\partial z} + \left(\frac{\rho k}{\mu \theta_a} \nabla P\right) * C \qquad [F.1]$$

The continuity equation for transport by advection and diffusion considering reactions:

$$\theta_a \frac{\partial C_g}{\partial t} = D_e \frac{\partial^2 C_g}{\partial z^2} - \frac{\nu C_g}{\delta z} - \theta_w \frac{\partial C_w}{\partial t} - R \qquad [F.2]$$

To estimate whether O_2 can diffuse downward from the column headspace into the soil column against the pressure gradient caused by the incoming methane, the Peclet number was calculated considered the maximum mass loading to the column was $5 m^3$/min, the length of soil in the column was approximately 0.70m and the diffusion coefficient for oxygen in free air (a conservative value) is approximately 1.8×10^{-5} m^2/s:

$$P_e = \frac{\nu L}{D} = \frac{(8.3 \times 10^{-8} ms^{-1})(0.7m)}{1.8 \times 10^{-5} m^2 s^{-1}} = 0.003 \qquad [F.3]$$

$\therefore$ diffusive transport dominates advective transport

Taking into consideration that diffusive transport dominates over advective transport, the advective term can be canceled out of the continuity equation, yielding the diffusion only variant of the continuity equation:

$$\boldsymbol{\theta_a \frac{\partial C_g}{\partial t} = D_e \frac{\partial^2 C_g}{\partial z^2} - \theta_w \frac{\partial C_w}{\partial t} - R} \qquad \textbf{[F.4]}$$

Appendix G: MATLAB® numerical model

```
function Scale_Assignment3_Model1

clc, close all

[z1,VWC]=load_VWC;

[v,HFC,Da0,Dw0,nP,nS,Cbot,Ctop,Th,ThL1,ThL2,tmax,dz,dt,H,t,z,nt,nz,p,C0,JD,JT]=define_
var;

[A,De,thetaeq,AP,AS,DeP,DeS,thetaeqP,thetaeqS,thetawP,thetawS,thetaaP,thetaaS,thetae
qFC]=define_layers(VWC,z,z1,ThL1,nP,nS,H,Da0,Dw0,p);


[t1,t2,t3,t4,C1,C2,C3,C4,tmed,cmed]=load_observed;


[t,CD]=ode15s(@DiffFun,t,C0,[],nz,HFC,JD,De,Cbot,dz,thetaeq,thetaeqFC);% Initial
Conditions


[t,CT]=ode15s(@TotalFun,t,C0,[],v,nz,HFC,JT,De,Cbot,dz,thetaeq,thetaeqFC);  % Call
subfunction that calculates t and CT(modeled adv-diff C)


% Fit mean experimental data w/ polynomial

poly_fit(tmed,cmed)


% Plot CO2 concentration w/ depth below ground surface (DBGS)

CO2_DBGS(CT,z,dt)


% Plot VWC of cover soil w/ DPGS

VWC_DBGS(VWC,z1)


% Plot model and CO2 conc. measured in SFC

model_fun(t,CD,CT,t1,t2,t3,t4,C1,C2,C3,C4)


% Plot model and mean CO2 conc. (measured in SFC)

model_mean(t,CD,CT,tmed,cmed)


function model_fun(t,CD,CT,t1,t2,t3,t4,C1,C2,C3,C4)

figure('Color',[1 1 1])                    % Change backgroun color of plot to white
```

```
% subplot(2,1,1)                          % Plot in subplot (OPTIONAL)
p1=plot(t,CD(:,end),'r',t,CT(:,end),'b');  % Create plot w/ diff-only and adv-diff models as red and black lines
set(p1(1),'LineWidth',1.75)               % Set model linewidth
set(p1(2),'LineWidth',1.75)               % Set model linewidth
hold on                                   % Retain plot
p11=plot(t1,C1,'o',t2,C2,'o',t3,C3,'o',t4,C4,'o');      % Plot field data from 4xFC
set(p11(1),'MarkerSize',4)                % Set marker size for C1
set(p11(2),'MarkerSize',4)                % Set marker size for C2
set(p11(3),'MarkerSize',4)                % Set marker size for C3
set(p11(4),'MarkerSize',4)                % Set marker size for C4
ylim([0 0.25])                            % Set y-axis limits
l1=legend('Diff Only','Adv-Diff','FC1','FC2','FC3','FC4','Location','Southoutside','Orientation','Horizontal'); % Set Legend
set(l1,'FontSize',11)                     % Set Legend font size
legend boxoff                             % Remove box outline from Legend
xlabel('Duration [hr]','FontSize',16)     % Label x-axis
ylabel('Concentration CO_{2} [%]','FontSize',16)       % Label y-axis
set(gca,'FontSize',12)                    % Set chart area font size


function model_mean(t,CD,CT,tmed,cmed)


figure('Color',[1 1 1])                   % Change background color of plot to white
% subplot(2,1,2)                          % Create subplot (OPTIONAL)
p2=plot(t,CD(:,end),'r',t,CT(:,end),'b');  % Plot diff-only and adv-diff models as red and black lines
set(p2(1),'LineWidth',1.75)               % Set linewidth of red diff-only
set(p2(2),'LineWidth',1.75)               % Set linewidth of black adv-diff
hold on                                   % Retain plot
p22=plot(tmed,cmed,'ko');                 % Plot mean CO2 conc. from field data
set(gca,'FontSize',12)                    % Set chart area font size
l2=legend('Diff Only','Adv-Diff','Mean','Location','Southoutside','Orientation','Horizontal');  % Set legend
```

```
set(l2,'FontSize',11)                          % Set font size of legend
legend boxoff                                  % Turn off box around legend
xlabel('Duration [hr]','FontSize',16)          % Label x-axis and set font size
ylabel('Concentration CO_{2} [%]','FontSize',16)       % Label y-axis and set font size
set(gca,'FontSize',12)                         % Set font size of chart area
ylim([0 0.25])                                 % Set y-axis limits

function VWC_DBGS(VWC,z1)
figure('Color',[1 1 1])                        % Change background color of plot to white
v=plot(VWC,z1);                                % Plot VWC w/ DPGS
set(gca,'ydir','reverse')                      % Reverse the dir. of the y-axis
set(v(1),'LineWidth',1.75)                     % Change linewidth of VWC
xlabel('VWC [%]','FontSize',14)                % Label x-axis and set font size
ylabel('Depth BGS [m]','FontSize',14)          % Label y-axis and set font size
set(gca,'FontSize',12)                         % Set font size of chart area

function CO2_DBGS(CT,z,dt)
figure('Color', [1 1 1])                       % Change background color of plot to white
plot(CT(1,1:end-1),z(1:end-1),'g*','LineWidth',2)      % Plot initial [CO2] w/ DPGS (not FC)
and assign color and linewidth
hold on                                        % Retain plot
plot(CT(end,1:end-1),z(1:end-1),'r*','LineWidth',2)    % Plot final [CO2] w/ DPGS (not FC)
and assign color and linewidth
hold on                                        % Retain plot
plot(CT(2:(10*dt):end-1,1:end-1),z(1:end-1),'k')       % Plot adv-diff w/ DPGS for soil layers
below FC and assign marker color
hold on                                        % Retain plot
plot(CT(2:(10*dt):end-1,end),z(end),'k.')      % Plot adv-diff w/ DPGS for FC layer and
assignn marker color
hold on                                        % Retain plot
plot(CT(1,end),z(end),'g*','LineWidth',2)      % Plot initial [CO2] in FC and assign color
and linewidth
plot(CT(end,end),z(end),'r*','LineWidth',2)    % Plot final [CO2]in FC and assign color
and linewidth
```

```
hold on                                    % Retain plot
set(gca,'ydir','reverse','FontSize',12)          % Change dir. of y-axis and set font size
xlabel('CO_2 concentration [%]','FontSize',14)     % Label x-axis and set font size
ylabel('Depth BGS [m]','FontSize',14)            % Label y-axis and set font size
l3=legend('Initial','Final','Location','Southoutside','Orientation','Horizontal');  % Set legend
set(l3,'FontSize',9.5)                     % Set font size of Legend
legend boxoff                              % Turn off box around Legend

function poly_fit(tmed,cmed)
n=2;                                       % Set nth order polynomial
PF = polyfit(tmed,cmed,n);                 % Fit an nth order polynomial

min_tmed=min(tmed);                        % Min time in tmed
max_tmed=max(tmed);                        % Max time in tmed
xx=[min_tmed:(max_tmed-min_tmed)/100:max_tmed];     % Create an array of ~100 pts

yy=polyval(PF,xx);                         % Find polynomial value at each pt

resid = polyval(PF,tmed)-cmed;             % Calculate residual values
figure('Color',[1 1 1])                    % Change background color of plot to white
plot(tmed,cmed,'*',xx,yy)                  % Plot mean CO2 field data and polynomial
hold on                                    % Retain plot
for i=1:numel(tmed)                        % Plot mean conc. value w/ polynomial
   xxx=[tmed(i) tmed(i)];
   yyy=[cmed(i) interp1(xx,yy,tmed(i))];

plot(xxx,yyy,'k')                          % Plot lines connecting to residuals
end
grid on                                    % Turn grid on
title([num2str(n),' order fit'])           % Title plot with polynomial order
xlabel('Duration [hr]','FontSize',14)          % Label x-axis and set font size
ylabel('Concentration CO_2 [%]','FontSize',14)     % Label y-axis and set font size
```

```
set(gca,'FontSize',12)                    % Set font size of chart area

function [z1,VWC]=load_VWC

data=csvread('Water_Contents2.csv');          % Read VWC w/ DBGS data from Excel
file

z1=data(:,1);                          % Assign variable "z1" to elevation (DBGS) data
VWC=data(:,2);                         % Assign variable "VWC" to water content data

function
[v,HFC,Da0,Dw0,nP,nS,Cbot,Ctop,Th,ThL1,ThL2,tmax,dz,dt,H,t,z,nt,nz,p,C0,JD,JT]=define_
var

% Definte parameters
Cbot=0.45;                             % Bottom CO2 constant concentration boundary
condition [%]
Ctop=0.03;                             % Top CO2 constant concentration boundary
condition [%]
ThL1=0.3;                              % Thickness of first soil layer [m]
ThL2=1.2;                              % Thickness of second soil layer [m]
Th=ThL1+ThL2;                          % Thickness of cover soil [m]
tmax=40;                               % Duration of purge test experiment [hr]
dz=0.1;                                % cover soil space step [m]
dt=0.5;                                % time step [hr]
H=0.03;                                % Henry's Law Constant for CO2
p=3.3;                                 % Material constant
v=0.005;                               % Pore-gas velocity [m/hr]
HFC=0.3048;                            % Height of flux chamber (HFC)

% Define De variables
Da0=0.0576;                            % Diffusion coefficient in free air [m2/hr]
Dw0=0.000008;                          % Diffusion coefficient in water [m2/hr]
nP=0.75;                               % Total porosity of peat layer
```

```
nS=0.4;                                  % Total porosity of subsoil


% Generate finite difference grid
t=0:dt:tmax;                             % Initialize time matrix
z=[Th-dz/2:-dz:dz/2 (-0.3048/2)];        % Initialize coversoil thickness matrix (for
block centered grid)including FC

nt=numel(t);                             % # of elements in time matrix
nz=numel(z);                             % # of elements in cover soil thickness matrix

C0=(((Cbot-Ctop)/Th)*z)+Ctop;            % Assign initial CO2 concentration
conditions in soil
C0(end)=0;                               % Assign zero initial CO2 concentration in FC

JD=zeros(nt,nz);                         % Initialize diffusive-only initial flux matrix
JT=zeros(nt,nz);                         % Initialize advective-diffusive initial flux matrix

function
[A,De,thetaeq,AP,AS,DeP,DeS,thetaeqP,thetaeqS,thetawP,thetawS,thetaaP,thetaaS,thetae
qFC]=define_layers(VWC,z,z1,ThL1,nP,nS,H,Da0,Dw0,p)

thetawP=mean(VWC(z1<ThL1));              % Average VWC of peat during purge
test (0-0.3m)
thetawS=mean(VWC(z1>ThL1));              % Average VWC of subsoil during purge
test (0.3-1.5m)

thetaaP=nP-thetawP;                      % Air-filled porosity for peat
thetaaS=nS-thetawS;                      % Air-filled porosity for subsoi

thetaeqP=thetaaP+H*thetawP;              % Equivalent air content for peat
thetaeqS=thetaaS+H*thetawS;              % Equivalent air content for subsoil
thetaeqFC=1;
```

```
DeP=10*(1/nP^2)*((Da0*thetaaP^p)+(Dw0*thetawP^p));      % Effective diffusion coefficient
for peat
DeS=(1/nS^2)*((Da0*thetaaS^p)+(Dw0*thetawS^p));        % Effective diffusion coefficient for
subsoil

AP=DeP/thetaeqP;                          % Constant for peat to shorten code
AS=DeS/thetaeqS;                          % Constant for subsoil to shorten code

% Define soil layer properties
A(z<0.3,:)=AP;                          % Assign AP (peat) at depths < 0.3m
De(z<0.3,:)=DeP;                          % Assign DeP (peat) at depths < 0.3m
thetaeq(z<0.3,:)=thetaeqP;                    % Assign thetaeqP (peat) at depths < 0.3m

De(z>0.3,:)=DeS;                          % Assign DeS (subsoil) at depths > 0.3m
A(z>0.3,:)=AS;                          % Assign AS (subsoil) at depths > 0.3m
thetaeq(z>0.3,:)=thetaeqS;                    % Assign thetaeqS (subsoil) at depths > 0.3m

function [t1,t2,t3,t4,C1,C2,C3,C4,tmed,cmed]=load_observed
% Import data from 4xFC purge test
data=csvread('Excel_Data.csv');                 % Read data from 4xFC purge test

t1=data(:,1);                           % Assign "t" variable to time data
t2=data(:,3);
t3=data(:,5);
t4=data(:,7);
C1=data(:,2);                           % Assign "C" variable to CO2 concentration data
C2=data(:,4);
C3=data(:,6);
C4=data(:,8);

ts=[t1 t2 t3 t4];                         % Create array containing all time measurements
tmed=mean(ts,2);                          % Calculate mean time representative of
sampling time for all 4 flux chambers
```

```
cs=[C1 C2 C3 C4];                          % Create array containing all CO2
measurements
cmed=mean(cs,2);                           % Calculate mean [CO2] representative of all 4
flux chambers


function [dCDdt]=DiffFun(t,CD,nz,HFC,JD,De,Cbot,dz,thetaeq,thetaeqFC)


% Bottom flux BC
JD(1,1)=-De(1,1)*((CD(1,1)-Cbot)/(dz/2));          % "Fudged" constant CO2 conc. bottom
BC


% Internal fluxes
for i=2:nz-1
   dCD=CD(i,1)-CD(i-1,1);
   R=(De(i,1)+De(i-1,1))/2;                % Average De for each space step in order to
account for fringe zone at soil interface
   JD(i,1)=-R.*(dCD/dz);
end



dCD=CD(nz,1)-CD(nz-1,1);
JD(nz,1)=-De(nz-1,1)*dCD/(dz/2);               % Calculate fluxes for internal points not
including FC
JD(nz+1,1)=0;                              % No flux out of FC


% Continuity
dzz=HFC;                                   % Assign "dzz" variable as HFC
i=1:nz;                                    % For all "i" up to, but not including, final "end" i
dCDdt(i,:)=-(JD(i+1,1)-JD(i,1))./(dz*thetaeq(i,1));
dCDdt(nz,1)=-(JD(nz+1,1)-JD(nz,1))./(dzz*thetaeqFC);     % Changing space step for FC


function [dCTdt]=TotalFun(t,CT,v,nz,HFC,JT,De,Cbot,dz,thetaeq,thetaeqFC)
```

```
% Bottom flux BC

JT(1,1)=v*CT(1,1)-De(1,1)*((CT(1,1)-Cbot)/(dz/2));       % "Fudged" constant CO2 conc. bottom BC


% Internal fluxes

for i=2:nz-1

   dCT=CT(i,1)-CT(i-1,1);

   A=(De(i,1)+De(i-1,1))/2;                    % Average De for each space step in order to account for fringe zone at soil/soil interface

   JT(i,1)=v*CT(i-1)-A.*(dCT/dz);

end


dCT=CT(nz,1)-CT(nz-1,1);

A=De(nz-1,1);                                  % Average thetaeq and De for each space step in order to account for fringe zone at soil/soil interface

JT(nz,1)=v*CT(nz,1)-A*dCT/(dz/2);                  % Calculate fluxes for internal points not including FC

JT(nz+1,1)=0;                                  % No flux out of FC


% Continuity

dzz=HFC;                                       % Assign "dzz" variable as HFC

i=1:nz;                                       % For all "i" up to, but not including, final "end" i


dCTdt(i,:)=-(JT(i+1,1)-JT(i,1))./(dz*thetaeq(i,1));

dCTdt(nz,1)=-(JT(nz+1,1)-JT(nz,1))./(dzz*thetaeqFC);     % Changing space step for FC
```